Mutagenesis and Mechanistic Studies of Dienelactone Hydrolase: Conversion to Dienelactone Isomerase

by

Ian Walker

BSc (Hons) Curtin

A thesis submitted for the degree of Doctor of Philosophy

of

The Australian National University

December 2001

Declaration

The work described in this thesis is original and has not previously been submitted for a degree or diploma in any other University or College, and to the best of my knowledge, does not contain material previously published or presented by another person, except where due reference is made in the text.

I give my consent to this copy of my thesis, when deposited at the University Library, being available for loan and photocopying.

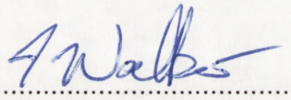

.....

Ian Walker

December 2001

Publication

Some of the work described in this thesis has been reported in the following publication:

Walker, I., Easton, C.J., Ollis, D.L. (2000) Site-directed mutagenesis of dienelactone hydrolase produces dienelactone isomerase. *Chemical Communications*. **8**:671-672.

Corrigendum

Page 1, paragraph 2, line 2 "chorocatechol' should read "chlorocatechol".

Figure 1. "malelyacetate" should read "maleylacetate".

Figure 2. β-sheet numbering "1, 2, 3, 4, 5, 6, 7, 8" should read left to right "1, 2, 4, 3, 5, 6, 7, 8".

Page 25, line 3 "debri" should read "debris".

Page 29, line 5 "sort" should read "sought".

Page 31, line 6 delete "from" preceding "the fragment".

Page 40, line 10 "25 0.1 °C" should read " 25 ± 0.1 °C".

Page 60, last sentence: delete "a" preceding "full'

"analyses" for "analysis"

"adopted" for "adapted".

Acknowledgments

I would like to thank my supervisors Chris Easton and David Ollis. Their support, guidance and encouragement has been invaluable. I also thank Chris for giving me the opportunity to study in a field in which I had little knowledge. I would also like to thank Eong Cheah for her help in getting me started and her wisdom of DLH. To Cy Jefferies for pointing me in the right direction for mutagenesis and general discussions about DLH. To Jian-Wei (JW) Liu for being a molecular biology wizz, for making and purifying some of the mutants used in this work, and for some proof-reading. To James Kelly for showing me the finer points of HPLC and for having a crack at some of the synthesis. I thank John Morrison for his comments on some of my early results. To Hideki, Connie and David for their assistance in providing some late night chemistry information.

Special thanks go to my family for all of their support and for encouraging me to go back and study in the first place.

To Dad

Abstract

A new and refined method for the purification of DLH has been developed ensuring that this enzyme retains high catalytic activity. The pH/pD dependence of wt DLH shows that proton transfer in the free enzyme and the enzyme-substrate complex is rate-determining. The magnitude of these proton transfers between water and deuterium oxide suggest that they occur *via* a general base mechanism.

The proposed catalytic mechanism of DLH was studied using site-directed mutagenesis and kinetic analysis of the mutant proteins using the *E*- and *Z*-dienelactones. The mechanism of hydrolysis of the *Z*-dienelactone by DLH is in agreement with that proposed by X-ray crystallography. Hydrolysis of the *E*-dienelactone is in general agreement with this mechanism, the major exception being that the process of substrate-induced activation of the nucleophile when hydrolysing the *E*-dienelactone appears to be different from that for the *Z*-dienelactone. The *E*-dienelactone does not interact with R206 in the Michaelis complex; the key residue that couples substrate binding to the activation of the nucleophile. Therefore, to hydrolyse the *E*-dienelactone, it appears that an active site conformational change occurs. There appears to be no role for S203 in the formation of the Michaelis complex for either isomer of dienelactone. A role for W88 is proposed here where this residue assists in the formation of the Michaelis complex, probably *via* forming π-π interactions with the lactone ring hydrogens. A role for Y85 as a general acid catalyst is not definitively supported here.

The kinetic characterisation of the C123S mutant enzyme has shown that this enzyme is an isomerase (DLI) and not a hydrolase, as previously assumed. A thermodynamic equilibrium is reached for the isomerisation of the *E*- and *Z*-dienelactones. Active site residues that are important for the formation of the Michaelis complex in DLH are also important for this role in DLI. Additionally, these residues are shown to be critical for the reaction of the substrate isomers once bound, probably by securing the position of the enolate formed in the acyl enzyme intermediate. DLI was shown to isomerise the

tert-butyl esters of dienelactone. The C123D mutant enzyme isomerises the *E*-dienelactone to the *Z*-isomer and hydrolyses the activated ester *p*-NPA.

Table of Contents

Declaration ii

Publication iii

Acknowledgments iv

Abstract vi

Table of Contents viii

List of Figures xv

List of Tables xix

List of Abbreviations xxi

Chapter 1 Introduction 1

1.1 **The *ortho*-cleavage and modified *ortho*-cleavage enzyme pathways for the degradation of aromatic compounds** 1

1.1.1 The reactions of the *ortho*-cleavage pathway 2

1.1.2 The reactions of the modified *ortho*-cleavage pathway 2

1.1.3 A comparison of the *ortho*- and modified *ortho*-cleavage pathway enzymes 4

1.1.4 Genes expressing the modified *ortho*-cleavage pathway of *Pseudomonas* sp. 5

1.2 **Determination of at least three different DLH types** 5

1.2.1 DLH type I 5

1.2.2 DLH type II 7

1.2.3 DLH type III 7

1.2.4 DLH from *Rhodococcus opacus* 1CP 8

1.3 **The X-ray crystallographic structure of DLH type III from *Pseudomonas putida* (pAC27)** 8

1.3.1 The overall structure of DLH 8

1.3.2 The α/β hydrolase fold 8

1.3.3 The active site of DLH 9

1.4 **The catalytic mechanism of DLH type III (pAC27)** 11

1.4.1 The active site and inhibitor binding 11

1.4.2 Substrate induced activation and the catalytic mechanism 12

1.4.3 Mechanistic comparisons with the serine and cysteine proteases 14

1.4.4 Limitations to our understanding of the proposed mechanism of catalysis by DLH 17

1.5 **Thesis proposal** 17

Chapter 2 Materials and Methods 18

2.1 **Materials** 18

2.1.1 Chemicals 18

2.1.2 Enzymes 19

2.1.3 The plasmid, bacterial strain, and the deoxyribo-oligonucleotides 19

2.1.4 The *clc*D gene encoding DLH 20

2.2 **Methods** 20

2.2.1 General 20

2.2.2 Substrate synthesis 21

2.2.2.1 *exo-3,6-Epoxy-1,2,3,6-tetrahydrophthalic anhydride* 21

2.2.2.2 *tert-Butoxycarbonylmethylenetriphenylphosphorane* 23

2.2.2.3 *E- and Z-dienelactone tert-butyl esters* 23

2.2.2.4 *E- and Z-dienelactones* 24

2.2.3 Cell culture 25

2.2.4 Purification of DLH 25

2.2.5 Enzyme assays 27

2.2.5.1 *Activity measurements during purification* 27

2.2.5.2 *Determination of the kinetic constants for purified DLH* 27

2.2.6 DLH mutants and their purification 29

2.2.6.1 *Method i) Generation of the E36D, E36Q, R81K and R206A mutants* 29

2.2.6.2 *Method ii) Generation of the remaining DLH mutants* 33

2.2.6.3 *DLH mutant purification, protein concentration and the determination of kinetic constants* 34

2.2.7 Determination of the pH dependence of DLH at low and high substrate concentrations 35

2.2.8 Determination of the pD dependence of DLH at high and low substrate concentrations 36

2.2.9 Determination of the pH dependence of the E36D, R206A and R81A mutants of DLH at low substrate concentrations 36

2.2.10 Measurement of kinetic activity using HPLC 37

2.2.10.1 *The elution of the E- and Z-dienelactones and their hydrolysis product(s)* 37

2.2.10.2 *Activity measurements of wt DLH using the E- and Z-dienelactones* 37

2.2.10.3 *Activity measurements of C123S, C123S/R81A and C123S/R206A mutants using the E- and Z-dienelactones* 38

2.2.10.4 *Activity measurements of C123S using the E- and Z-dienelactone tert-butyl esters* 38

2.2.10.5 *Activity measurement of DLH using the E-dienelactone tert-butyl ester* 39

2.2.10.6 *Activity measurement of C123D using the E-dienelactone* 39

2.2.11 Hydrolysis of *p*-nitrophenyl acetate by DLH, C123S and C123D enzymes 40

Chapter 3 Purification and preliminary kinetic analysis of DLH 41

3.1 **DLH purification** 41

3.2 **Optimisation of the purification of DLH** 41

3.3 **The effect of sodium chloride on DLH activity** 45

3.4 **Conclusion** 48

Chapter 4 Mutagenesis of DLH, overexpression of the mutant proteins and preliminary determination of their pH dependence 49

4.1 **Mutagenesis** 49

4.2 **Overexpression and purification of the mutant proteins of DLH** 50

4.3 **Confirmation of the size of the expressed DLH proteins** 50

4.4 **The pH and pD dependence of the kinetic parameters of DLH** 51

4.4.1 Determination of the pH profile for wt DLH 52

4.4.2 Observation of non-Michaelis-Menten kinetics below pH 7.5 55

4.4.3 Determination of the pD profile for wt DLH 55

4.4.4 Summary of the pH and pD dependence of wt DLH 58

4.5 **Determination of the pH profiles for the E36D, R81A and R206A mutants of DLH at low substrate concentrations** 58

4.6 **Conclusion** 63

Chapter 5 Kinetic analysis of the hydrolysis of the *E*- and *Z*-dienelactones catalysed by DLH mutants 64

5.1 **Hydrolysis of the *Z*-dienelactone** 64

5.1.1 E36D mutant 64

5.1.2 R206A, R81A, and R206A/R81A mutants 66

5.1.3 R81K and R206K mutants 68

5.1.4 Y85F mutant 70

5.1.5 W88A mutant 70

5.1.6 Summary of the hydrolysis of the *Z*-dienelactone by DLH mutant enzymes 72

5.2 **Hydrolysis of the *E*-dienelactone** 73

5.2.1 E36D mutant 74

5.2.2 R206A, R81A and R206A/R81A mutants 75

5.2.3 R81K and R206K mutants 77

5.2.4 Y85F mutant 78

5.2.5 W88A mutant 79

5.2.6 Summary of the hydrolysis of the *E*-dienelactone by DLH mutant enzymes 79

5.2.7 Active site conformational change in DLH for hydrolysing the *E*-dienelactone 80

5.3 **Hydrolysis of the *E*- and *Z*-dienelactones by S203 mutant enzymes** 84

5.3.1 Hydrolysis of the *Z*-dienelactone 85

5.3.1.1 *S203A mutant* 85

5.3.1.2 *S203H mutant* 86

5.3.1.3 *S203D mutant* 87

5.3.2 Hydrolysis of the *E*-dienelactone 88

5.3.2.1 *S203A mutant* 88

5.3.2.2 *S203H mutant* 88

5.3.2.3 *S203D mutant* 89

5.3.3 Summary of the hydrolysis of the *E*- and *Z*-dienelactones by S203 mutant enzymes 89

5.4 **Conclusion** 90

Chapter 6 Kinetic analysis of the reactions of the *E*- and *Z*-dienelactones catalysed by C123S and C123D mutant enzymes 91

6.1 **Observation of isomerase and not hydrolase activity by the C123S mutant enzyme** 91

6.2 **Kinetic analysis of the isomerase activity of DLI by HPLC** 93

6.3 **Kinetic analysis of the isomerisation of the *E*- and *Z*-dienelactones by DLI using UV spectroscopy** 96

6.3.1 Isomerisation of the *Z*-dienelactone 96

6.3.2 Isomerisation of the *E*-dienelactone 97

6.3.2.1 *Active site conformational change when isomerising the E-dienelactone* 99

6.3.3 Summary of the isomerase activity of DLI with the *E*- and *Z*-dienelactones 99

6.4 **Kinetic analysis of the reactions of the *E*- and *Z*-dienelactones catalysed by DLI mutants** 100

6.4.1 Reaction of the *Z*-dienelactone analysed using HPLC 100

6.4.2 Reaction of the *Z*-dienelactone analysed using UV spectroscopy 100

6.4.2.1 *DLI R206A mutant* 102

6.4.2.2 *DLI R81A mutant* 103

6.4.2.3 *Observation of a burst with the arginine mutants of DLI when reacting with the Z-dienelactone* 104

6.4.3 Reaction of the *E*-dienelactone analysed using HPLC 106

6.4.3.1 *DLI* 108

6.4.3.2 *DLI R206A mutant* 108

6.4.3.3 *DLI R81A mutant* 109

6.4.4. Summary of the reaction of the *E*- and *Z*-dienelactones by DLI mutant enzymes 110

6.5 **Reaction of the *E*- and *Z*-dienelactone *tert*-butyl esters catalysed by DLI analysed using HPLC** 110

6.5.1 Reaction of the *E*-dienelactone *tert*-butyl ester with DLH analysed using HPLC 113

6.6 **Kinetic analysis of the C123D mutant** 115

6.6.1 Reaction of the *E*-dienelactone analysed using HPLC 115

6.6.2 Hydrolysis of *p*-nitrophenyl acetate by C123D analysed using UV spectroscopy 116

6.7 **Conclusion** 118

References 119

Appendences

Appendix 1 128

Synthesis of the E- and Z-dienelactams

Protein Crystallography

Appendix 2 130

Kinetic data used in Chapter 3

Appendix 3 132

Kinetic data used in Chapter 4

Appendix 4 146

Kinetic data used in Chapter 5

Appendix 5 156

Kinetic data used in Chapter 6

List of Figures

Figure 1. Comparison of the *ortho*-cleavage and modified *ortho*-cleavage pathways. 3

Figure 2. Topology of the hydrolase fold of DLH. 9

Figure 3. The substrates *E*- and *Z*-dienelactone and the inhibitor *Z*-dienelactam. 12

Figure 4. The active site of DLH in the absence of substrate. 13

Figure 5. The active site of DLH in the presence of substrate. 14

Figure 6. Synthetic pathway for the production of the *E*- and *Z*-dienelactones. 22

Figure 7. The relative activity of DLH after incubation in increasing concentrations of β-ME. 45

Figure 8. The effects of NaCl concentration on the activity of wt DLH hydrolysing the *E*-dienelactone. 46

Figure 9. Comparison of the kinetics of hydrolysis by wt DLH without and in the presence of 100 mM NaCl. 47

Figure 10. Reaction scheme for the ionisations of the free enzyme and the enzyme-substrate complex. 52

Figure 11. The k_{cat}/K_m profile in water (pH) and deuterium oxide (pD) for wt DLH. 54

Figure 12. The k_{cat} profile in water (pH) and deuterium oxide (pD) for wt DLH. 54

Figure 13. K_m *vs* pD profile and pH profile for wt DLH. 57

Figure 14. The pH profile in water for wt DLH with the *E*-dienelactone at 0.3 x K_m. 61

Figure 15. The pH profile in water for E36D with the *E*-dienelactone at 0.3 x K_m. 61

Figure 16. The pH profile in water for R206A with the *E*-dienelactone at 0.3 x K_m. 62

Figure 17. The pH profile in water for R81A with the *E*-dienelactone at 0.3 x K_m. 62

Figure 18. Comparison of the side chain length and charge distribution of a lysine residue to an arginine residue. 69

Figure 19. The possible role of Y85 in the hydrolysis of the *Z*-dienelactone. 71

Figure 20. A schematic of the distance(s) that W88 is from the ring hydrogens of the lactam inhibitor *Z*-dienelactam in the C123S mutant enzyme. 72

Figure 21. Demonstration of the deviation from Michaelis-Menten kinetics for the DLH hydrolysis of the *E*-dienelactone. 81

Figure 22. The distance in angstroms that S203 and R206 are from the carboxylate of the inhibitor *Z*-dienelactam. 86

Figure 23. Concentrations of the *Z*-dienelactone, the *E*-dienelactone and the hydrolytic product after reaction of a) the *Z*-dienelactone and b) the *E*-dienelactone with DLI, as determined by HPLC. 94

Figure 24. Concentrations of the *Z*-dienelactone, the *E*-dienelactone and the hydrolytic product after reaction of a) the *Z*-dienelactone with DLH and b) the *E*-dienelactone with DLH, as determined by HPLC. 95

Figure 25. Isomerisation of the *E*-dienelactone by DLI. 98

Figure 26. Concentrations of the *Z*-dienelactone, the *E*-dienelactone and the hydrolysis product after the reaction of the *Z*-dienelactone with DLI R206A, as determined by HPLC. 101

Figure 27. Concentrations of the *Z*-dienelactone, the *E*-dienelactone and the hydrolysis product after the reaction of the *Z*-dienelactone with DLI R81A, as determined by HPLC. 101

Figure 28. Securing the position of the enolate in the acyl enzyme intermediate by ionic interactions with R206 and R81. 104

Figure 29. Concentrations of the *Z*-dienelactone, the *E*-dienelactone and the hydrolytic product after the reaction of the *E*-dienelactone with DLI R206A, as determined by HPLC. 107

Figure 30. Concentrations of the *Z*-dienelactone, the *E*-dienelactone and the hydrolytic product after the reaction of the *E*-dienelactone with DLI R81A, as determined by HPLC. 107

Figure 31. The *tert*-butyl esters of dienelactone. 111

Figure 32. Concentrations of the *Z*-dienelactone *tert*-butyl ester, the *E*-dienelactone *tert*-butyl ester and the hydrolysis product after

reaction of the *Z*-dienelactone *tert*-butyl ester with DLI, as determined by HPLC. 111

Figure 33. Concentrations of the *Z*-dienelactone *tert*-butyl ester, the *E*-dienelactone *tert*-butyl ester and the hydrolysis product after reaction of the *E*-dienelactone *tert*-butyl ester with DLI, as determined by HPLC. 112

Figure 34. Concentrations of the *E*-dienelactone *tert*-butyl ester and the hydrolytic product after reaction with DLH, as determined by HPLC. 114

Figure 35. DLH hydrolysis of the *E*-dienelactone *tert*-butyl ester to the *tert*-butyl ester of maleylacetate. 114

Figure 36. Isomerisation of the *E*-dienelactone to the *Z*-isomer by C123D. 116

List of Tables

Table 1. Comparison of the properties of enol lactone hydrolase with the different types of dienelactone hydrolase. 6

Table 2. Salt gradient used for the purification of wt and mutant DLH with the DEAE Fractogel column. 26

Table 3. The extinction coefficients (ε) for the *E*- and *Z*-dienelactones. 28

Table 4. Oligonucleotides used for the site-directed mutagenesis of wt DLH and the C123S mutants. 30

Table 5. PCR protocol for Method i). 31

Table 6. PCR protocol used for sequencing of the DLH gene. 33

Table 7. PCR protocol for Method ii). 34

Table 8. Specific activity of DLH for the hydrolysis of the *E*-dienelactone after each step during purification. 43

Table 9. Specific activity of DLH stored for several days at 4 °C in buffer A. 44

Table 10. The p*K* values of DLH in buffered solutions of water (pH) and deuterium oxide (pD) obtained from the k_{cat}/K_m and k_{cat} profiles. 53

Table 11. Kinetic data for the interaction of wt DLH and various active site mutants with the *E*-dienelactone. 59

Table 12. Values of p*K* calculated from pH profiles for wt and mutant DLHs using a single low substrate concentration of the *E*-dienelactone such that $s<K_m$. 60

Table 13. Kinetic data for the interaction of wt DLH and various active site mutants with the *Z*-dienelactone. 65

Table 14. Kinetic data for the interaction of wt DLH and various active site mutants with the *E*-dienelactone. 74

Table 15. Comparison of the kinetics of wt DLH with various mutants of the active site residue S203. 85

Table 16. Kinetic data for the isomerisation of the *E*- and *Z*-dienelactones by DLI. 97

Table 17. Kinetic data for the interaction of DLI R206A and DLI R81A with the *Z*-dienelactone. 102

Table 18. Estimation of the rate constants for the isomerisation of the *Z*-dienelactone to the *E*-isomer by the arginine mutants of DLI. 106

Table 19. Kinetic data for the interaction of DLI and various active site mutants with the *E*-dienelactone. 109

Table 20. Kinetic data for the interaction of C123D, DLH and DLI with *p*-nitrophenyl acetate. 117

List of Abbreviations

Abbreviation	Meaning
A	Alanine
C	Cysteine
D	Aspartate
E	Glutamate
F	Phenylalanine
H	Histidine
I	Isoleucine
K	Lysine
L	Leucine
Q	Glutamine
R	Arginine
S	Serine
W	Tryptophan
Y	Tyrosine

Chapter 1

Introduction

Dienelactone hydrolase (EC 3.1.1.45) is an enzyme involved in the degradation of chloroaromatic compounds and occurs in a diverse range of bacteria (Schmidt and Knackmuss, 1980). In nature the degradation of these aromatic compounds is essential for their mineralisation. Microorganisms that express the enzymes necessary for the degradation of these aromatic compounds can utilise them as their sole carbon and energy source (Harwood and Parales, 1996; Reineke and Knackmuss, 1988). Some can also participate in the degradation of a variety of xenobiotic industrial pollutants (*eg.* chloroanilines and chlorobiphenyls) introduced into the environment. Dienelactone hydrolase (DLH) is the third of four enzymes in the modified *ortho*-cleavage or chlorocatechol branch of the β-ketoadipate pathway that converts chlorocatechols into β-ketoadipate for incorporation into the tricarboxylic acid (TCA) cycle (Schmidt and Knackmuss, 1980). DLH catalyses the hydrolysis of dienelactone (4-carboxymethylenebut-2-en-4-olide) to maleylacetate (4-hydroxy buta-1,3-diene-1,4-dicarboxylate).

1.1 The *ortho*-cleavage and modified *ortho*-cleavage enzyme pathways for the degradation of aromatic compounds

The mineralisation of a wide range of complex aromatic and chloroaromatic compounds converges to either catechol or chorocatechol for degradation by the *ortho*- and the modified *ortho*-cleavage pathway, respectively. The pathway for the aerobic degradation of catechols was first deciphered by Ornston (1966) where he noted that catechol was degraded *via ortho* (intradiol)-cleavage. The *ortho*-cleavage (β-ketoadipate) pathway is involved in the breakdown of catechols derived from compounds as diverse as naphthalene, mandelate and cinnamate.

Early observations were made of a parallel pathway for the degradation of 4-chlorophenoxyacetate that was distinct from the *ortho*-cleavage pathway (Evans *et al.*, 1971). The degradation of 3-chlorobenzoate by a Pseudomonad using a similar pathway to that of 4-chlorophenoxyacetate was noted later (Dorn *et al.*, 1974) and further characterisation of this pathway developed the understanding of the intermediates and enzymes of the modified *ortho*-cleavage pathway (Schmidt and Knackmuss, 1980). The chlorocatechols that enter this pathway come from compounds as diverse as chlorodibenzofuran, chlorodiphenyl ethers and chlorobenzenes.

1.1.1 The reactions of the *ortho*-cleavage pathway

The *ortho*-cleavage of catechol is accomplished by the enzyme catechol 1,2-dioxygenase to give *cis,cis*-muconate (Figure 1). Muconate cycloisomerase then cyclises the *cis,cis*-muconate. Isomerisation of the double bond from the 2- to the 3-position is catalysed by muconolactone isomerase. The product from this reaction is hydrolysed by enol lactone hydrolase to β-ketoadipate. Further degradation of β-ketoadipate to succinyl-CoA and acetyl-CoA by β-ketoadipate:succinyl-CoA transferase and β-ketoadipyl-CoA thiolase allows these products from the *ortho*-cleavage pathway to be incorporated as intermediates into the TCA cycle (Schlömann, 1994).

1.1.2 The reactions of the modified *ortho*-cleavage pathway

Degradation in the chlorocatechol pathway proceeds with the cleavage of a 3- or 4-substituted chlorocatechol at the *ortho* position by chlorocatechol 1,2-dioxygenase (EC 1.13.11.-) to give either the 2- or 3-chloro-*cis,cis*-muconate, respectively (Figure 1). Both of these pathway intermediates are cyclised by chloromuconate cycloisomerase (EC 5.5.1.7) and, after the spontaneous release of HCl, give dienelactone. DLH from *Pseudomonas* sp. B13 catalyses the hydrolysis of the *E*- and *Z*-isomers of dienelactone (4-carboxymethylenebut-2-en-4-olide) to 3-hydroxymuconate (2-hydroxybuta-1,3-

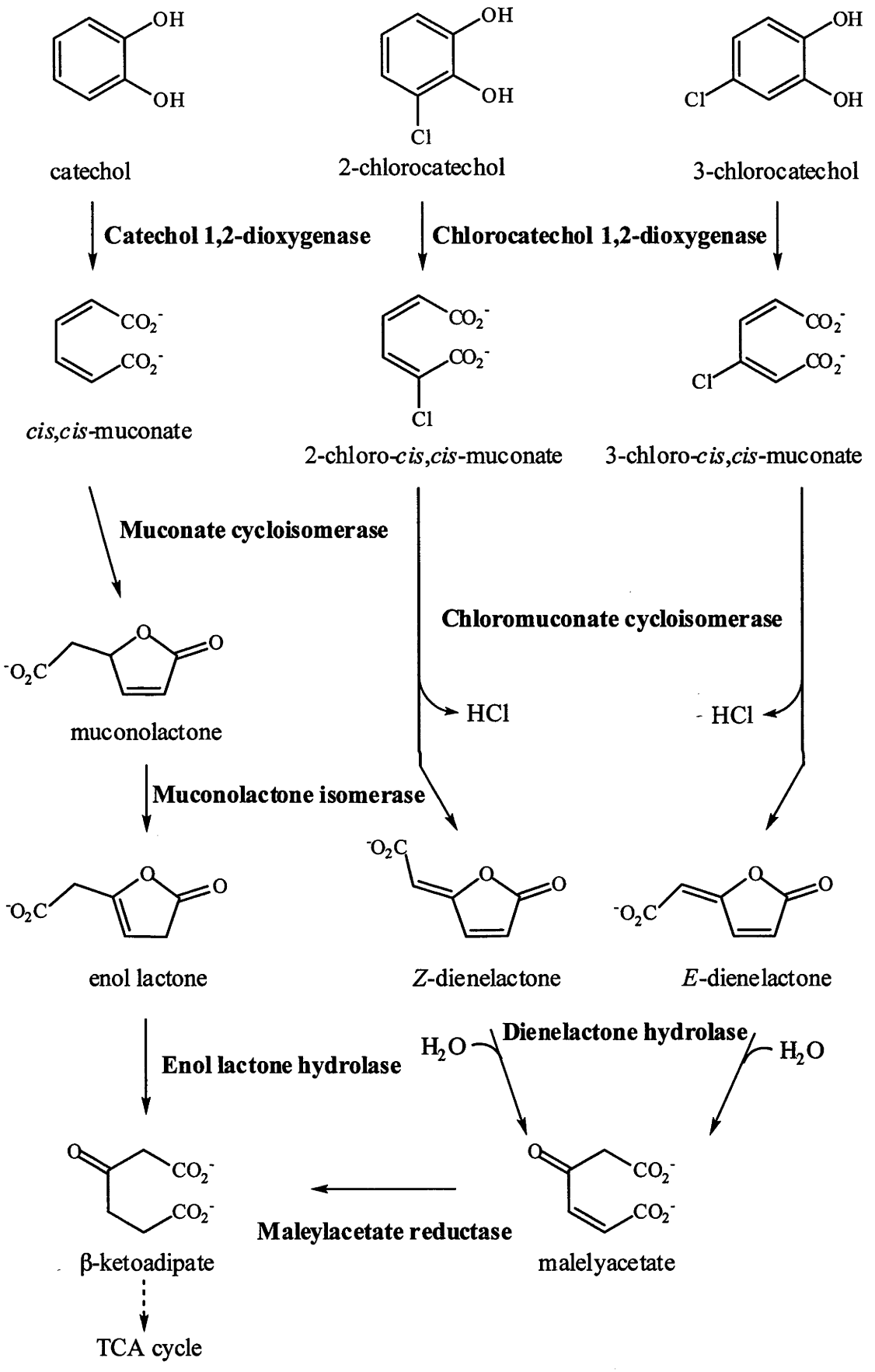

Figure 1. Comparison of the *ortho*-cleavage (left) and modified *ortho*-cleavage pathways. Adapted from Schlömann, 1994.

diene-1,4 dicarboxylate). This product of DLH hydrolysis is in tautomeric equilibrium with maleylacetate (2-oxo buta-1,3-diene-1,4-dicarboxylate). Maleylacetate is further reduced by maleylacetate reductase (EC 1.3.1.32) to β-ketoadipate which on further reduction to succinyl-CoA and acetyl-CoA can enter into the TCA cycle, as occurs in the *ortho*-cleavage pathway.

1.1.3 A comparison of the *ortho*- and modified *ortho*-cleavage pathway enzymes

As shown in Figure 1, the reactions catalysed in the *ortho*- and modified *ortho*-cleavage pathways are quite similar (Schlömann, 1994). However, important differences occur between these pathways, particularly after the cyclisation of the *cis,cis*-muconate and the chloro-*cis,cis*-muconate. The ester product from muconate cycloisomerase activity (muconolactone) is relatively stable. To permit ring cleavage of the lactone, isomerisation of the double bond from the 2- to the 3-position is first needed. The product derived from chloromuconate cycloisomerase (the *E*- or *Z*-dienelactone) does not require isomerisation of the double bond. A double bond at the 3-position of dienelactone is already present from the elimination of the chlorine-substituent during cyclisation. Kinetic analysis shows that the muconolactone produced after the cyclisation of *cis,cis*-muconate is not hydrolysed by DLH. Conversely, dienelactone produced by chloromuconate cycloisomerase is not degraded by the corresponding enzyme (ELH) of the *ortho*-cleavage pathway (Schmidt and Knackmuss, 1980).

The modified *ortho*-cleavage pathway utilises maleylacetate reductase that is not part of the *ortho*-cleavage pathway. This enzyme reduces the maleylacetate formed by DLH to β-ketoadipate, which then joins the *ortho*-cleavage pathway for incorporation into the TCA cycle. The genes that encode the modified *ortho*-cleavage pathway do not contain those genes that encode the remaining two enzymes for β-ketoadipate degradation. Therefore, for the full degradation of the β-ketoadipate generated by the modified *ortho*-cleavage pathway, microorganisms that express this pathway must also express the *ortho*-cleavage pathway.

1.1.4 Genes expressing the modified *ortho*-cleavage pathway of *Pseudomonas* sp.

The genes of the modified *ortho*-cleavage pathway are plasmid encoded. The expression of these genes from *Pseudomonas* sp. B13 (pWR1) is regulated by the *clc*R regulatory gene (Parsek *et al.*, 1994). These genes constitute *clc*A, *clc*B, *clc*D and *clc*E encoding for the proteins chlorocatechol 1,2-dioxygenase, chloromuconate cycloisomerase, dienelactone hydrolase and maleylacetate reductase, respectively. The DLH gene from pAC27 (derived from pAC25) of *Pseudomonas putida* AC866 (Chatterjee and Chakrabarty, 1982), as used in this work, was shown to encode for a DLH that is identical to that of pWR1 (Chatterjee and Chakrabarty, 1983; Frantz *et al.*, 1987). The *clc*D gene of pAC27 encodes for DLH (type III) as a 236 amino acid protein with a molecular weight of approximately 25500 Daltons (Frantz *et al.*, 1987).

1.2 Determination of at least three different DLH types

There are known to be at least three different types of DLH. They vary based on isomer preference (Schlömann, 1994; Schlömann *et al.*, 1990) and are shown in Table 1. Enol lactone hydrolase (ELH) is shown for a comparison of its physical and chemical properties to DLH. Although ELHs are remote in evolutionary terms to DLHs, as determined by sequence analysis, a common ancestry could be determined by three-dimensional structural alignment (Schlömann, 1994). The ability of ELH to be inhibited by *p*-chloromercuribenzoate (a cysteine specific inhibitor) is deceptive since this enzyme has a serine residue as the nucleophile and not a cysteine (Hartnett and Ornston, 1994; Schlömann, 1994).

1.2.1 DLH type I

DLH type I will only hydrolyse the *Z*-isomer of dienelactone. Interestingly, this enzyme type also hydrolyses enol lactone and may therefore be an intermediate in the

Table 1. Comparison of the properties of enol lactone hydrolase with the different types of dienelactone hydrolase. Adapted from Schlömann, 1994.

Enzymes	Substrate Converted			Molecular mass	Inactivation[a]		pH optimum
(Representative strains or encoding plasmids)	enol lactone	*Z*-dienelactone	*E*-dienelactone	(kDa)	*p*-CMB	EDTA	
Enol lactone hydrolase (*eg. P. putida*)	+[b]	-	-	29.1-34.5[c]	+	n.d.	7.5-9.0
DLH type I (*eg. A. eutrophus* 335)	+	+	-	58[d]	+	+	7.5
DLH type II (*eg. B. cepacia* ATCC 17759)	-	-	+	32.4[e]	-	-	5.5
DLH type III (*eg.* pAC27, pJP4)	-	+	+	25.4-25.8[c]	+	-	7.5
DLH from *R. opacus* (*erythropolis)* 1CP	-	-	+	30[f]	+	-	7.8-8.0

[a] Inactivation by *p*-chloromercuribenzoate (*p*-CMB) and ethylenediaminetetraacetic acid (EDTA), respectively.
[b] + = high turnover rate; - = low or zero turnover rate.
[c] Monomeric enzymes with molecular masses predicted from DNA sequences.
[d] Determined by gel filtration.
[e] Determined by SDS-PAGE.
[f] Determined by SDS-PAGE and gel filtration.
n.d. Not determined.

evolution between dienelactone hydrolases and enol lactone hydrolases (Schlömann, 1994). Type I DLHs are Mn^{2+} dependent with a molecular mass that is approximately two fold larger than that of the other DLH types. The pH optimum and reactivity with *p*-chloromercuribenzoate (*p*-CMB) of type I DLH is similar to that of ELH and DLH type III enzymes.

1.2.2 **DLH type II**

Type II DLH will only hydrolyse the *E*-isomer of dienelactone. Binding of this isomer is relatively weak with a K_m value of approximately 600 μM. The catalytic activity of this enzyme is estimated to be 49000 min^{-1} (Schlömann *et al.*, 1993). This DLH type appears to be very different from the other DLH types (and ELH) in its physical and reaction properties such as pH optimum, behaviour with *p*-CMB and amino acid composition (Schlömann *et al.*, 1993). It is suggested that DLH of type II is, at best, distantly related to the other DLH types (Schlömann, 1994; Schlömann *et al.*, 1993). DLH type II enzymes have arisen *via* convergent and not divergent evolution.

1.2.3 **DLH type III**

Dienelactone hydrolases of type III will equally hydrolyse both the *E*- and *Z*-dienelactones. However, there is an approximate 27 fold preference in binding the *Z*-isomer over the *E*-isomer for DLH encoded by *Pseudomonas* sp. B13 (K_m = 15 μM and 400 μM, respectively; Schmidt and Knackmuss, 1980). There is no difference in the rates of hydrolysis of these isomers at 1800 min^{-1} (Ngai *et al.*, 1987). The discrimination in binding these isomers by DLH type III encoded by pJP4 is substantially less (K_m = 110 and 140 μM for the *Z*- and *E*-isomers, respectively; Schlömann, 1994). Titration of DLH type III from *Pseudomonas* sp. B13 with *p*-CMB showed that per mole of enzyme 0.94 sulfhydryl groups reacted (Ngai *et al.*, 1987). This inactivation was completely reversed by dithiothreitol and suggested a cysteine is important for enzymatic activity, possibly positioned in or near the active site. Although the DLH from *Pseudomonas* sp. B13 has two cysteine residues, it is thought that the other cysteine residue is buried, possibly in a hydrophobic region that results in it being inaccessible to *p*-CMB (Ngai *et al.*, 1987). The pH optimum (7.5) was measured using "initial velocities" for substrate hydrolysis between pH 5 to 9 (Ngai *et al.*, 1987).

1.2.4 DLH from *Rhodococcus opacus* 1CP

The DLH from *Rhodococcus opacus* 1CP appears to have evolved independently from those mentioned above (Eulberg *et al.*, 1998). Although this enzyme hydrolyses only the *E*-dienelactone and has a molecular weight of approximately 30 kDa (similar to that of DLH type II), it appears to be more closely related to the DLH type III enzymes (Eulberg *et al.*, 1998; Schlömann, 1984). Protein sequence alignment of DLH from Rhodococcus with DLH type III enzymes indicates that both proteins have the same catalytic triad (Eulberg *et al.*, 1998).

1.3 The X-ray crystallographic structure of DLH type III from *Pseudomonas putida* (pAC27)

1.3.1 The overall structure of DLH

The structure of DLH type III was initially solved by Pathak *et al.* (1988) at 2.8 Å and was later refined to 1.8 Å (Pathak and Ollis, 1990). DLH can be described as an α/β protein with a central β-pleated sheet composed of eight strands that are shielded from the polar exterior by seven helices (Figure 2). Of these strands, seven are parallel and one anti-parallel (strand 2). The structure of DLH is in many ways typical of α/β proteins. The interior sheet is twisted and the strands are connected by right handed crossovers.

1.3.2 The α/β hydrolase fold

As mentioned above, DLH has an α/β hydrolase fold which is common for what appears to be evolutionary remote enzymes (Ollis *et al.*, 1992). The topology and three-dimensional structure of these enzymes align the catalytic triads. These triads comprise a nucleophile (C, S, or D), a histidine and an acid (D or E) although in the primary sequence the order is nucleophile, acid and histidine. The nucleophile appears

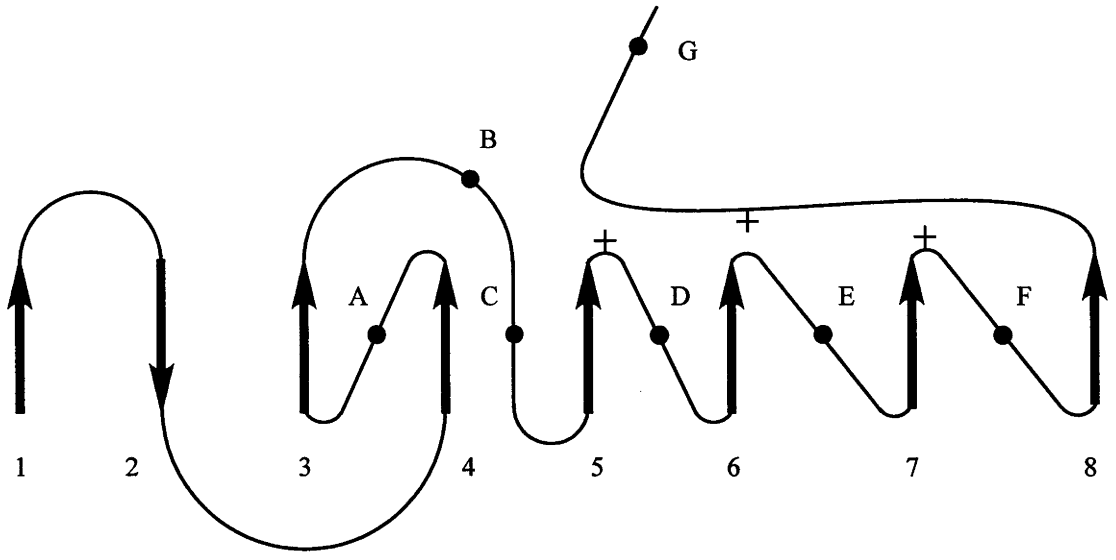

Figure 2. Topology of the hydrolase fold of DLH (Ollis *et al.*, 1992). The β-sheets are represented by arrows (1-8) and the α-helices by circles (A-G). The catalytic triad is represented by +.

at a sharp γ-like turn (the 'nucleophile elbow') with the recurring sequence of Sm-X-Nu-X-Sm-Sm (Sm = small residue, X = any residue, Nu = nucleophile) which is important for the positioning of this nucleophile. The catalytic histidine and acid both appear on loops at the end of strand eight and strand seven, respectively.

1.3.3 **The active site of DLH**

The position of the active site in DLH from pAC27 was established after the examination of its structure and was later confirmed by numerous experiments (Cheah *et al.*, 1993a; Cheah *et al.*, 1993b; Pathak and Ollis, 1990). Like other α/β proteins the active site occurs at the strand switch point of the protein, in this case, after strand 5. The active site contains three hydrogen bonded residues that form the catalytic triad. The catalytic triad of DLH comprises a nucleophilic cysteine (C123), a histidine (H202), and an aspartate (D171) residue (Pathak *et al.*, 1991).

Cysteine 123 lies at the N-terminus of helix C and is the central residue in a γ-like-turn that links strand five and helix C (Pathak and Ollis, 1990; Pathak *et al.*, 1991). This

sharp γ-like-turn appears to have a number of functions. It reverses the direction of the peptide chain so that the nucleophile is readily accessible to the substrate in the active site. The sharp turn also places the nucleophile at the base of helix C where the negatively charged thiolate can be stabilised by the dipole moment of helix C (Hol *et al.*, 1978). This dipole effect is enhanced by the very hydrophobic nature of this helix.

In the crystal structure of DLH, the side-chain of C123 exists either in an active or an inactive conformation. The Sγ is capable of rotating about the Cα-Cβ bond so that it can swing into the active site or away from it (Cheah *et al.*, 1993a; Cheah *et al.*, 1993b; Pathak *et al.*, 1991). In the active conformer the C123 thiol lies 3.41 Å from Nε2 of H202, coplanar with the imidazole ring. It is centred at the base of helix C, perfectly positioned to take full advantage of the helix C dipole. In the inactive conformer the C123 thiol is swung towards the interior of the enzyme away from the active site and is placed 3.47 Å from Oε2 of E36, a residue which lies very close to but not actually within the active site cleft. In the X-ray crystal structure of the active site of DLH, C123 is partially oxidised to the sulfinic acid which locks it into the 'activated state'. The catalytic cysteines of papain and actinidin are similarly afflicted with the problem of oxidation which may be promoted by the proximity of the sulfur to the oxyanion hole (Warshel, 1978). Oxyanion holes function to stabilise the oxyanion in the tetrahedral intermediate that is formed after the attack of the nucleophile on the substrate. Previous studies have suggested that prior to oxidation, the side chain of C123 in DLH exists in equilibrium between the above two conformers (Cheah *et al.*, 1993b). In the absence of substrate, the equilibrium lies toward the inactive or resting state of the enzyme and a scheme has been proposed for the activation of the enzyme by substrate. The switch between the conformations is thought to occur after the substrate binds into the active site which then activates this conformational change. This activation will be described in detail later.

The other triad residues of DLH are found on loops that emerge from strands seven and eight. H202 lies on a loop between strand eight and helix G. This loop comprises three

consecutive type I β turns and is the longest stretch of peptide in DLH without any secondary structure (Pathak *et al.*, 1988; Pathak and Ollis, 1990). The Nε2 of H202 faces the nucleophile with Nδ1 facing the triad acid. The Nε2 is 3.43 Å from the oxidised Sγ of C123 with the Nδ1 2.62 Å from Oδ1 of D171 (Pathak and Ollis, 1990). Aspartate 171 also lies on a reverse turn but unlike the other two catalytic residues, it lies away from the active site cleft. The Oδ2 of D171 is distal to the histidine and is hydrogen bonded to the backbone amide of F173.

1.4 The catalytic mechanism of DLH type III (pAC27)

1.4.1 The active site and inhibitor binding

Inhibitor binding studies with the *Z*-dienelactam (Cheah *et al.*, 1993a; Cheah *et al.*, 1993b) have established the location of the active site with an inhibitor that is iso-structural with the substrate (Figure 3). These studies were done with the wt enzyme and with the active site mutant C123S. Problems associated with oxidation of the cysteine nucleophile necessitated the use of the C123S mutant to obtain a clearer understanding of the enzyme/inhibitor contacts in the bound complex.

The C123 nucleophile is in a hydrophobic region of the active site cleft, with R81 and R206 toward the hydrophilic entrance of this cleft. The side regions of the active site are formed by helix B and the loop between strand eight and helix G. On helix B are found R81 and Y85 while on the loop between strand eight and helix G there is S203, R206, and S208. Deeper in the active site cleft the walls are formed by part of the loop between strand three and helix A and the loop between strand six and helix D. E36 forms the rear of this recess - the region furthest from the aqueous exterior.

When the inhibitor is bound in the active site, the acyl carbon is in close proximity to the cysteine nucleophile (C123) in the active conformation. The carbonyl oxygen is positioned close to the oxyanion hole that comprises the backbone amides of I37 and

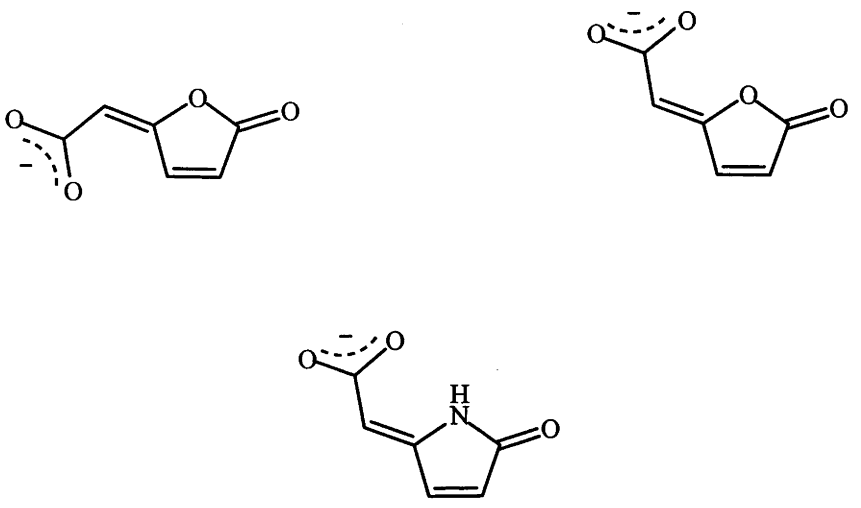

Figure 3. The substrates *E*- and *Z*-dienelactone and the inhibitor *Z*-dienelactam.

L124. The inhibitor ring hydrogens are in close contact with W88 while the amide of the inhibitor ring faces the exterior of the enzyme (Cheah *et al.*, 1993b). The dienelactam carboxylate is positioned towards the entrance of the active site and forms ion-pairs with R206 and R81. An additional hydrogen bond is proposed to occur between the side chain of S203 and the inhibitor carboxylate.

1.4.2 **Substrate induced activation and the catalytic mechanism**

Based on the differences observed in the active site of DLH between the free and inhibitor bound crystal structures, a mechanism was proposed for the hydrolysis of the *Z*-dienelactone. In the absence of substrate, two ion-pairs are thought to be important in the active site (Figure 4). One ion-pair is formed between R206 and E36. As mentioned above, E36 also forms a hydrogen bond to the C123 thiol (the inactive conformer). The second ion-pair is formed between H202 and D171. It is proposed that when the substrate binds its carboxylate group makes a close approach to R206 and forms a new ion-pair with this residue (Figure 5). The presence of the substrate causes the R206-E36 ion-pair to weaken resulting in the carboxylate of E36 shifting away from R206 and towards the C123 thiol. The E36 carboxylate becomes a much stronger base in the hydrophobic environment and abstracts the proton from the thiol of C123. The

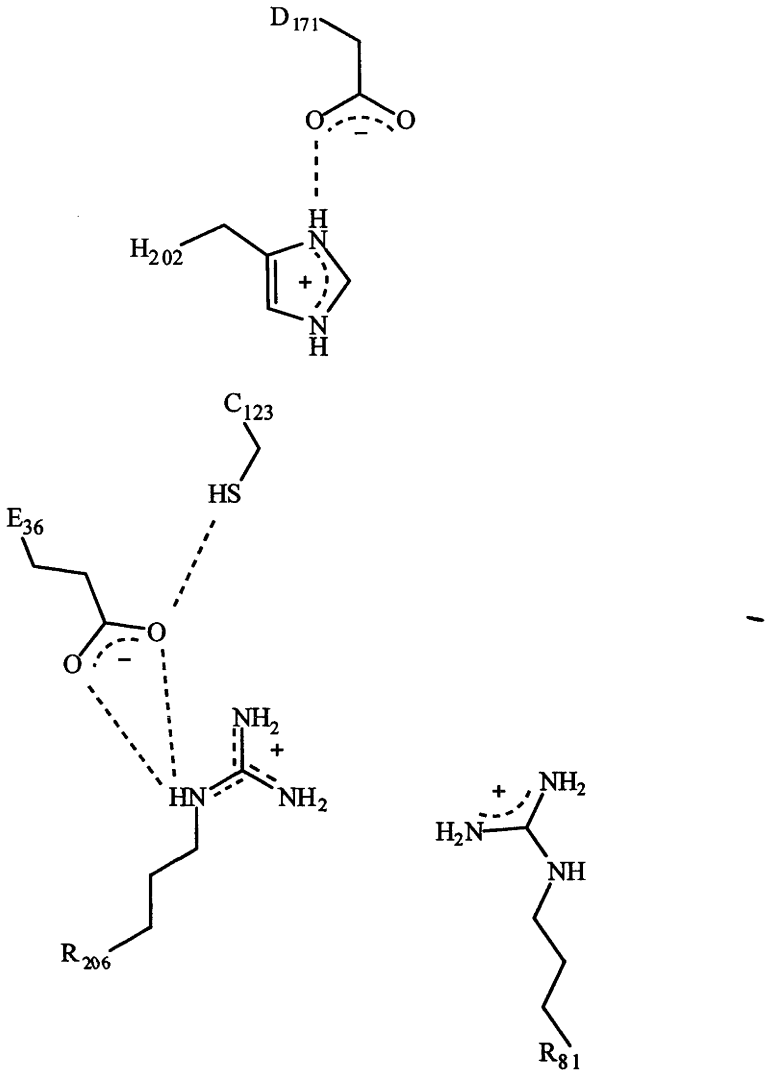

Figure 4. The active site of DLH in the absence of substrate.

thiolate now shifts into the active conformer where it can be electrostatically stabilised by the imidazolium of H202 and the dipole moment of helix C. In this active conformation, the thiolate of C123 is adjacent to the substrate. This sequence of events is also supported by theoretical studies (Beveridge and Ollis, 1995).

The activated nucleophile then attacks the acyl carbon of dienelactone forming the first tetrahedral intermediate. The oxyanion is stabilised in the oxyanion hole by interactions with I37 and L124, as mentioned above. The tetrahedral intermediate then collapses, cleaving the ring and expelling the heterocyclic oxygen to give the reasonably stable

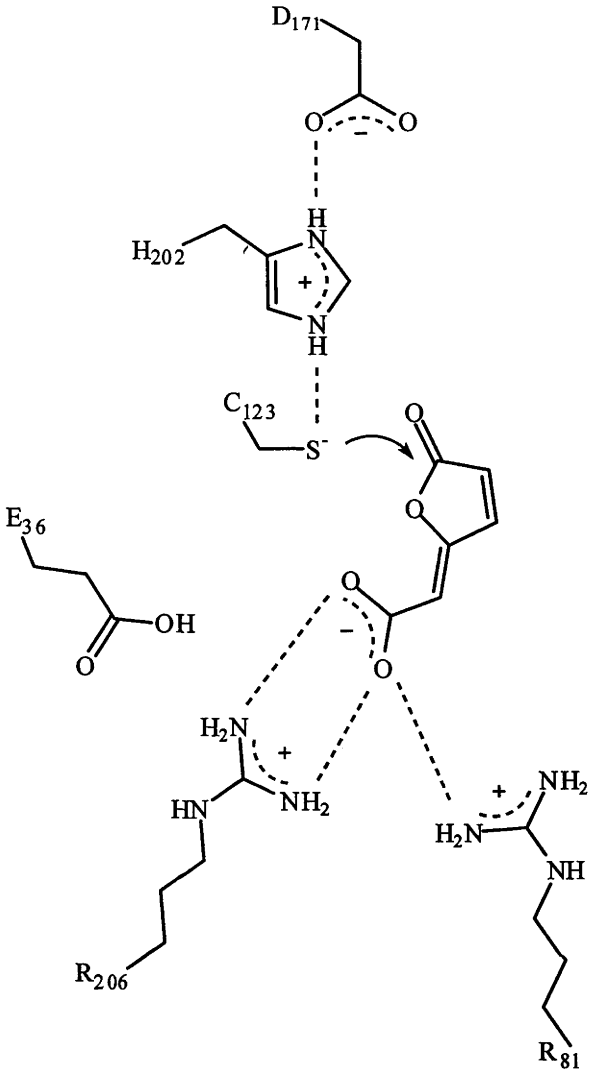

Figure 5. The active site of DLH in the presence of substrate.

enolate intermediate. The enolate can then act as a general base in the breakdown of the covalent intermediate by abstracting a proton from water. The resulting hydroxide then attacks the acyl enzyme forming the second tetrahedral intermediate that subsequently collapses to release the product and the free enzyme.

1.4.3 **Mechanistic comparisons with the serine and cysteine proteases**

The catalytic mechanism of DLH (Cheah *et al.*, 1993a; Pathak *et al.*, 1991) was initially proposed based on similarities to those of the serine and cysteine proteases in regard to

the triad histidine's role as a general acid/base catalyst. However, there are significant differences between the mechanisms.

In the serine proteases, it is generally accepted that the imidazole of the triad histidine acts as a general base and abstracts a proton from the serine hydroxyl which then attacks the polarised acyl carbon forming the first tetrahedral intermediate. The former carbonyl oxygen is now an oxyanion and is stabilised in the oxyanion hole (Henderson, 1970). The tetrahedral intermediate is protonated at the substrate nitrogen by the triad imidazolium ion before the first proteolytic product (RNH_2) is released (Fastrez and Fersht, 1973). The tetrahedral intermediate does not accumulate and quickly collapses to form the acyl enzyme (acylation). The second proteolytic product is released from the enzyme by the process of deacylation. The imidazole abstracts a proton from a nearby water molecule with the resulting hydroxyl group attacking the acyl carbon. The second proteolytic product (RCO_2^-) is released with regeneration of the serine hydroxyl.

Like the serine proteases, cysteine proteases such as papain (and actinidin) go through a tetrahedral and an acyl enzyme intermediate. In contrast to serine proteases, the cysteine proteases such as papain are 'activated' enzymes (Lewis *et al.*, 1981; Migliorini and Creighton, 1986; Polgár, 1974; Polgár and Asbóth, 1986). That is, the active site cysteine occurs as an ion-pair with the triad histidine ($ImH^+\cdots S^-$) in the resting state. In both papain and actinidin, the thiolate is further stabilised by a helix dipole (Baker, 1980; Hol *et al.*, 1978; Kamphuis *et al.*, 1984). The imidazole ring is oriented with the Nδ1 facing the nucleophile (Kamphuis *et al.*, 1984); this differs from trypsin and DLH where Nε2 faces the nucleophile.

With the peptide substrate in the active site, the acyl carbon is polarised by the interaction of the carbonyl oxygen with the proposed oxyanion hole (Drenth *et al.*, 1976). This polarisation facilitates the attack of the thiolate nucleophile on the acyl carbon of the substrate. Protonation of the leaving group nitrogen by the imidazolium ion is proposed to occur prior to or in concert with nucleophilic attack (Arad *et al.*,

1990; Howard and Kollman, 1988). For protonation to occur, it is suggested that the imidazolium ring rotates approximately 30° about the Cβ-Cγ bond from the position it holds in the resting state into the plane of the leaving group (Drenth *et al.*, 1976). The former acyl carbon assumes a tetrahedral configuration with the carbonyl oxygen now as the oxyanion stabilised in the oxyanion hole (Drenth *et al.*, 1976; van Duijnen *et al.*, 1979; Ménard *et al.*, 1991; Rullmann *et al.*, 1989). A protein helix dipole is also proposed to contribute to the stabilisation of the oxyanion in the tetrahedral intermediate (van Duijnen *et al.*, 1979; Rullmann *et al.*, 1989). As both the resting state and the intermediate are in a zwitterionic form, they do not have to be stabilised by a counter charge from the third triad member; papain and actinidin have an asparagine (Baker, 1980) instead of the aspartate of serine proteases and that of DLH. The collapse of the tetrahedral intermediate and release of the first proteolytic product (RNH_2) forms the acyl enzyme. The triad imidazole abstracts a proton from a nearby water molecule with the resulting hydroxyl group attacking the acyl carbon to form the second tetrahedral intermediate. The collapse of this tetrahedral intermediate releases the second product (RCO_2^-) from the hydrolysis of the peptide substrate and regenerates the resting state of the enzyme.

The role that the triad histidine has in protonating the leaving group and in deacylation in the serine and cysteine proteases differs significantly from that for DLH. Modelling studies of DLH that assumed a role for the triad histidine in deacylation were futile (Cheah *et al.*, 1993a). Steric constraints limit the ability of the imidazolium ion to participate in the protonation of the leaving enolate group prior to or after the collapse of the first tetrahedral intermediate and then in the deprotonation of a nearby water molecule for its attack on the acyl carbon. In this sense a new mechanism has been proposed, as discussed above, that accounts for the distinct differences in the catalytic mechanism of DLH as opposed to those of the serine and cysteine proteases. These differences may explain why DLH does not hydrolyse the amide analogues of dienelactone (Cheah *et al.*, 1993a). The highly unstable nature of the enamine anion would require it to be protonated prior to its release from the first tetrahedral

intermediate.

1.4.4 Limitations to our understanding of the proposed mechanism of catalysis by DLH

This understanding of the activation and catalytic mechanism of DLH is based mainly on structural studies with some preliminary kinetic analysis. The native structure gave clear indications of the active site location and it also showed that the potential nucleophile was pointed away from the active site and hence required activation before catalysis could occur. Inferences about this activation process were provided by crystal structures with the *Z*-dienelactam bound. The idea that the resting state of the enzyme is 'inactive' is supported by the resistance of C123 to chemical modification (Cheah *et al.*, 1993b). However, direct structural evidence for the details of the mechanism of hydrolysis of the *E*-dienelactone was not available. It should also be noted that the limited kinetic data supporting the proposed mechanism had been obtained only with the *E*-dienelactone.

1.5 Thesis proposal

On the basis of the limitations stated above, further kinetic evidence was needed to investigate the proposed catalytic mechanism of DLH. It was anticipated that this evidence would be provided by kinetically characterising DLH using both isomers of dienelactone and by site-directed mutagenesis of DLH. It was to be expected that these kinetic studies would help clarify the catalytic mechanism of DLH by indicating the residues that are important for substrate binding and for reaction of the substrate once bound.

Chapter 2

Materials and Methods

2.1 Materials

2.1.1 Chemicals

Solutions were made with Milli-Q® ultra pure reverse osmosis water (Millipore®, USA). All reagents used were of analytical grade. Univar® hydrochloric acid, anhydrous acetic acid, benzene, absolute ethanol, hexane, petroleum spirit (40-60 °C), sodium hydroxide pellets, and anhydrous diethyl ether were obtained from Ajax Chemicals, Australia. AnalaR grade dried magnesium sulfate, ethyl acetate, methanol, dichloromethane, acetone, sodium chloride, EDTA (ethylenediaminetetraacetic acid) and SDS (sodium dodecyl sulfate) were from BDH Chemicals Ltd, England. TFA (trifluoroacetic acid), *tert*-butyl chloroacetate, triphenylphosphine, maleic anhydride, tetramethylammonium hydroxide and ammonium sulfate were obtained from Aldrich®. Acetonitrile was HPLC Grade from EM Science. Chloroform-d, acetone-d_6, and methanol-d_4 were from Cambridge Isotope Laboratories, USA. HEPES (*N*-[2-hydroxyethyl]piperazine-*N*'-[2-ethanesulfonic acid]), MES (2-[*N*-morpholino]ethanesulfonic acid), TEMED (*N,N,N,N*-tetramethylethylenediamine), light white mineral oil, ethanolamine, *p*-toluenesulfonic acid, *p*-nitrophenylacetanilide, *p*-nitrophenyl acetate, ethidium bromide (*L*-arginine-2,7-diamino-10-ethyl-9-phenyl phenanthridium bromide), Trizma® hydrochloride (tris[hydroxymethyl]amino methane hydrochloride), Bicine (*N,N*-bis[2-hydroxyethyl]glycine), glycerol, potassium phosphate and guanidine (aminomethanamidine) hydrochloride were from Sigma®. Agarose (standard low-m_r) and ammonium persulfate were supplied by Bio-Rad Laboratories, USA. Bacto® yeast extract, Bacto® tryptone and Bacto® agar were purchased from Difco Laboratories, USA. Premixed acrylamide/bisacrylamide solution (37.5:1), ampicillin, the DNA

Molecular Marker X and 'protease free' bovine serum albumin were purchased from Roche Molecular Biochemicals, Germany. Coomassie brilliant blue and β-mercaptoethanol were obtained from Progen Industries (Australia) and Riedel-de Haën (Germany), respectively. Sodium citrate dihydrate was obtained from Mallinckrodt® Inc, USA. 3-Acetylacrylic acid was from Lancaster Synthesis Ltd, England.

2.1.2 **Enzymes**

The DNA restriction endonuclease enzymes Mlu1, Ksp1, Nde1, Stu1, and EcoR1, were purchased from Roche at a concentration of 10 units/μl as were the dNTPs (2.5 mM of each) and T4 Ligase (1 unit/μl) with the T4 Ligase buffer. SuRE/Cut® restriction endonuclease buffers B, H, and L, alkaline phosphatase (from calf intestine, 1 unit/μl) and alkaline phosphatase 10x reaction buffer were purchased from Roche. Vent™ DNA polymerase (2000 units/ml), the 10x ThermoPol® PCR reaction buffer and DNA/nuclease free $MgSO_4$ (100 mM solution) were obtained from New England Biolabs® Inc (USA). The restriction endonuclease Dpn1 (10 units/μl), Pfu DNA polymerase (2.5 units/μl) and the 10x Pfu polymerase reaction buffer were purchased from Stratagene® (USA).

2.1.3 **The plasmid, bacterial strain, and the deoxyribo-oligonucleotides**

The plasmid vector pND704 (Love *et al.*, 1996) and *Escherichia coli* AN1459 were supplied by Dr Nick Dixon from The Centre for Molecular Structure and Function, Research School of Chemistry, ANU (Canberra, ACT). The desalted oligonucleotides for the introduction of the site-directed mutations of DLH were purchased from Bresatec Pty Ltd (Australia), or GeneWorks (Australia). Primer 9 and the universal primer m13/pUC were obtained through Bresatec Pty Ltd (Australia) and Roche, respectively.

Sequencing was performed using the ABI PRISM™ Dye Terminator Cycle Sequencing

Ready Reaction Kit at the Biomolecular Resource Facility in the Centre for Molecular Structure and Function, ANU (ACT).

2.1.4 The *clc*D gene encoding DLH

The gene encoding DLH was previously cloned into *E. coli* from *Pseudomonas putida* (Frantz and Chakrabarty, 1987). This sequence contained some of the gene that encoded for the *clc*E protein (maleylacetate reductase, E.C. 1.3.1.32). The expression of DLH commonly suffered from read-through into the clcE gene (Robinson, 1999) which was eliminated by insertion of two strong stop codons (Jefferies, 1998). The gene encoding *clc*D only was cloned into the pND704 plasmid, which comprises a heat-inducible over-expression system, and transformed into the *E. coli* strain AN1459 (Jefferies, 1998).

2.2 Methods

2.2.1 General

Melting points were determined on a Kofler hot-stage melting point apparatus under a Reichert microscope and are uncorrected.

Analytical thin layer chromatography was performed using Merck Kieselgel 60 F_{254} silica on aluminium backing plates with visualisation either under a UV lamp (254 nm) or by potassium permanganate dip. Preparative chromatography was performed using positive pressure flash chromatography using Merck Kieselgel 60 (230-400 mesh ASTM).

Anhydrous diethyl ether was obtained by distillation from sodium benzophenone ketyl. Drying and purification of other solvents and reagents was performed using standard laboratory procedures (Armarego and Perrin, 1996).

Nuclear magnetic resonance spectra were recorded on a Varian Gemini 300 spectrometer. Proton nuclear magnetic resonance (^{1}H NMR) spectra were recorded at 300 MHz and carbon nuclear magnetic resonance (^{13}C NMR) spectra were recorded at 75.5 MHz. Chemical shifts from the NMR spectra are quoted as δ in parts per million. The chemical shifts were either referenced to the residual non-deuterated solvent (^{1}H/^{13}C: D_2O δ 4.70, CD_3OD δ 3.31/49.0, CD_3COCD_3 δ 2.17, $CDCl_3$ δ 7.25) or to the internal standard tetramethylsilane (TMS; 0.00 ppm). Multiplicities are abbreviated to: s, singlet; d, doublet; m, multiplet; br, broad.

Low and high resolution electron impact (EI) mass spectra were performed by technical staff using a VG Autospec double-focussing trisector mass specrometer operating at 70 eV. Electrospray ionisation (ESI) mass spectra were performed by technical staff using a Fisons VG Quatro II triple quadrupole mass spectrometer controlled by MassLynx software at 120 eV. Mass spectral data are listed as mass-to-mass charge ratio (intensity relative to the base peak).

2.2.2 **Substrate synthesis**

The synthesis of both the *E*- and *Z*-dienelactones was essentially that of Massy-Westropp and Price (1980), with some modifications (Figure 6).

2.2.2.1 *exo-3,6-Epoxy-1,2,3,6-tetrahydrophthalic anhydride* (1)

To 98 g (1 mol) of maleic anhydride in 1.2 L of dry diethyl ether under a nitrogen atmosphere was added furan (68 ml, 1 mol) dropwise with stirring at 35 °C over approximately 1 hour. After the furan was added the solution was stirred at this temperature for a further 10 minutes, cooled to room temperature then stirred overnight. The solution stood at room temperature for a further 3 days after which time the white precipitate was filtered, dried, and then recrystallised from ethanol. Yield 71.8 g (1), 43%; ^{1}H NMR ($CDCl_3$, 0.1% TMS) δ = 6.58 (s, 2H), 5.49 (s, 2H), 3.18 (s, 2H); mp

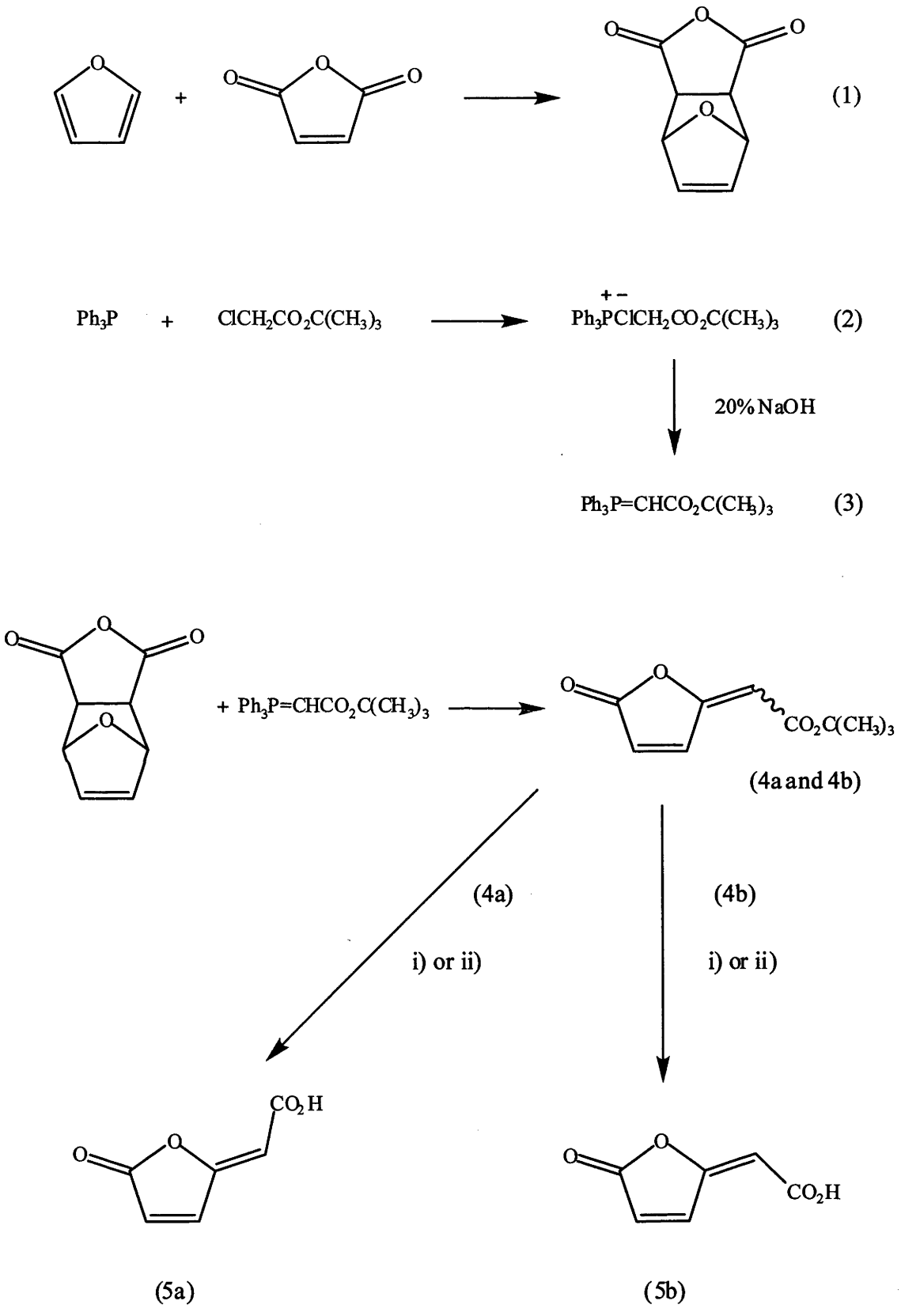

Figure 6. Synthetic pathway for the production of the *E*- and *Z*-dienelactones (Massy-Westropp and Price, 1980).

124 °C, (Massy-Westropp and Price, 1980; 125 °C).

2.2.2.2 *tert-Butoxycarbonylmethylenetriphenylphosphorane* (3)

Triphenylphosphine (75 g, 0.286 mol) was added to 30.2 ml of *tert*-butyl chloroacetate (31.8 g, 0.211 mol) in dry benzene (150 ml) under a nitrogen atmosphere and the mixture was heated at reflux for 6 hours. The solution was cooled to room temperature and the white precipitate of the chloride salt that formed was filtered and washed (2 x 50 ml) with cold diethyl ether and dried. Yield 65 g (2), 55%; ^{1}H NMR ($CDCl_3$, 0.1% TMS) δ = 7.50 (m, 15H, Ph_3), 5.60 (d, $J_{P,CH}$ = 14.1 Hz, 2H), 1.26 (s, 9H, ^{t}Bu); mp 217 °C, (Massy-Westropp and Price, 1980; 219-221 °C).

The chloride salt (59 g, 0.143 mol) was dissolved in Milli Q water then the temperature was reduced to 4 °C. With vigorous stirring 20% NaOH was added with the formation of a white precipitate. The precipitate was filtered and washed with water. The solution had more NaOH added until no further precipitate formed. Yield 49 g (3), 94%; ^{1}H NMR ($CDCl_3$, 0.1% TMS) δ = 7.51 (m, 15H, Ph_3), 2.65 (br, =CH), 1.20 (s, 9H, ^{t}Bu); mp 149-152 °C, (Massy-Westropp and Price, 1980; 152-153 °C).

2.2.2.3 *E- and Z-dienelactone tert-butyl esters* (4a and 4b)

The phosphorane (3) (15.0 g, 0.0412 mol) was added to a solution of (1) (6.84 g, 0.0412 mol) in dry benzene (450 ml) under a nitrogen atmosphere and the mixture was heated at reflux for 6 hours. The solution was cooled to room temperature and the resulting dark solution was applied to a short (5 cm x 3 cm) silica column (silica gel 60, Merck) then the column was washed (3 x 50 ml) with cold diethyl ether. The resulting yellow solution was evaporated under reduced pressure without heating. The residue was resuspended in diethyl ether (100 ml) and the solution was filtered to remove triphenylphosphine oxide. The *tert*-butyl esters were separated on silica *via* flash chromatography (20 cm x 2.5 cm) with 1:1 diethyl ether/petroleum spirit (40-60°C).

The *E*-dienelactone *tert*-butyl ester (4b) (R_F 0.73, 4.6 g, 57%) after recrystallisation from petroleum spirit (40-60°C); ^{1}H NMR ($CDCl_3$, 0.1% TMS) δ = 8.36 (d, J = 5.6 Hz, C2-H), 6.43 (d, J = 5.5 Hz, C3-H), 5.86 (s, C5-H), 1.52 (s, 9H, ^{t}Bu); mp 106 °C, (Massy-Westropp and Price, 1980; 107-109 °C). The *Z*-dienelactone *tert*-butyl ester (4a) (R_F 0.30, 0.162 g, 2%) after recrystallisation from petroleum spirit (40-60°C); ^{1}H NMR ($CDCl_3$, 0.1% TMS) δ = 7.40 (d, J = 5.5 Hz, C2-H), 6.42 (d, J = 5.5 Hz, C3-H), 5.4 (s, C5-H), 1.53 (s, 9H, ^{t}Bu); mp 155 °C, (Massy-Westropp and Price, 1980; 156 °C).

2.2.2.4 *E- and Z-dienelactones* (5a and 5b)

The final acids were prepared in two ways. The first (i) involved reaction of the *tert*-butyl esters (4a and 4b) with *p*-toluenesulfonic acid and the second deprotection (ii) was *via* reaction with TFA. The reactions of both isomers by either method yielded similar results.

i).

To 0.40 g (0.0020 mol) of (4b) dissolved in dry benzene (50 ml) was added 0.20 g (0.001 mol) *p*-toluenesulfonic acid under a nitrogen atmosphere and the solution was heated at reflux for 6 hours. The solvent was evaporated under reduced pressure and the residue washed (2 x 40 ml) with cold diethyl ether. The precipitate was then dissolved in ethyl acetate and left at room temperature until the product precipitated from solution as white crystals. Yield 0.151 g (5b), 53%; ^{1}H NMR (CD_3COCD_3) δ = 8.42 (d, J = 5.5 Hz, C2-H), 6.69 (d, J = 5.5 Hz, C3-H), 5.96 (s, C5-H); mp 165-166 °C, (Massy-Westropp and Price, 1980; 164-165 °C).

ii).

To 0.47 g (0.0024 mol) of (4a) was added 20 ml of dry dichloromethane. TFA (5 ml, 0.065 mol) was added dropwise with vigorous stirring and the resulting solution was

stirred at room temperature for 4 hours. The solvent was removed under a stream of nitrogen and the precipitate recrystallised from ethyl acetate. Yield 0.144 g (5a), 43%; ^{1}H NMR (CD_3COCD_3) δ = 7.87 (d, J = 5.5 Hz, C2-H), 6.64 (d, J = 5.5 Hz, C3-H), 5.68 (s, C5-H); mp 243 °C, (Massy-Westropp and Price, 1980; 244 °C).

2.2.3 **Cell culture**

Cells were taken from a freezer stock (-70 °C) in DMSO (7%) and grown overnight at 30 °C on LBTA (Luria-Bertani broth supplemented with 0.4 mM thymine and 50 μg/ml ampicillin) plates (with 1.5% agar). Colonies were then transferred to a starter culture in the above LBTA media (pH 7.6) and grown overnight at 30 °C in a orbital shaking water bath (model OW1412, Paton Scientific, Pty Ltd.). The culture was then added to 1 litre of LBTA in baffled flasks (1:100 dilution) and grown to an OD_{595} of 0.5-0.6. The culture temperatures were then rapidly elevated to 42 °C (over approximately 1 minute) with stirring in a 75 °C water bath and then grown, as above, at 42 °C for 2 hours to allow the protein to overexpress. The cells were collected by centrifugation (Sorvall) at 11000 g for 25 minutes at 4 °C.

2.2.4 **Purification of DLH**

The purification of DLH was carried out according to a modification of the method of Pathak *et al.* (1988) and Cheah *et al.* (1993b).

All steps for the purification were performed at 4 °C and the pH of the buffer solutions was corrected for this temperature. The cell pellet was resuspended in buffer A (20 mM HEPES, 1 mM EDTA, 1 mM β-ME, adjusted to pH 7.0) and the solution was passed once through a French® press (SLM Aminco, SLM Instruments, Inc.). The lysed cells were centrifuged at 39000 g for 45 minutes to remove cell debri and the lysate applied to an anion exchange Fractogel® (Merck) EMD DEAE - 650 (M) column (80 ml) previously equilibrated with buffer A. The column was washed with one column

Table 2. Salt gradient used for the purification of wt and mutant DLH with the DEAE Fractogel column (80 ml).

Time (minutes)	% Buffer B[#]
0	0
80	0
190	5
470	11
550	20
551	100
631	100
632	0
712	0

[#] 0% buffer B corresponds to 0 mM NaCl and 100% buffer B to that of 1 M NaCl.

volume of buffer A to remove unbound proteins. The column was then eluted with a non-linear of buffer B (buffer A containing 1 M NaCl; Table 2). DLH eluted between 90 mM and 100 mM NaCl (by comparison to a DLH standard, Cheah *et al.*, 1993b) as determined by gel electrophoresis (15% acrylamide, 0.1% SDS and stained with coomassie brilliant blue). The fractions containing DLH were pooled and then applied to a 200 ml size exclusion column (Sephadex® G 75 superfine, Pharmacia Biotech) equilibrated in buffer A. DLH was then determined to be approximately >98% pure by gel electrophoresis, as described above. The fractions containing the pure protein were dialysed overnight in a 12000-14000 Dalton cutoff semi-permeable membrane (Spectra/Por) against 2 litres of 20 mM HEPES buffer containing 1 mM EDTA, at pH 7.0 to remove β-ME. The dialysis was repeated for a further 2 hours in fresh buffer. The protein was concentrated in Centriplus concentrators (Amicon) with a 10000 Dalton cutoff to approximately 7 mg/ml and stored at -70 °C. Protein concentrations of the pure enzyme were determined by measuring absorbance at 280 nm in 6 M guanidium hydrochloride and 20 mM phosphate buffer, at pH 6.5, with an extinction coefficient (ε)

of 32670 M^{-1} cm^{-1} based on the protein sequence for the wt enzyme (Gill and von Hippel, 1989).

2.2.5 **Enzyme assays**

2.2.5.1 *Activity measurements during purification*

The *E*-dienelactone was dissolved in an equimolar concentration of sodium hydroxide. Determination of enzyme activity during DLH purification was measured in 20 mM HEPES buffer containing 1 mM EDTA, at pH 7.0 and 25.0 ± 0.1 °C. The enzyme/buffer solution was equilibrated for 5 minutes in at this temperature then 'zeroed' before the substrate was added. Accurate substrate concentrations were determined from the absorbance (ε 17000 M^{-1} cm^{-1}) of the reaction solutions at the beginning of the reaction. The rate of reaction was determined from the data collected over a two minute period where approximately 5-10% of the substrate was consumed. The measurements were made in triplicate in a final volume of 1 ml in quartz cuvettes (Starna Pty Ltd, Australia) using 50 μM of the *E*-dienelactone in a Shimadzu (UV-2101PC) UV/Vis spectrophotometer using the UV-2101PC Kinetics software. Activity was expressed as specific activity (per mg of protein) after hydrolysing 1 μM of the substrate. Total protein concentrations were determined *via* the method reported by Stevens (1992), where absorbance due to nucleic acids (A_{260}) in the preparation was subtracted from the total protein concentration (Equation 1).

$$[\text{protein}]\ (\text{mg/ml})^{1\%} = 1.55(A_{280}) - 0.76(A_{260}) \qquad (1)$$

2.2.5.2 *Determination of the kinetic constants for purified DLH*

The apparent kinetic constants for wt DLH using the *E*- and *Z*-dienelactones were collected in 20 mM HEPES buffer containing 1 mM EDTA, at pH 7.0 and 25 ± 0.1 °C with the addition of "protease free" BSA (Sigma). Linearity of the response of different

Table 3. The extinction coefficients (ε) for the *E*- and *Z*-dienelactones.

Wavelength (nm)	*E*-dienelactone (ε; M^{-1} cm^{-1})	*Z*-dienelactone (ε; M^{-1} cm^{-1})
280[#]	17000	15625
300	9391	7089
310	4466	2263
316	2336	889
320	1445	487
325	807	325

[#] The extinction coefficient at 280 nm are previously quoted values (Schmidt and Knackmuss, 1980; Schlömann, *et al.*, 1990) and were used as the reference for determining the extinction coefficients (M^{-1} cm^{-1}) for the other wavelengths.

enzyme concentrations at one substrate concentration was checked. The extinction coefficients for both isomers of dienelactone that were used are presented in Table 3. The data that was collected over a wide substrate concentration range (using one enzyme concentration) were fit to the Michaelis-Menten equation *via* non-linear regression (Equation 2) to obtain the apparent kinetic constants V_{max} and K_m using the KaleidaGraph® (Version 3.0.1) graphics package. The curve fits in this package are based on the Levenberg-Marquart algorithm. The linearity of the data was checked by transformation of the Michaelis-Menten equation to generate s/*v* against s plots (Hanes plots, Equation 3). k_{cat} was estimated by dividing V_{max} by the spectrophotometerically determined enzyme concentration, as described above.

$$v = \frac{V_{max} \times s}{K_m + s} \qquad (2)$$

$$\frac{s}{v} = \frac{K_m + s}{V_{max}} \qquad (3)$$

2.2.6 **DLH mutants and their purification**

Site-directed mutagenesis of DLH was achieved using two methods. The first PCR based (polymer chain reaction) method (Method i) of mutagenesis involved the amplification of a single oligonucleotide (reverse complement) that contained the mutated amino acid of interest. However, this method proved slow in generating the desired mutations of interest so a second method of site-directed mutagenesis was sort. This method (Method ii) was based on that developed by Papworth *et al.* (1996) for the amplification of the whole plasmid using two complementary primers that incorporate the desired mutation. Oligonucleotides (oligos) used for mutagenesis *via* both methods are shown in Table 4.

2.2.6.1 *Method i) Generation of the E36D, E36Q, R81K and R206A mutants*

To determine the optimal conditions for amplification of the desired mutation, a plasmid and $MgSO_4$ concentration screen was conducted, as described by Jefferies (1998). Briefly, the plasmid template (10 ng and 100 ng) and $MgSO_4$ (0, 1, 2, 3, and 7 mM) concentrations were altered to ensure maximal amplification of the mutant oligos while minimising the amplification of non-specific DNA. The optimal conditions found for the generation of the above mutants were by using a plasmid template (pND704 containing wt DLH) concentration of 100 ng and a $MgSO_4$ concentration of 1 mM. The mutant oligos were added to the above concentrations of template and $MgSO_4$ with 0.25 mM dNTP, 18 ng of primer 9 (a primer that binds specifically upstream from the polylinker region of pND704 that is upstream of the 5' region of the start of the *clc*D gene) in ThermoPol® buffer in a total volume of 50 µL. Vent® DNA polymerase was added to a final concentration of 20 units and the reaction mix covered with 2 drops of light white mineral oil and the PCR performed in a Corbett Research FTS-1C Fast Thermal Sequencer (Corbett Research, Australia) using the cycling temperature protocol illustrated in Table 5. The annealing temperature was adjusted for the relevant oligonucleotide.

Table 4. Oligonucleotides used for the site-directed mutagenesis of wt DLH and the C123S mutants.

Mutation	Oligonucleotide[#]
E36D	CATGAACGCGTTCACACCAAATATTTGTTGAGCGATCAC
E36Q	CATGAACGCGTTCACACCAAATATGTCTTGAGCGATCAC
R81A-1	CAGGATGAGGCGCAGGCAGAGCAAGCCTAC
R81A-2	GTAGGCTTGCTCTGCCTGCGCCTCATCCTG
R81K	GTCGAAGGCCTGCCAGAGCTTGTAGGCTTGCTCTTTCTGC GCTC
Y85F-1	AGAGAGCAAGCCTTCAAGCTCTGGCAG
Y85F-2	CTGCAAGAGCTTGAAGGCTTGCTCTCT
W88A-1	GCCTACAAGCTCGCGCAGGCCTTCGAC
W88A-2	GTCGAAGGCCTGCGCGAGCTTGTAGGC
C123D-1	TTGGTGGGGTATGATCTGGGCGGTGCG
C123D-2	CGCACCGCCCAGATCATACCCCACCAA
S203A-1	GAGGCCGGACACGCGTTCGCCAGGACG
S203A-2	CGTCCTGGCGAACGCGTGTCCGGCCTC
S203D-1	GAGGCCGGACACGATTTCGCCAGGACG
S203D-2	CGTCCTGGCGAAATCGTGTCCGGCCTC
S203H-1	GAGGCCGGACACCATTTCGCCAGGACG
S203H-2	CGTCCTGGCGAAATGGTGTCCGGCCTC
R206A	CAACGCCGCGGCACTCGCCACATAGCCCGAACTGCTCGT CGCGGCGAACGAG
R206K-1	GAGGCCGGACACTCGTTCGCCAAGACGAGCAGTTC
R206K-2	GAACTGCTCGTCTTGGCGAACGAGTGTCCGGCCTC

[#] The oligonucleotides that contain a 1 (forward) or a 2 (reverse) were complementary and were used for the Stratagene® method of mutagenesis, whereas the other oligos were of the reverse complement that amplified this region of the gene only. The underlined bases indicate the mutated region. The R81A/R206A double mutant was made using the R206A plasmid as the template to introduce the R81A mutation. The arginine (R81A and R206A) mutations in the C123S protein were made by using the C123S plasmid as the template and using the relevant oligos.

Table 5. PCR protocol for Method i).

Cycle	Step	Temperature (°C)	Time (minutes)	Cycle Iterations
1	1	94	5	1
2	1	94	0.5	-
2	2	60	1	-
2	3	72	1	32
34	1	72	20	-
34	2	4	5	1

After the PCR, the reaction mix (added to 50% glycerol, 0.2% bromophenol blue) was then separated by gel electrophoresis on a 2% agarose gel using ethidium bromide for the detection of the DNA bands under UV light. The mutated PCR fragment was then run onto DEAE filter paper (NA45; Schleicher and Schuell), then removed from the DEAE membrane using a high salt solution (1 M NaCl and 50 mM arginine) at 70 °C and then ethanol (50%) precipitated for 1 hour at -70 °C. After removing from the fragment from -70 °C, it was spun down at 4°C, then was washed with 70% ethanol (4 °C), the supernatant then removed, the pellet dried and then resuspended in 10 mM Tris-HCl buffer at pH 7.6. The purified fragment and the pND704 plasmid were then digested with the restriction enzymes Nde1 and Mlu1 (20 units each) in a total volume of 100 µl in a buffer compatible with both enzymes (buffer H) for 4 hours at 37°C. The R81K mutant fragment (after PCR and gel purification) was digested with the Nde1 and Stu1 restriction enzymes (20 units each in buffer B). R206A was digested in 2 steps as the restriction enzymes used were not compatible in the same digestion buffer. The R206A PCR fragment and the plasmid were first digested with Nde1 (20 units in buffer H), gel purified, then digested with Ksp1 (20 units in buffer L) and then gel purified, as described above. The digested plasmids were then dephosphorylated with calf intestinal phosphatase (1 unit) for 1 hour at 37 °C after adding 5 µl of the 10x dephosphorylation buffer to the digestion reaction mix. The reaction mix was then placed in a 75 °C water

bath for 15 minutes (for denaturation of the restriction enzymes) and then placed on ice for 15 minutes. The digested fragment and plasmid were then gel purified, precipitated, and resuspended, as described above.

The digested fragment (40 ng) was then ligated into the digested (and dephosphorylated) plasmid (80 ng) with T4 ligase (1 unit) in T4 ligation buffer. This ligation reaction was done in a final volume of 50 µl and performed at 14 °C for approximately 12-14 hours. The ligation mixture was placed on ice for 10 minutes and then mixed with 100 µl of competent cells (AN1459) and kept on ice for a further 30 minutes. The cells were heat shocked at 30 °C for 2 minutes then added to 1 ml of sterile LBT (Luria-Bertani broth supplemented with 0.4 mM thymine) at 30 °C and left to incubate for 3 hours at this temperature. After this time the transformed cells were plated out (20-100 µL) on LBTA plates, as described above, and grown overnight at 30 °C. To assess the success of the ligation and subsequent transformation, 12 single colonies were removed at random from the plates and streaked out onto two 6-sector LBTA plates (singles) and grown overnight at 30 °C. A single colony was chosen at random from 6 of the streaked 'singles' and grown as a 3 ml overnight culture, with agitation, in LBTA media at 30 °C. The culture was then 'minipreped' (BRESAspin Plasmid Mini Kit, Bresatec) and the resulting plasmid resuspended in Tris-HCl buffer (pH 7.6). The average concentration of plasmid obtained *via* this method was 40 ng/µl. The plasmids were then checked for total size and the size of the ligated insert. The insert size was determined by a rapid digestion (1 hour) of the plasmid with the NdeI and EcoR1 (1.5 units in 8 µl) restriction enzymes (in buffer H) that cut at the 5' and 3' end of the DLH gene, respectively (Jefferies, 1998). The digested and undigested plasmids were then run on a 0.8%, 35 ml agarose gel with ethidium bromide and viewed under UV light. Four of the plasmids (and the inserts) that were of the correct size were chosen at random for gene sequencing using the Big Dye terminator reaction. The plasmids (320 ng) were added to the sequencing mix containing primer 9 (18 ng) in a total volume of 20 µl and amplified, as summarised in Table 6. The PCR reaction mix was precipitated using sodium acetate (pH 5.2) and ethanol (a final concentration of 0.2 M and 70%, respectively) and left on

Table 6. PCR protocol used for sequencing of the DLH gene.

Cycle	Step	Temperature (°C)	Time (minutes)	Cycle Iterations
1	1	96	0.50	-
1	2	50	0.25	-
1	3	60	4	25
26	1	4	5	1

ice for 10 minutes. The precipitated 'sequence' oligonucleotide was spun down, washed, and then dried, as mentioned above. The plasmids that contained the mutated gene of interest were transformed into AN1459 *E. coli* cells (using 1.5 µl of minipreped plasmid), as described above, with a single colony grown as an overnight culture in LBTA media and stored (1 ml) as a DMSO (7%) stock solution.

2.2.6.2 *Method ii) Generation of the remaining DLH mutants*

The method used for the generation of the remainder of the mutations in Table 4 was based on the method developed by Papworth *et al.*, (1996). The protocol is outlined in the QuickChange® Site-Directed Mutagenesis Kit supplied by Stratagene® (USA).

In a final volume of 50 µl was added 50 ng of plasmid (either wt DLH or the C123S mutant), the two complementary oligonucleotide primers containing the desired mutation (125 ng each), 1 µl of dNTP mix (0.25 mM of each), 5 µl of the 10x Pfu reaction buffer, 1 µl of Pfu DNA polymerase (2.5 units) and covered with 2 drops of light white mineral oil. The above reaction mix was amplified in the thermal cycliser (as mentioned above) according to the cycle protocol set out in Table 7. The number of cycle iterations (16) and elongation time (10 minutes) were those that are recommended by Stratagene for single amino acid changes and the size of the plasmid used (approximately 5 kb), respectively. After the amplification reaction was complete 1µl

Table 7. PCR protocol for Method ii).

Cycle	Step	Temperature (°C)	Time (minutes)	Cycle Iterations
1	1	95	0.5	1
2	1	95	0.5	-
2	2	55	1	-
2	3	68	10	16
18	1	4	5	1

(10 units) of the restriction enzyme Dpn1 was added to the amplification reaction below the oil layer, mixed, and microcentrifuged for 1 minute. The reaction mix was placed in a 37 °C water bath for 1 hour to digest the parental DNA plasmid. The digestion mix (2 µl) was used for transformation into AN1459 competent cells (as described above), plated out (50 µl and 100 µl) onto LBTA plates and grown overnight at 30 °C. The plasmids were minipreped, as described above, and sequenced *via* the Big Dye terminator method. Since the entire gene is amplified by this Stratagene method of site-directed mutagenesis, the DLH gene was sequenced in the reverse direction, in addition to the forward direction using primer 9, by using the universal primer M13 (18 ng) to ensure no further mutations were present.

2.2.6.3 *DLH mutant purification, protein concentration and the determination of kinetic constants*

The purification of the DLH mutant proteins and the determination of their concentration and kinetic constants were essentially the same as the methods used for the wt enzyme.

2.2.7 Determination of the pH dependence of wt DLH at low and high substrate concentrations

A 'three buffer system' was chosen for the pH dependence studies of wt DLH which were based on the program designed by Ellis and Morrison (1987). This system reduces a change in the ionic strength of the buffer solution when changing its pH. The three buffer system was checked over the pH range studied (pH 5 to pH 10) against several different buffers that also covered this pH range and the system was found to have no substantial effect on enzyme activity. The buffers chosen were MES, HEPES, and ethanolamine (10 mM; 10 mM; 20 mM, respectively) containing 1 mM EDTA. A 10x stock solution was made and diluted when necessary. The pH values were checked with an Orion pH meter (model 520A), with a temperature probe, calibrated with pH buffer standards 4.0, 7.0, and 10.0 (BDH) at the relevant temperature. Adjustments to the pH of the buffer solution was with HCl and tetramethylammonium hydroxide. At all the pH values measured, the buffer was equilibrated for five minutes in quartz cuvettes in the UV spectrometer before the enzyme (10 μL, in 20 mM HEPES buffer containing 1 mM EDTA, at pH 7.0) was added, mixed and then the *E*-dienelactone added (≤1.5% of the total volume) to start the reaction (1 ml final volume). Preliminary studies showed that a variation in pH due to the hydrolysis of the substrate was not substantial over a 10 minute period. The rate of enzyme hydrolysis of the *E*-dienelactone was corrected for the background hydrolysis of this substrate at pH values ≥8.0. The pH of the reaction solution was determined immediately after the reaction was complete. The data corresponding to k_{cat} and k_{cat}/K_m were fit to Equation 4, where y is k_{cat} or k_{cat}/K_m, C is the limiting value of y, K_1 and K_2 are the ionisation constants, and $[H^+]$ is the proton concentration in solution.

$$y = \frac{C}{1 + \frac{[H^+]}{K_1} + \frac{K_2}{[H^+]}} \qquad (4)$$

2.2.8 Determination of the pD dependence of wt DLH at high and low substrate concentrations

Solvent isotope effects in deuterium oxide (99.75% pure; Cambridge Isotopes Laboratories, USA) were determined in the three buffer system, as described for the pH profiles. The buffers MES and HEPES and EDTA were dissolved in deuterium oxide (D_2O), freeze dried, and resuspended to the desired concentration in D_2O with the addition of ethanolamine. After the addition of the enzyme, and correcting for the addition of ethanolamine, the final D_2O concentration in the cuvette was presumed to be 97.5%. The *E*-dienelactone was dissolved in an equimolar concentration of NaOD made by dissolving NaOH pellets in D_2O, evaporating to dryness, then resuspension in D_2O. This procedure was repeated three times. During the incubation period the cuvettes were covered to minimise the exposure of the D_2O to the atmosphere. All preparations and transfers involving D_2O were carried out in a glove bag under a positive pressure of nitrogen passed through a 300 cm x 1.5 cm column filled with anhydrous calcium chloride and dried silica. Adjustment to pD was with DCl or deuterated tetramethylammonium hydroxide, prepared similarly to NaOD, then adding 0.4 to the reading given by the pH meter (Glasoe and Long, 1960). The data were fit to Equation 4 after background hydrolysis of the *E*-dienelactone was subtracted from the enzyme catalysed reaction at pH $\geq$8.0.

2.2.9 Determination of the pH dependence of the E36D, R206A and R81A mutants of DLH at low substrate concentrations

It was not practical to perform a full kinetic analysis at each pH for the E36D, R206A and R81A mutants of DLH. A pH profile at one substrate concentration was chosen such that $s<K_m$. This concentration (approximately 0.3 x K_m) was changed for each mutation depending on the value of K_m determined from the full kinetic analysis in 20 mM HEPES buffer containing 1 mM EDTA, at pH 7.0 and 25 ± 0.1 °C.

2.2.10 Measurement of kinetic activity using HPLC

Some activity measurements for the wt DLH, C123S (and mutants thereof) and the C123D enzyme were made using a Waters Symmetry® 5µm C18 column (4.5 mm x 250 mm) at a flow rate of 1.5 ml/min on a Waters 2690 HPLC separations module (with autosampler) controlled by the Millenium[32] chromatography software. Peak detection was with a Waters 996 photodiode array detector at 210 nm and 280 nm.

All conditions used were tested for substrate stability. The appropriate controls (that is, without enzyme) were also performed under the same conditions as the reactions and the data subtracted from the enzyme catalysed rate, if required.

2.2.10.1 *The elution of the E- and Z-dienelactones and their hydrolysis product(s)*

The retention times of the authentic *E*- and *Z*-dienelactones (9.0 and 4.2 minutes, respectively), maleylacetate (2.6 minutes), and *trans*-acetylacrylic acid (5.1 minutes) were determined using 10% ACN and 0.1% TFA in water. The peak corresponding to maleylacetate was determined by NaOH (17 mM) hydrolysis of the *E*- and *Z*-dienelactones and by monitoring DLH hydrolysis of these same substrates (Schmidt and Knackmuss, 1980). A further peak was observed at 3.5 minutes which was thought to correspond to the product of the decarboxylation of maleylacetate to form *cis*-acetylacrylic acid (Schmidt and Knackmuss, 1980) which is predominantly in a cyclic form at low pH (Seltzer and Stevens, 1968).

2.2.10.2 *Activity measurements of wt DLH using the E- and Z-dienelactones*

In a final volume of 1.80 ml in 20 mM HEPES buffer containing 1 mM EDTA, at pH 7.0 was added DLH and BSA (25 µg/ml). After 5 minutes equilibration in a water bath at 25 ± 1 °C, the reaction was initiated by the addition of either substrate (55 µM). At designated time points an aliquot (150 µl) of the reaction mix was removed and quickly

quenched with 17 µl of 1% TFA in 99% ACN. The final ACN concentration was 10%. The samples were immediately frozen in liquid N_2 and thawed at room temperature prior to injection (100 µl) onto the above column in 10% ACN and 1% TFA in water.

2.2.10.3 *Activity measurements of C123S, C123S/R81A, and C123S/R206A mutants using the E- and Z-dienelactones*

In a final volume of 250 µl of 20 mM HEPES buffer containing 1 mM EDTA, at pH 7.0 was added the relevant enzyme, BSA (400 µg/ml) and then equilibrated in a water bath at 25 ± 1 °C for 5 minutes. The reaction was initiated by the addition of the substrate. Aliquots (20 µl) of the reaction mix were removed at designated time points and mixed with 100 µl of 12% ACN (10% final) in H_2O with 0.1% TFA and frozen in liquid N_2. The samples were then thawed to room temperature prior to injection (18 µl) onto the above column in 10% ACN and 0.1% TFA in water.

2.2.10.4 *Activity measurements of C123S using the E- and Z-dienelactone tert-butyl esters*

In a final volume of 1.30 ml of 20 mM HEPES buffer containing 1 mM EDTA, at pH 7.0 was added the enzyme, BSA (400 µg/ml), ACN and equilibrated in a water bath at 25 ± 1 °C for 5 minutes. The reaction was initiated by the addition of substrate (1.0 mM of either isomer) dissolved in HPLC grade ACN to give a final concentration of 10%. At designated time points an aliquot (60 µl) of the reaction mix was removed and added to 60 µl of 90% ACN (50% ACN final) and frozen in liquid N_2. The samples were thawed to room temperature prior to injection (40 µl) onto the column using a 50% ACN in water mobile solvent phase. The *E*-dienelactone *tert*-butyl ester eluted with a retention time of 9.0 minutes with the *Z*-isomer eluting at 5.2 minutes. A further peak appeared at 2.5 minutes that corresponded to the NaOH (17 mM) catalysed hydrolysis of either ester.

2.2.10.5 *Activity measurement of DLH using the E-dienelactone tert-butyl ester*

In a final volume of 1.30 ml was added DLH (998 nM), ACN (10% final concentration) and buffer (20 mM HEPES containing 1 mM EDTA, at pH 7.0) and incubated at 25 °C for 5 minutes prior to the addition of 1.01 mM of the *E*-dienelactone *tert*-butyl ester (dissolved in ACN). At designated time points an aliquot (100 µl) of the reaction mix was removed and added to 1000 µl of 55% ACN (50% ACN final) and frozen in liquid N_2. The samples were thawed to room temperature prior to injection (100 µl) onto the column using a 50% ACN in water mobile solvent phase. The substrate, *E*-dienelactone *tert*-butyl ester, eluted with a retention time of 9.0 minutes with an additional peak at 2.9 minutes.

To identify the above reaction product, the reaction was repeated on a larger scale with the reaction monitored by HPLC as above. In a final volume of 15 ml in 20 mM HEPES buffer containing 1 mM EDTA, at pH 7.0 was added DLH (1.3 µM) and ACN (10% final concentration). After 5 minutes of equilibration at 25 °C, the *E*-dienelactone *tert*-butyl ester (1.01 mM) in ACN was added to initiate the reaction. The reaction was complete after approximately 100 minutes. The reaction mix was acidified to pH 1.0 with 1 M HCl and the protein separated by ultrafiltration through a 10000 Dalton cutoff Centricon (Amicon) at 4 °C. The filtrate was extracted 4 times with 50 ml dichloromethane, the organic phase dried over magnesium sulfate, and the solvent removed under reduced pressure without heating. ^{1}H NMR ($CDCl_3$, 0.1% TMS) δ = 7.21 (d, J = 5.4 Hz, C2-H), 6.18 (d, J = 5.4 Hz, C3-H), 2.85 (d, J = 15.9 Hz, C5-1H), 2.66 (d, J = 15.9 Hz, C5-1H), 1.51 (s, 9H, ^{t}Bu); MS (ESI)$^+$, 214.3.

2.2.10.6 *Activity measurement of C123D using the E-dienelactone*

To a final volume of 150 µl of C123D (21.8 µM) in 20 mM HEPES buffer containing 1 mM EDTA, at pH 7.0 was added BSA (133 µg/ml) and equilibrated for 5 minutes at 25 ± 0.1 °C in the temperature controlled sample compartment of the HPLC system. The

reaction was initiated by the addition of 2.01 mM of the *E*-dienelactone. Injections (8 µl) were made at designated time points onto the column in 10% ACN and 0.1% TFA in water. The buffer used for the control reaction consisted of the buffer used in the final step of dialysis. This was necessary to ensure the same buffer concentration, pH, and ionic strength conditions were used for both the enzyme and the control reaction.

2.2.11 **Hydrolysis of *p*-nitrophenyl acetate by DLH, C123S and C123D enzymes**

In a final volume of 1.0 ml of 20 mM HEPES containing 1 mM EDTA, at pH 7.0 was added the relevant enzyme, BSA, ACN (to give a final concentration of 2%) and incubated at 25 0.1 °C for 5 minutes prior to the addition of *p*-nitrophenyl acetate (dissolved in ACN). The reaction was monitored at 400 nm in a UV spectrometer using an extinction coefficient for the *p*-nitrophenol/*p*-nitrophenolate ion of 8740 M^{-1} cm^{-1} (Pathak *et al.*, 1991). The data were fit to Equation 2.

Chapter 3

Purification and preliminary kinetic analysis of DLH

Previous methods for the purification of DLH were essentially those of Pathak *et al.*, (1988) with some modifications (Cheah *et al.*, 1993b). The method involves passing the overexpressed protein twice through a DEAE anion exchange column. However, this method of purification was found to be unsatisfactory yielding protein approximating 85-90% purity. Crystallisation of this protein yielded DLH of high purity but this method of purification is time consuming (about 1 week). The purpose of the work presented in this chapter was to develop a new rapid method of purifying DLH that would not involve crystallisation of the protein or oxidation of the catalytic cysteine.

3.1 DLH purification

After cell growth (see Materials and Methods) the cells were pelleted, resuspended in buffer A (20 mM HEPES, 1 mM EDTA, 1 mM β-ME at pH 7.0) and lysed through a French Press. The lysate, after centrifugation, was loaded directly onto a DEAE Fractogel® anion exchange column. DLH was eluted with a linear gradient of buffer B (buffer A and 1 M NaCl) between 90-110 mM NaCl and the fractions containing DLH (as determined by SDS-PAGE stained with coomassie blue) were pooled and loaded onto a Sephadex G-75 (superfine) size-exclusion column equilibrated with buffer A. Again, the fractions were analysed by SDS-PAGE to check for the purity of DLH with the relevant fractions pooled and concentrated by ultrafiltration before storage at -70 °C. Purification of DLH *via* this method yielded pure protein, as determined by coomassie blue staining, in a short time period.

3.2 Optimisation of the purification of DLH

Initial attempts to purify DLH resulted in an enzyme activity (k_{cat}) with the *E*-

dienelactone that was well below the literature value of 1800 min^{-1} (Ngai *et al.*, 1987; Schmidt and Knackmuss, 1980). Measured values were approximately 300 min^{-1}. To understand the cause of the low k_{cat} values obtained for DLH, the method of purification was investigated.

Activity measurements of DLH were made after each step of the purification. After the DEAE column, the protein sample was dialysed against buffer A before activity measurements were taken. The kinetic measurements were made in 20 mM HEPES buffer containing 1 mM EDTA, at pH 7.0 and 25 °C using the *E*-dienelactone (50 μM) and are summarised in Table 8.

The measurement of the specific activity (units/mg of protein) after the final purification step resulted in an activity of 52 U/mg of protein for the first batch of DLH purified (purification 1) using the newly established protocol.

To determine if the DEAE and/or the Sephadex columns were degrading DLH during the purification, the above purified protein (52 U/mg of activity) was passed through these columns again (purification 2). The activity measured after these steps (58-60 U/mg) was not substantially different from the 52 U/mg of activity measured for this protein initially. Based on this observation it was evident that the column media used for purification of DLH was not contributing to its reduced activity.

To further investigate the low enzyme activity of DLH compared to the literature values, the possible oxidation of the catalytic cysteine was examined. To minimise oxidation of the cysteine, the buffers used in the purification were sonicated then degassed by bubbling nitrogen gas through them for approximately 45 minutes prior to their use. After 3 attempts (purifications 3, 4 and 5) of purifying DLH using this modified procedure, it appeared that this protocol did not substantially increase the specific activity of DLH (80 U/mg).

Table 8. Specific activity of DLH for the hydrolysis of the *E*-dienelactone after each step during purification. The numbers 1-6 refer to the number of times DLH was purified. Numbers 3-6 refer to DLH purified with buffers that were sonicated then bubbled with nitrogen gas (N_2(g)) before use.

Purification Step	Specific Activity (U/mg) Sonication/N_2(g)					
	1	2*	3	4	5	6
Lysate	13	-	14	15	9	16
DEAE	18	58	30	38	30	56
Sephadex	52	60	60	80	80	145

* Rechromatography of the previous sample (*ie.* the sample with 52 U/mg activity).

The last batch of DLH purified (purification 6) *via* the above modified procedure had a specific activity that was substantially increased (145 U/mg). However, the cause of the increased activity was uncertain. The only difference in the procedure was that the purification of this last batch of DLH took longer than normal. Therefore, the effect of time on enzyme activity was studied.

The samples from the last batch of DLH purified (that is, purification 6) were stored at 4 °C. These samples were tested for 9 days after the final purification step to monitor possible changes in activity over time with the results presented in Table 9. It is evident that the specific activity of DLH increased over these 9 days from 145 U/mg to a peak of 209 U/mg on day 6 then declining thereafter to 198 U/mg on day 9.

Based on these observations, it seemed possible that whatever was inhibiting DLH activity was either breaking down over this time period or was dissipating from the buffered enzyme solution. In addition to the 20 mM HEPES buffer (pH 7.0), the solution contained 1 mM EDTA and 1 mM β-ME. The HEPES buffer had previously been used for the kinetic analysis of DLH (Cheah *et al.*, 1993a; Pathak *et al.*, 1991) and was not expected to adversely affect enzyme activity here. Generally, EDTA is added

Table 9. Specific activity of DLH stored for several days at 4 °C in buffer A.

Day	0	2	5	6	8	9
Activity (U/mg)	145	166	206	209	204	198

to buffered enzyme solutions to remove metal ions that may inhibit enzyme activity and/or it is added to inhibit proteases that rely on metal ions for activity. DLH is not metal dependent (Ngai *et al.*, 1987) and therefore the addition of EDTA should not affect enzyme activity. β-ME is also sometimes added during the purification of proteins as a reducing agent for the enzyme of interest, to protect against the oxidation of thiols, or as an inhibitor of proteases by reducing their disulfide bonds. The reduction of these bonds interferes with the structural integrity of the proteases and inhibits their proteolytic activity. The effect of β-ME on DLH was not clear.

Since β-ME is volatile, over time a reduction in the concentration of this compound in the buffered enzyme solution may affect DLH activity. To investigate the possibility that β-ME inhibits DLH activity it was added to buffered enzyme solutions in increasing concentration and the results are presented in Figure 7.

Addition of β-ME to the enzyme solution in increasing concentrations to a maximum of 20 mM substantially decreases the hydrolytic activity of DLH. β-ME was removed from the initial enzyme sample by dialysis. The inhibition is non-linear with respect to β-ME concentration with the effect approaching saturation. At a concentration of 20 mM β-ME, the rate of hydrolysis of the *E*-dienelactone (480 μM) by DLH was inhibited to approximately 20% of the rate without β-ME.

It is shown that β-ME has an adverse affect on DLH activity although the exact nature of this inhibition is not clear. One explanation could be that β-ME positions itself within the active site and so reduces the ability of the enzyme to bind the substrate.

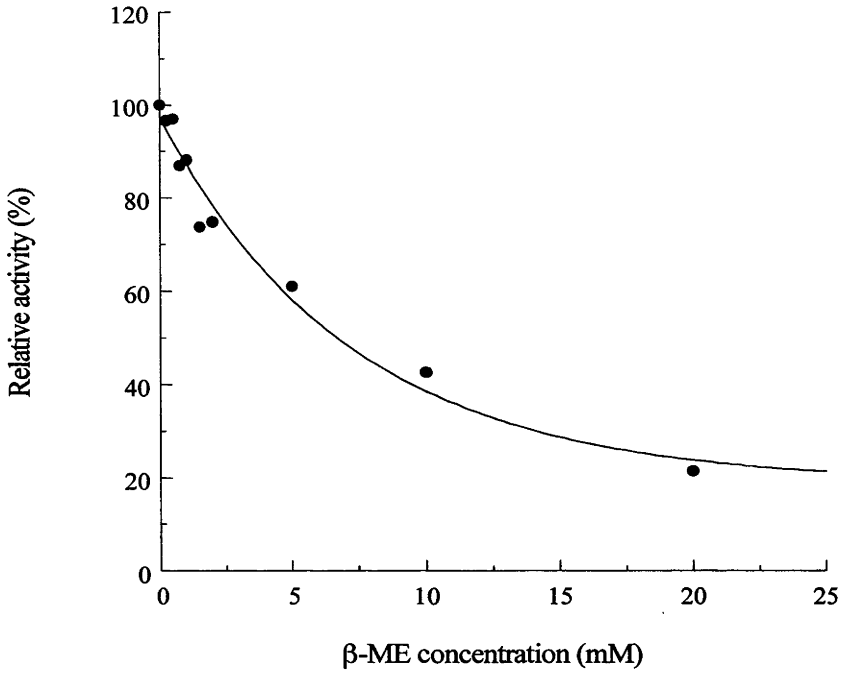

Figure 7. The relative activity of DLH after incubation in increasing concentrations of β-ME. The data were collected in 20 mM HEPES buffer, 1 mM EDTA, at pH 7.0 and 25 °C. The enzyme solution was equilibrated with the added β-ME in a sealed cuvette for 5 minutes prior to addition of the *E*-dienelactone to a final concentration of 480 μM.

To stop the inhibitory response of β-ME on DLH, it was dialysed after the final purification step, prior to concentration, to remove it from the enzyme solution. Constant enzyme activities were then obtained upon enzyme purification in reasonable agreement to the value obtained in the literature (Ngai *et al.*, 1987, Schmidt and Knackmuss, 1980).

3.3 The effect of sodium chloride on DLH activity

The salt content of an enzyme solution is an important parameter for the optimal functioning of many enzymes. It is common practice to add a salt to an enzyme solution to increase the ionic strength of the solution to maintain protein stability. As sodium chloride (NaCl) is used in the purification of DLH, the effect of this salt's concentration on enzyme activity was assessed. The effect of increasing NaCl concentration on DLH activity was determined in 20 mM HEPES buffer containing 1 mM EDTA, at pH 7.0 and 25 °C and the results are shown in Figure 8.

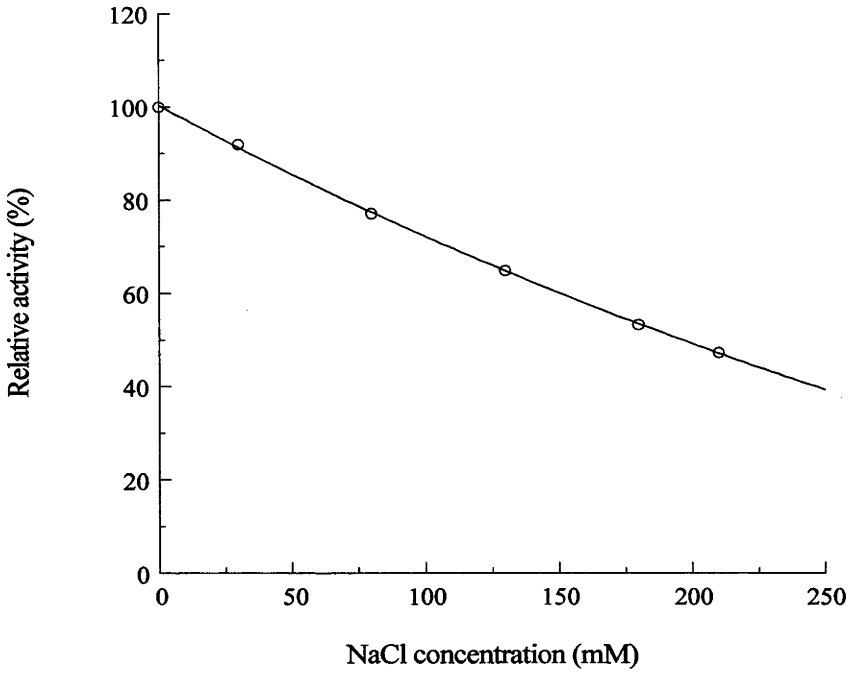

Figure 8. The effects of concentration on the activity of wt DLH hydrolysing the *E*-dienelactone. The data were collected in 20 mM HEPES buffer containing 1 mM EDTA, at pH 7.0 and 25 °C.

When the concentration of NaCl is increased there is a concomitant decrease in enzyme activity when hydrolysing the *E*-dienelactone (50 μM). At a NaCl concentration of 210 mM (the maximum tested) there is an approximate 50% inhibition to the catalytic rate of DLH.

To further investigate the effect of NaCl on DLH activity, a more complete kinetic analysis of DLH in the presence and absence of 100 mM NaCl was carried out and the results are shown in Figure 9. Again it is clear that 100 mM NaCl affects the activity of DLH. The NaCl appears to decrease the affinity of the enzyme for the substrate, that is, it increases K_m. The K_m value without NaCl is 177 μM and the K_m value with the added 100 mM NaCl is 278 μM. The apparent V_{max} value of 19.6 μM min^{-1} without NaCl and that of 19.3 μM min^{-1} with 100 mM NaCl are very similar.

It appears that NaCl reduces the enzymatic activity of DLH by decreasing the affinity of the enzyme for the substrate and not by reducing the rate of the reaction of the

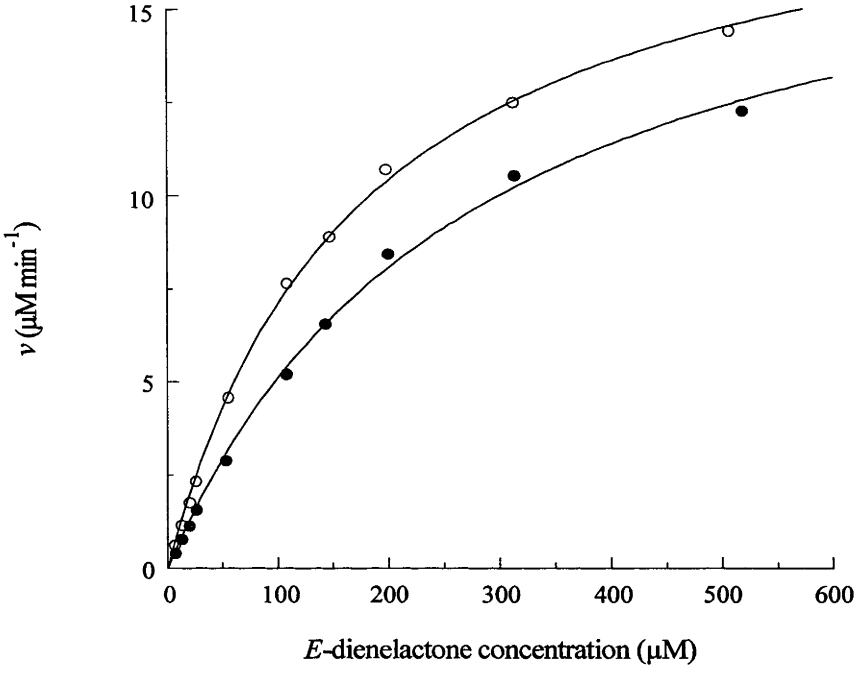

Figure 9. Comparison of the kinetics of hydrolysis by wt DLH without (O) and in the presence (●) of 100 mM NaCl. The data were collected in 20 mM HEPES buffer containing 1 mM EDTA, at pH 7.0 at 25 °C.

substrate once bound. This indicates that the enzyme is not being denatured by the increased NaCl concentration. To determine if NaCl is directly competing with the substrate for binding sites within the enzyme or affecting the conformation of the active site and thereby altering substrate binding, the ionic strength of the reaction solution was altered by changing buffer strength.

Ellis and Morrison (1987) have developed a '3 buffer system' for obtaining pH profiles over a wide pH range while minimising changes in the ionic strength of the buffered solution. Preliminary studies using this buffer system suggest that the ionic strength of the reaction solution is an important criterion for the activity of DLH. The hydrolysis of the *E*-dienelactone (50 μM) in buffers based on this system (MES, HEPES and ethanolamine) was studied at an ionic strength of 5 mM at pH 5.45 and 25 °C. The activity of DLH at 5 mM ionic strength was approximately 40% higher than at 20 mM ionic strength using the same buffers, pH, and temperature. An additional trial was made at pH 6.0 with the above buffers maintaining an ionic strength of either 20 mM or

40 mM. The doubling of the ionic strength of the reaction solution decreased the activity of DLH by 30%. From this study it appears that the ionic strength of the enzyme reaction solution is an important feature for DLH activity.

Changes to the ionic strength of the enzyme reaction solution by either changing buffer concentration or NaCl concentration appear to have a similar affect on DLH activity. Therefore, it appears unlikely that competition for binding sites by NaCl results in the observed decrease in enzyme activity unless the buffers used also competed for similar substrate binding sites in DLH. These results indicate the importance of maintaining constant reaction conditions while kinetically characterising this protein.

3.4 Conclusion

A new and refined method has been developed for the rapid purification of DLH. The refinement includes the removal of β-ME from the purified enzyme solution. This compound was shown to inhibit the activity of DLH. Additionally, care is needed in retaining a constant ionic strength of the buffered enzyme solution as modest changes in this strength can have an adverse effect on the activity of DLH.

Chapter 4

Mutagenesis of DLH, overexpression of the mutant proteins and preliminary determination of their pH dependence

The previous chapter described a new method of purifying DLH while retaining high enzyme activity. One objective of the work described in this chapter was to prepare site-directed mutants of DLH within the active site. These mutants were to be used later to probe the catalytic mechanism of DLH. After the purification of these mutant proteins using the method developed in Chapter 3, attempts were made to confirm the size of the overexpressed proteins using ESI mass spectrometry. Additionally, the pH and pD dependence of wt DLH and selected mutant proteins was examined to assess the role that pH has in controlling the catalytic mechanism.

4.1 Mutagenesis

The method of choice for site-directed mutagenesis was that based on the protocol of Stratagene®. This method (method (ii) in the Materials and Methods) gave a consistently high ratio of the desired mutated gene to the wt gene. For example, using this technique, after transformation and making 'singles' plates, four single colonies were chosen for sequencing. Of these four colonies on average three returned as having the desired mutated gene. Method ii) consists of amplifying the whole double stranded plasmid template while incorporating the double stranded oligonucleotide primer containing the desired mutation. The rate of isolating plasmid that contained the desired mutated gene by method i) (amplifying only a short single stranded mutant oligonucleotide by PCR and its ligation into plasmid) was very low possibly as a result of the more extensive protocol that was involved. This method (i) frequently required screening of more than 10 colonies before the desired mutation was obtained. For simplicity and the rapid generation of mutant genes, method ii) was chosen for the production of most of the mutant proteins used here.

All mutant genes were sequenced using the relevant primer(s) by the Big Dye terminator reaction to confirm the desired mutation.

4.2 Overexpression and purification of the mutant proteins of DLH

The overexpression of wt DLH is reported to approximate 58 mg/L of bacterial culture (Robinson, 1999). One group of mutant proteins which retain the cysteine nucleophile (C123) overexpressed very well with concentrations ranging from an approximate low of 22 mg/L for S203H to 53 mg/L for R81A. One mutant (E36Q) did not overexpress and purification of this protein was limited to the background level of protein produced within the *E. coli* (AN1459) bacterial cells (<1 mg/L). The other group of mutant proteins has a serine as the nucleophile (C123S). This group of proteins expressed at levels between 15 mg/L for C123S/R206 to a high of 22 mg/L for C123S.

The mutant proteins were purified by the same method as used for the wt protein, as outlined in the Materials and Methods. There was little difference in the elution pattern from both the anion exchange and size-exclusion chromatography columns of the various mutants compared to that of the wt enzyme. This suggests that all the proteins are of a similar structure and that the mutant proteins are not misfolded.

4.3 Confirmation of the size of the expressed DLH proteins

The wt DLH protein was analysed by electrospray ionisation mass spectrometry (ESI-MS) to determine its correct mass (using horse myoglobin as the standard). The mass of DLH is 25401 ± 0.7 Daltons, similar to the predicted mass as given by the protein sequence (25400.7 Daltons). The mutants of DLH were sensitive to the method of sample preparation for the ESI-MS analysis, precipitating out of solution. For ESI-MS analysis, proteins are extensively dialysed against 0.1% formic acid. This method removes salts from the sample while the addition of formic acid aids in the reliable ionisation of the protein for the ESI-MS analysis. Attempts were made to prevent the

protein from precipitating out of solution by reducing the formic acid concentration during the dialysis (0.05%) or by adding the formic acid at the point of sample injection. However, these attempts were unsuccessful. This suggests that the mutant proteins of DLH are unstable at extreme pH.

4.4 The pH and pD dependence of the kinetic parameters of DLH

The determination of a pH profile of an enzyme may help to identify groups that participate in its catalytic mechanism. As discussed in the Introduction, several groups in the active site of DLH are involved in the hydrolysis of dienelactone. The effect that pH can have on the k_{cat}/K_m and k_{cat} values during the reaction of the enzyme with substrate can provide information about the state of ionisation of the 'free' enzyme or the enzyme-substrate complex.

The simplified reaction scheme illustrated in Figure 10 corresponds to a bell-shaped enzyme activity *vs* pH curve with ionisations for the free enzyme and the enzyme-substrate complex. From this, two molecular protonation constants are apparent for the free enzyme (K_{E1} and K_{E2}) at low substrate concentration and two others for the enzyme-substrate complex at substrate saturation (K_{ES1} and K_{ES2}). Two assumptions are made with this scheme. Firstly, only EH^- binds to the substrate and only EH^-S reacts to give products. EH_2 and E^{2-} (and EH_2S and $E^{2-}S$) are inactive (Cornish-Bowden, 1995). Secondly, the catalytic reaction only involves two steps, similar to the Michaelis-Menten mechanism. Under these conditions, ionisations of the free enzyme are represented in the k_{cat}/K_m *vs* pH profile at low substrate concentration and ionisations of the enzyme-substrate complex are reflected at substrate saturation in the k_{cat} *vs* pH profile (Tipton and Dixon, 1979). In Figure 10 k_{cat}/K_m is indicated by the constants k_1/k_{-1} and k_{cat} by k_2. The K_m value refers to $(k_{-1}+k_2)/k_1$.

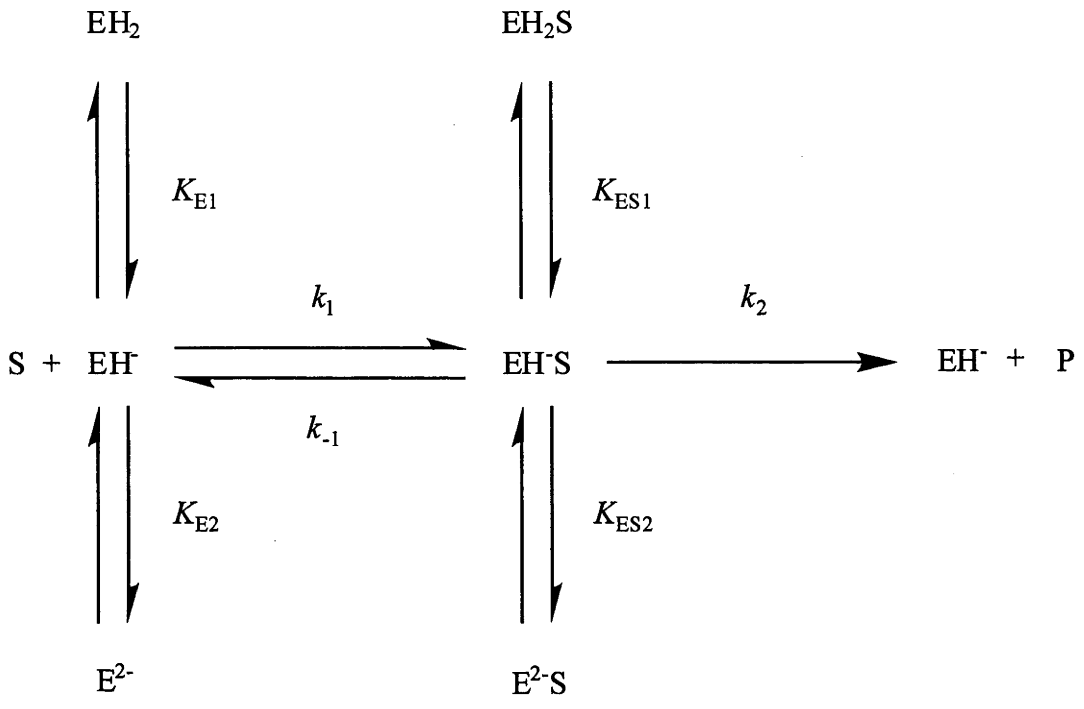

Figure 10. Reaction scheme for the ionisations of the free enzyme and the enzyme-substrate complex.

4.4.1 Determination of the pH profile for wt DLH

The k_{cat}/K_m and k_{cat} values were obtained from a full kinetic analysis of wt DLH hydrolysing the *E*-dienelactone at different pH values in buffered aqueous solutions (10 mM MES, 10 mM HEPES and 20 mM ethanolamine with 1 mM EDTA adjusted to the required pH and at 25 °C) with the view to maintaining constant ionic strength (Ellis and Morrison, 1987). The p*K* values (pK_1 and pK_2) were derived from a theoretical fit to the k_{cat}/K_m and k_{cat} pH profiles and are summarised in Table 10 and presented in Figures 11 and 12.

The non-linear fits to the pH profiles were done using KaleidaGraph®. The curve fits were optimised using the Levenberg-Marquart algorithm and the errors displayed are the standard errors of these parameters. As shown in Figures 11 and 12, the actual fits to the data are relatively poor. Therefore, errors given in Table 10, as derived from the theoretical fit to the data, are likely to be underestimated.

Table 10. The pK values of DLH in buffered solutions of water (pH) and deuterium oxide (pD) obtained from the k_{cat}/K_m and k_{cat} profiles.

	pH		pD		SKIE[#]
	pK_1	pK_2	pK_1	pK_2	
k_{cat}/K_m	5.5 ± 0.1	8.9 ± 0.1	5.9 ± 0.1	9.4 ± 0.1	2.8 ± 0.1
k_{cat}	5.6 ± 0.1	8.5 ± 0.1	5.6 ± 0.1	9.1 ± 0.1	3.3 ± 0.2

[#] The solvent kinetic isotope effects (SKIE) were estimated from the pH/pD maximum region of the respective profiles.

k_{cat}/K_m profile

As mentioned above, the k_{cat}/K_m pH profile refers to ionisation of the 'free' enzyme at low substrate concentration or it can refer to ionisation of the substrate. In the k_{cat}/K_m profile determined for wt DLH, ionisation of the substrate would not appear since its pK value is below that of the pH range tested.

The determination of the k_{cat}/K_m pH profile for wt DLH between pH 5.0 and pH 10.0 results in a bell-shaped curve. In this profile pK_1 is 5.5 ± 0.1 and pK_2 is 8.9 ± 0.1 with a pH maximum of 7.2.

k_{cat} profile

As mentioned above, the k_{cat} pH profile indicates the pKs of groups ionising on the enzyme at substrate saturation.

The k_{cat} pH profile between pH 5.0 and pH 10.0 is also bell-shaped with a pK_1 of 5.7 ± 0.1 and a pK_2 of 8.5 ± 0.1. The pH maximum is 7.05.

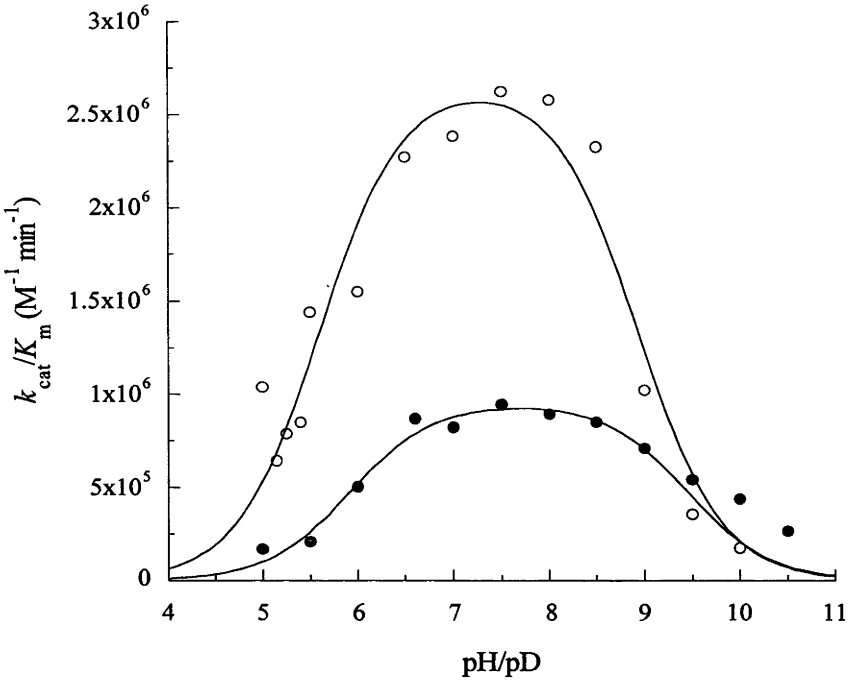

Figure 11. The k_{cat}/K_m profile in water (pH; O) and deuterium oxide (pD; ●) for wt DLH. The k_{cat}/K_m values were determined at each pH from a full kinetic analysis in a three buffer system at 25 °C. The data at pD 9.5-10.5 were excluded from the theoretical fit to the experimental data; see text for details.

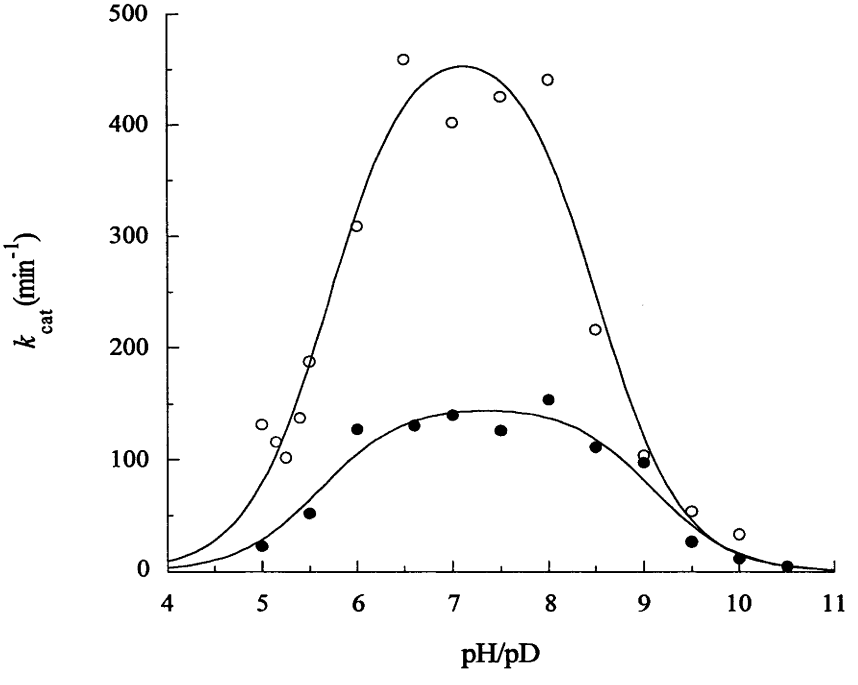

Figure 12. The k_{cat} profile in water (pH; O) and deuterium oxide (pD; ●) for wt DLH. k_{cat} values were determined at each pH from a full kinetic analysis in a three buffer system, as above.

4.4.2 Observation of non-Michaelis-Menten kinetics below pH 7.5

An anomaly was observed in the kinetics of DLH at pH values less than 7.5. Transformation of the rate data at increasing substrate concentrations for the hydrolysis of the *E*-dienelactone and replotting as a Hanes plot shows the data are not linear. The non-linearity occurs at low substrate concentrations where the rate of hydrolysis of the *E*-dienelactone is slower than would be expected. This anomaly is discussed in further detail in Chapters 5 and 6.

4.4.3 Determination of the pD profile for wt DLH

Exchange of the solvent water with deuterium oxide (pD profile) can influence acid dissociable functional groups that are important in the catalytic mechanism of an enzyme (Hwang and Cook, 1998). This effect is shown as an increase in the p*K* value in deuterium oxide (D_2O) compared to that in H_2O (an equilibrium solvent deuterium isotope effect) generally by about 0.3-0.6 pH units (Venkatasubban and Schowen, 1984). Additionally, comparison of the rates of reaction in water and D_2O can be used to evaluate the extent of proton transfer in a rate-determining or partially rate-determining step in the overall reaction.

The p*K* values derived from a theoretical fit to the k_{cat}/K_m and k_{cat} profiles in D_2O at different pDs using the *E*-dienelactone as substrate are summarised in Table 10 and illustrated in Figures 11 and 12. The same buffers, EDTA concentration and temperature were used for determining the pH and pD profiles. As mentioned above, the values and standard errors shown for pK_1 and pK_2 should be viewed with some caution.

k_{cat}/K_m profile

As mentioned above, the p*K* values determined from a k_{cat}/K_m profile refer to ionisations

of the free enzyme at low substrate concentration. The k_{cat}/K_m pD profile of wt DLH is bell-shaped with a pK_1 of 5.9 ± 0.1 and a pK_2 of 9.4 ± 0.1. The pD maximum is 7.65. The pK_1 value in D_2O is increased by 0.4 of a pH unit with the pK_2 value being increased by 0.5 of a pH unit when compared to the corresponding values in water.

To the extent that the pK_1 and pK_2 values may be assumed to be correct, the increases in the pK_1 and pK_2 values in D_2O are in the average range of 0.3-0.6 expected when the dissociable group comprises oxygen, nitrogen, or sulfur (Venkatasubban and Schowen, 1984). As discussed in the Introduction, with wt DLH it is proposed that substrate binding interrupts the ion-pair between E36 and R206. The E36 carboxylate then moves towards and deprotonates C123. The thiolate rotates about its Cα-Cβ bond into the active conformation where it is stabilised by the protonated H202 residue prior to acylation. The increase in the observed pK_1 and pK_2 values in D_2O may refer to any of the above events since these side chain residues contain the above mentioned dissociable groups.

In determining the pK_2 value, the data points at pD 9.5, 10.0, and 10.5 were omitted when fitting the theoretical curve (Figure 11). At these pD values the values of K_m were substantially less, by approximately 3, 6, and 9 fold at pD 9.5, 10.0 and 10.5, respectively, than those seen at lower pDs (Figure 13). This decrease in K_m contributes to the observed broadness of the k_{cat}/K_m profile. As mentioned above, it is generally assumed that the K_m term includes the constants k_1, k_{-1} and k_2 and a change in any of these values will affect the value of K_m. The decrease in K_m may indicate a decrease in either k_{-1} or in k_2. A similar decrease in K_m was not observed when determining the pH profile in water (Figure 13). This does not necessarily indicate that such a decrease does not occur. It is more likely that the decrease occurs but outside the range of pH values tested.

A comparison of the maximum or limiting k_{cat}/K_m values in water and D_2O shows a 2.8 ± 0.1 fold decrease in D_2O. The size of this isotope effect suggests that proton transfer

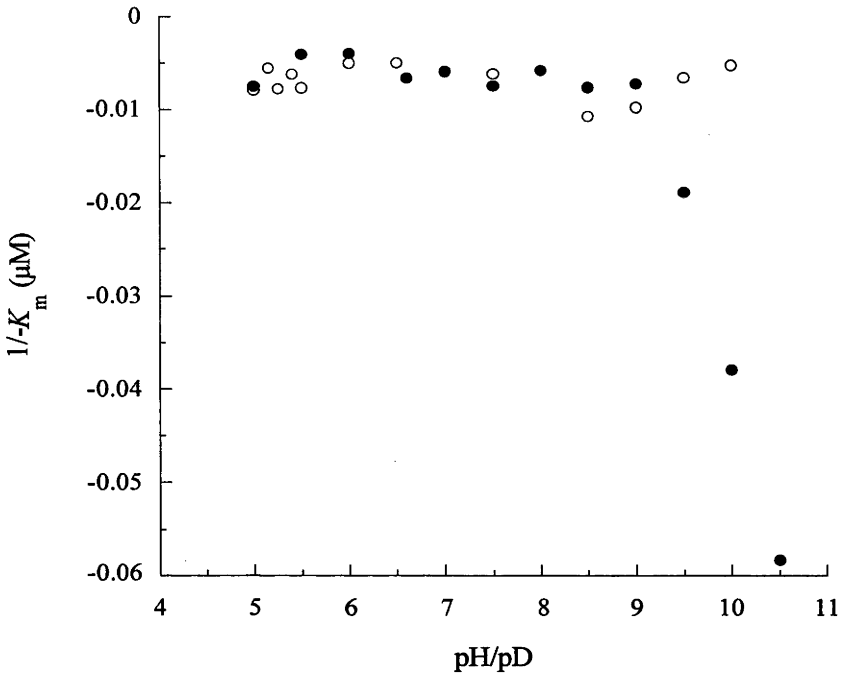

Figure 13. K_m *vs* pD profile (●) and pH profile (○) for wt DLH.

is rate-determining and is indicative of a general base mechanism for this proton transfer (Bender and Kézdy, 1964).

k_{cat} profile

As mentioned above, p*K*s obtained from k_{cat} profiles indicate the ionisation of groups in the enzyme-substrate complex at substrate saturation. The k_{cat} pD profile is bell-shaped with a pK_1 of 5.6 ± 0.1 and a pK_2 of 9.1 ± 0.1. The pD maximum is 7.35. The value of pK_1 obtained in D_2O did not change compared to that value in water. The value of pK_2 increased 0.6 of a unit in D_2O compared to that observed in water.

To the extent that the pK_1 and pK_2 values may be assumed to be correct, the lack of an equilibrium solvent deuterium isotope effect for pK_1 can be accounted for based on the proposed catalytic mechanism of DLH. For example, if pK_1 reflects deprotonation of E36, since E36 is thought to deprotonate C123 to produce the active state of the enzyme and does not participate further in the reaction, no isotope effect would be

expected. The shift in pK_2 between water and D_2O is normal. Such an isotope effect could be attributed to, for example, substrate assisted deprotonation of a water molecule which attacks the acyl carbon of the acyl enzyme.

Comparison of the maximum catalytic rate in water and D_2O shows a SKIE of 3.3 ± 0.2. This value shows that proton transfer is rate-determining during reaction of the substrate once bound. The size of this isotope effect is also indicative of a general base mechanism for proton transfer.

4.4.4 Summary of the pH and pD dependence of wt DLH

The pH and pD dependence of DLH has been determined to probe the proposed hydrolytic mechanism of this enzyme through kinetic analysis using the *E*-dienelactone. This analysis has shown that ionisable groups on the enzyme are important at low (k_{cat}/K_m) and high (k_{cat}) substrate concentrations. A solvent kinetic isotope effect is observed for both cases. The magnitude of these effects suggests that proton transfer is rate-determining in the overall reaction alluding to general base catalysis.

4.5 Determination of the pH profiles for the E36D, R81A and R206A mutants of DLH at low substrate concentrations

The determination as described above of the pH and pD profiles for wt DLH demonstrated the importance of ionisable groups on the enzyme activity. To further probe these ionisations in an attempt to assign them to specific residues of DLH, pH profiles of selected active site DLH mutants were analysed in the expectation that the mutations would perturb the ionisations.

It was not practical to carry out a full kinetic analysis of each mutant across a range of pH and pD values. Instead, since the pH maximum for wt DLH is approximately 7.0, this pH was used to obtain k_{cat}/K_m and k_{cat} values for the three mutants of DLH,

Table 11. Kinetic data for the interaction of wt DLH and various active site mutants with the *E*-dienelactone.

	k_{cat} [#] (min^{-1})	K_m (μM)	Ratio k_{cat}/K_m wt:mutant
wt DLH	870	184 ± 12	
E36D	44	257 ± 11	37
R206A	6	238 ± 21	960
R81A	650	1550 ± 88	15

[#] Non-linear regression of the kinetic data indicates that the error in the k_{cat} value is less than 5%.

analysed in 20 mM HEPES buffer containing 1 mM EDTA, at 25 °C and the results are summarised in Table 11. An *E*-dienelactone concentration of 0.3 x K_m was then used for the determination of the pH profiles for the three mutants. The use of a substrate concentration well below the K_m value minimises the effects of rate constants that pertain only to k_{cat}. Therefore, the velocity of substrate hydrolysis at a single low substrate concentration can be used to estimate the k_{cat}/K_m value using Equation 5 where v is the rate of hydrolysis of the *E*-dienelactone at 0.3 x K_m (s) and E is the enzyme concentration. For comparison, analogous data were obtained using wt DLH.

$$\frac{k_{cat}}{K_m} = \frac{v}{s \times E} \qquad (5)$$

The pH profiles were examined in buffered aqueous solutions (10 mM MES; 10 mM HEPES; 20 mM ethanolamine with 1 mM EDTA, adjusted to the required pH and at 25 °C) with a view to maintaining constant ionic strength (Ellis and Morrison, 1987). The pK values (pK_1 and pK_2) are derived from theoretical fits of the pH profiles and are summarised in Table 12 and presented in Figures 14, 15, 16 and 17. The profiles obtained using this method for wt DLH and the E36D, R81A and R206A mutants are all

Table 12. Values of pK calculated from pH profiles for wt and mutant DLHs using a single low substrate concentration of the *E*-dienelactone such that s<K_m.

k_{cat}/K_m (s<K_m)			
	pK_1	pK_2	$pH_{maximum}$
wt DLH	5.5 ± 0.03	8.5 ± 0.03	7.0
E36D	5.6 ± 0.02	8.7 ± 0.02	7.15
R206A	5.8 ± 0.04	9.4 ± 0.05	7.6
R81A	5.1 ± 0.05	9.1 ± 0.05	7.1

bell-shaped.

As shown in Table 12, pK_2 for wt DLH determined using this method is different to that presented above. However, these numbers must represent the same value. Therefore, the reliability of both data sets must be questioned. It does seem that the data illustrated in Figures 14, 15, 16 and 17 are probably the more reliable. Nevertheless, it is hard to determine roles of individual amino acids. It is shown that the R206A mutation increases pK_2. The R81A mutation also increases pK_2 and decreases pK_1. Therefore, the pK values cannot be associated directly with particular groups on the enzyme. As shown in Table 11, the R81A mutation increases the value of K_m indicating that this residue is important for substrate binding. The E36D and R206A mutations decrease the value of k_{cat} suggesting that they are important for the reaction of the substrate once bound. Therefore, these results suggest that a full kinetic analysis of DLH mutant enzymes are more informative about the catalytic mechanism of DLH, the approach adapted in the next chapter.

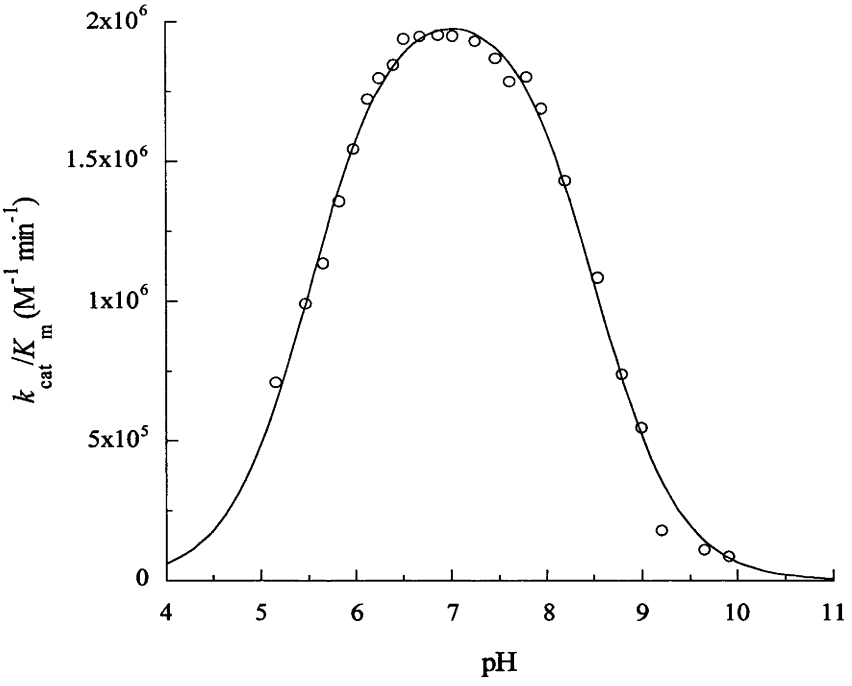

Figure 14. The pH profile in water for wt DLH with the *E*-dienelactone at 0.3 x K_m. k_{cat}/K_m was estimated at each pH using Equation 5.

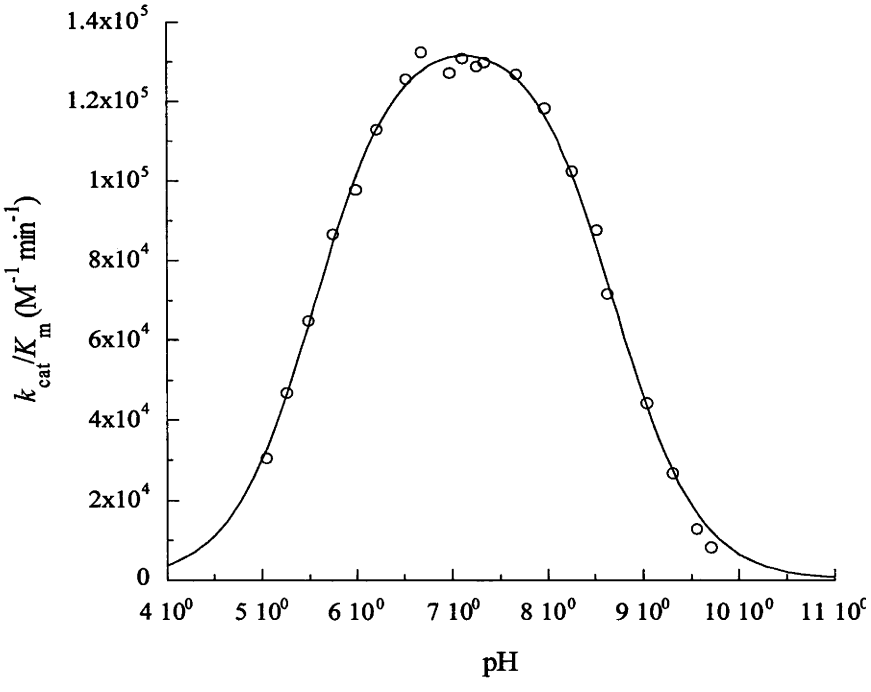

Figure 15. The pH profile in water for E36D with the *E*-dienelactone at 0.3 x K_m. k_{cat}/K_m was estimated at each pH using Equation 5.

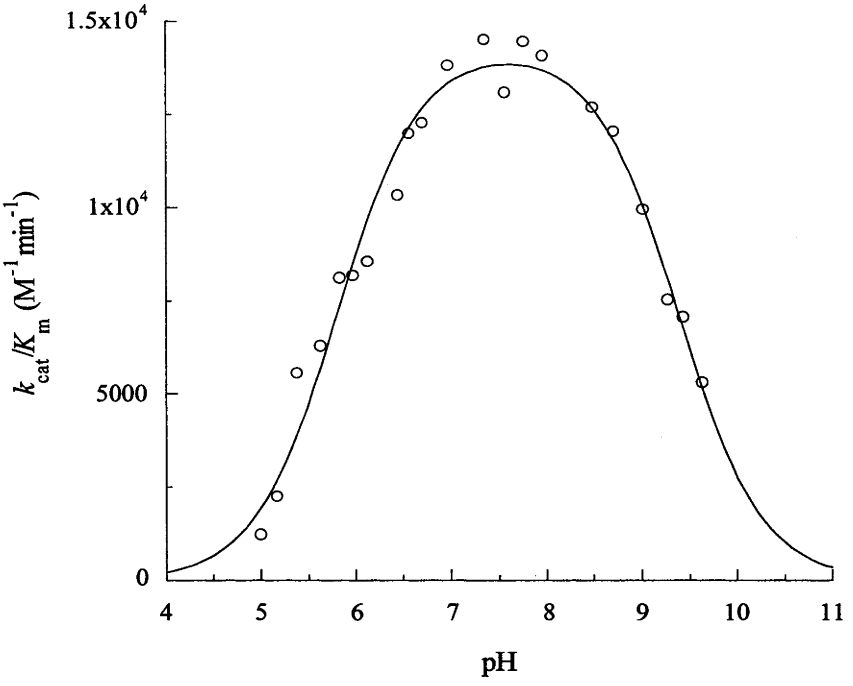

Figure 16. The pH profile in water for R206A with the *E*-dienelactone at 0.3 x K_m. k_{cat}/K_m was estimated at each pH using Equation 5.

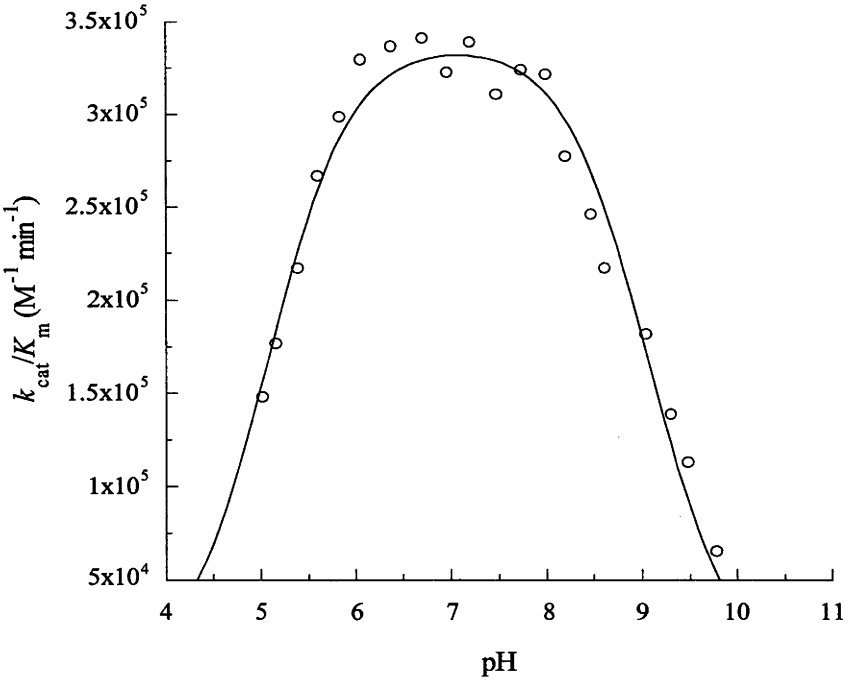

Figure 17. The pH profile in water for R81A with the *E*-dienelactone at 0.3 x K_m. k_{cat}/K_m was estimated at each pH using Equation 5.

4.6 Conclusion

This chapter has described the mutagenesis of DLH, the overexpression and purification of the mutant proteins and an analysis of the pH dependence of wt and selected mutants of DLH. The method of choice for mutagenesis was that based on the protocol of Stratagene® with the mutant genes confirmed by gene sequence analysis. All the mutant proteins overexpressed very well, with the exception of the E36Q mutant, and were purified by the same method as that used for the wt enzyme. Only the size of wt enzyme could be confirmed by ESI-MS analysis, the mutant proteins were too unstable for this analysis. The pH/pD dependence wt DLH suggests that proton transfer is a rate-determining step with the free enzyme and the enzyme-substrate complex at substrate saturation. A deviation from Michaelis-Menten kinetics occurs at low substrate concentrations at pH values less than 7.5.

Chapter 5

Kinetic analysis of the hydrolysis of the *E*- and *Z*-dienelactones catalysed by DLH mutants

The previous chapter highlighted the uncertainty in determining the contribution of specific residues in the active site of DLH to the catalytic mechanism. However, it has provided a pH optimum range for the wt and some selected mutants of DLH. As discussed in the Introduction, DLH catalyses the hydrolysis of the *E*- and *Z*-dienelactones to maleylacetate. The purpose of the work described in this chapter was to investigate the kinetics of the interactions of the lactones with site-directed mutants of DLH, in order to probe the catalytic mechanism.

5.1 Hydrolysis of the *Z*-dienelactone

The wt DLH and nine mutants were kinetically characterised with the *Z*-dienelactone to investigate the catalytic mechanism. One mutant, E36Q, did not overexpress. The very low activity and the low expression level of this mutant protein made a full kinetic analysis impossible. The kinetic data characterising the interaction of the *Z*-dienelactone with wt DLH and eight mutants are summarised in Table 13. The data were collected in 20 mM HEPES buffer containing 1 mM EDTA, at pH 7.0 and 25 °C. Under these conditions the hydrolysis of the lactone by the wt enzyme shows a catalytic rate constant (k_{cat}) of 1120 min^{-1} and a binding constant (K_m) of 11 ± 0.5 μM. Corresponding values of 1800 min^{-1} and 15 μM have been reported (Ngai *et al.*, 1987; Schmidt and Knackmuss, 1980) for this catalysis in 33 mM phosphate buffer at pH 6.5 and 25 °C, in reasonable agreement with the present work.

5.1.1 E36D mutant

Site-directed mutagenesis of the E36 residue to an aspartate results in an enzyme

Table 13. Kinetic data for the interaction of wt DLH and various active site mutants with the *Z*-dienelactone.

	k_{cat}[#] (min^{-1})	K_m (μM)	Ratio k_{cat}/K_m wt:mutant
wt DLH	1120	11 ± 0.5	
E36D	50	18 ± 1	37
R206A	37	350 ± 30	960
R81A	1070	160 ± 4	15
R206A/ R81A	2	880 ± 85	44800
R81K	1250	16 ± 0.5	1.3
R206K	96	25 ± 1	27
Y85F	670	19 ± 1	2.9
W88A	690	340 ± 21	50

[#] Non-linear regression of the kinetic data indicates that the error in the k_{cat} value is less than 5%.

(E36D) with a k_{cat} value of 50 min^{-1} which is 22 fold less than that of the wt protein. The K_m value of 18 ± 1 μM recorded with the mutant enzyme is similar to that observed with the wt enzyme (11 ± 0.5 μM). Overall the mutation results in a reduction in the k_{cat}/K_m value of 37 fold.

As discussed in the Introduction, it has been proposed that in the absence of a substrate E36 forms an ionic interaction with R206 in the wt enzyme. When the substrate binds through ion-pairing with R206, the R206-E36 interaction is weakened allowing E36 to deprotonate the active site cysteine (C123) for nucleophilic attack on the substrate (Cheah *et al.*, 1993b). Consistent with this hypothesis, the E36A mutant was found to be catalytically inactive. The low k_{cat} for the E36D mutant also illustrates the

importance of E36 in the reaction of the substrate once bound to the wt enzyme. Clearly the mutant enzyme does not function in the same manner. In the mutant protein D36 may still form an ion-pair with R206 which is disrupted on substrate binding, given that the similar K_m values for the wt and mutant protein indicate the mutation has little effect on the substrate-protein affinity. However, D36 appears to be unable to activate C123, probably because it is too far away. The results presented here for the E36D mutation suggest that the catalytic triad of DLH comprising C123, H202, and D171 cannot work independently of other residues in the active site for the catalysis of the *Z*-dienelactone. Cysteine activation by E36 is first required. This is in contrast to the cysteine (papain) and serine (trypsin) proteases where the catalytic triads of Cys, His, and Asn, and Ser, His, and Asp, respectively, appear to act alone to activate the nucleophile for reaction with bound substrate.

5.1.2 **R206A, R81A and R206A/R81A mutants**

The mutation of arginine 206 to an alanine (R206A) replaces a large, polar side chain with a short hydrophobic one. The R206A mutant protein shows a 30 fold decrease in the k_{cat} value (37 min^{-1}) compared to that of the wt enzyme. Additionally, this mutant protein shows a 32 fold increase in the K_m value (350 ± 30 μM) when compared to that of the wt enzyme. The R206A mutation results in a decrease in k_{cat}/K_m by 960 fold. It is clear that this mutation has a substantial effect on both substrate binding and reaction of the substrate once bound.

As discussed above, it is thought that the guanidino moiety of R206 in the wt enzyme interacts as an ion-pair with E36 (which deprotonates C123) and also binds the substrate in the active site. The large reduction in the k_{cat} value for the R206A mutant enzyme compared to that of the wt protein demonstrates the role that R206 has in catalysis once the substrate has bound. Replacement of the guanidinium side chain with an alanine eliminates the ion-pair between R206 and E36. This could result in an enzyme with increased activity where E36 would be free to deprotonate C123.

However, the low k_{cat} suggests otherwise, demonstrating that interruption of the R206-E36 ion-pair compromises the activity of DLH. The substantial increase in K_m for the R206A mutant enzyme also underlies the important functional role that this residue has in substrate binding into the active site.

The k_{cat} value for the hydrolysis of the *Z*-dienelactone by the R81A mutant enzyme (1070 min^{-1}) is similar to that of the wt enzyme. However, the K_m (160 ± 4 μM) is increased approximately 15 fold compared to that of wt DLH. In contrast to the R206A mutation, the R81A mutation only affected binding of the substrate in the active site and not the rate of reaction of the bound substrate.

The side chain of R81 is proposed to bind the substrate carboxylate in forming the Michaelis complex and during the reaction of the bound *Z*-dienelactone, as discussed in the Introduction. It is evident that R81 does not participate in the hydrolysis of the bound *Z*-dienelactone based on the similar k_{cat} value of the R81A mutant enzyme compared to that of the wt enzyme. The substantial increase observed for the K_m value for the R81A mutation is consistent with the role R81 has in binding the *Z*-dienelactone to form the Michaelis complex.

The R206A/R81A double mutant enzyme was tested to compare its activity to that of the single mutant enzymes in their role in the hydrolysis of the *Z*-dienelactone. This double mutant enzyme shows a 560 fold decrease in k_{cat} (2 min^{-1}) with an 80 fold increase in the K_m value (880 ± 85 μM), with a total reduction in k_{cat}/K_m of 44800 fold, when compared to that of wt DLH.

The R81A/R206A double mutant enzyme is inefficient in binding and catalysing the reaction of the bound *Z*-dienelactone compared to the wt enzyme. This result is not surprising given the role that R81 and R206 have in binding the *Z*-dienelactone and R206 has in the reaction of this substrate once bound, as noted above.

5.1.3 **R81K and R206K mutants**

The roles of R81 and R206 in the hydrolysis of the *Z*-dienelactone were further assessed by mutating each of these residues independently to a lysine residue. The mutation of an arginine to a lysine retains the positive charge of the side chain but reduces the charge distribution. The R81K mutation had little effect on the k_{cat} value (1250 min^{-1}) or the K_m value (16 ± 0.5 μM). Together, the k_{cat}/K_m value decreased only 1.3 fold.

As illustrated in Figure 18, the overall length of a lysine side chain is 1.0 Å shorter than the length of an arginine side chain. Additionally, the charge distribution and spatial flexibility of a lysine residue is substantially different to that of an arginine residue.

As discussed above with the R81A mutation and by Cheah *et al.* (1993a), the arginine side chain at position 81 is important for the formation of the Michaelis complex. Replacement of the arginine at position 81 with a lysine (R81K) does not substantially affect the formation of the Michaelis complex. Therefore, it appears that a lysine side chain functions essentially the same as an arginine side chain at this position. The higher concentration of charge of a lysine side chain compared to an arginine side chain must compensate for the shorter lysine side chain length. This indicates that an arginine at this position is not an essential residue.

To check that the above results were made by the R81K mutant enzyme only, the gene encoding for this protein was resequenced. The sequencing was done in both directions to ensure that the desired mutation, and only this mutation, was present. The correct sequence was obtained for the gene encoding the R81K mutant protein.

The R206K mutant enzyme has a 12 fold lower k_{cat} (96 min^{-1}) than wt DLH but with a K_m value (25 ± 1 μM) that is similar to that of the wt enzyme. Overall, k_{cat}/K_m was reduced 27 fold.

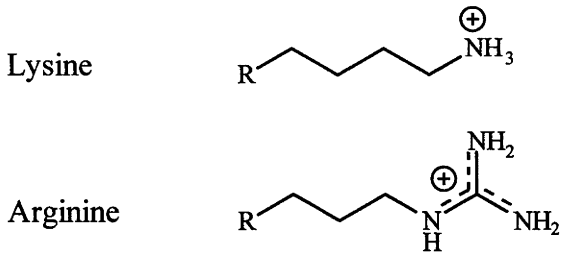

Figure 18. Comparison of the side chain length and charge distribution of a lysine residue to an arginine residue. These two side chain residues are approximately the same length (8.5 Å for lysine and 9.5 Å for arginine, Xu *et al.*, 2000) but differ significantly in their charge distribution.

As discussed above with the R206A mutation and by Cheah *et al.* (1993a), the R206 side chain is important for the formation of the Michaelis complex and in the reaction of the substrate once bound. The kinetic analysis of the R206K mutant enzyme suggests that a lysine side chain at this position does not substantially affect the formation of the Michaelis complex. This effect is in agreement with the argument above for the R81K mutation.

In contrast to the R206K effect on binding, this mutation substantially reduces the rate of reaction of the substrate once bound. The ionic interaction between R206 and E36 in the wt enzyme in the absence of substrate would be relatively weak because of the distribution of charge of an arginine side chain. In contrast to this, the concentration of charge of a lysine side chain would create a stronger ionic interaction with E36. It may be that this stronger interaction reduces the ability of E36 to deprotonate C123 for nucleophilic attack on the substrate and, therefore, reduces the rate of reaction of the substrate once bound.

As for the R81K mutant, the gene encoding the R206K mutant protein was resequenced in both directions and was found to be the desired gene.

5.1.4 **Y85F mutant**

The tyrosine to phenylalanine mutation removes the hydroxyl group of the tyrosine side chain at position 85. The Y85F mutation did not substantially change k_{cat} (670 min^{-1}) or K_m (19 ± 1 μM). There is only a 2.9 fold decrease in the k_{cat}/K_m value.

Mutation of the tyrosine at position 85 to a phenylalanine (Y85F) was used to probe the contribution that the tyrosine hydroxyl has in the catalytic mechanism of DLH. The position of the bound *Z*-dienelactam in the active site of DLH (Cheah *et al.*, 1993a) suggests that the tyrosine hydroxyl of Y85 is 3.74 Å from the C5 position of this inhibitor. In the reaction of DLH with the *Z*-dienelactone this corresponding distance may change after acylation of C123, placing the side chain of Y85 within a reasonable distance to donate its proton (H^+) to C5 of this substrate. This would stabilise the developing anion charge at this position associated with forming the enolate intermediate (Figure 19). If Y85 donates its proton before the rate-determining step, the Y85F mutant would then be expected to have a much lower k_{cat}. The small decrease in k_{cat} (1.7 fold) of the Y85F mutant enzyme compared to the k_{cat} of the wt enzyme suggests there is no interaction of the hydroxyl group of Y85 with the substrate during the reaction of the bound substrate, at least not before the rate-determining step of the reaction.

5.1.5 **W88A mutant**

The tryptophan to alanine mutation (W88A) changes the bulky residue of a tryptophan side chain to the small methyl group of an alanine. The W88A mutant enzyme k_{cat} value (690 min^{-1}) did not substantially change from the k_{cat} value of the wt enzyme. However, this mutant enzyme had an increased K_m for the *Z*-dienelactone of approximately 31 fold (340 ± 21 μM) when compared to that of the wt enzyme. Overall, a decrease in the k_{cat}/K_m value of 50 fold was observed.

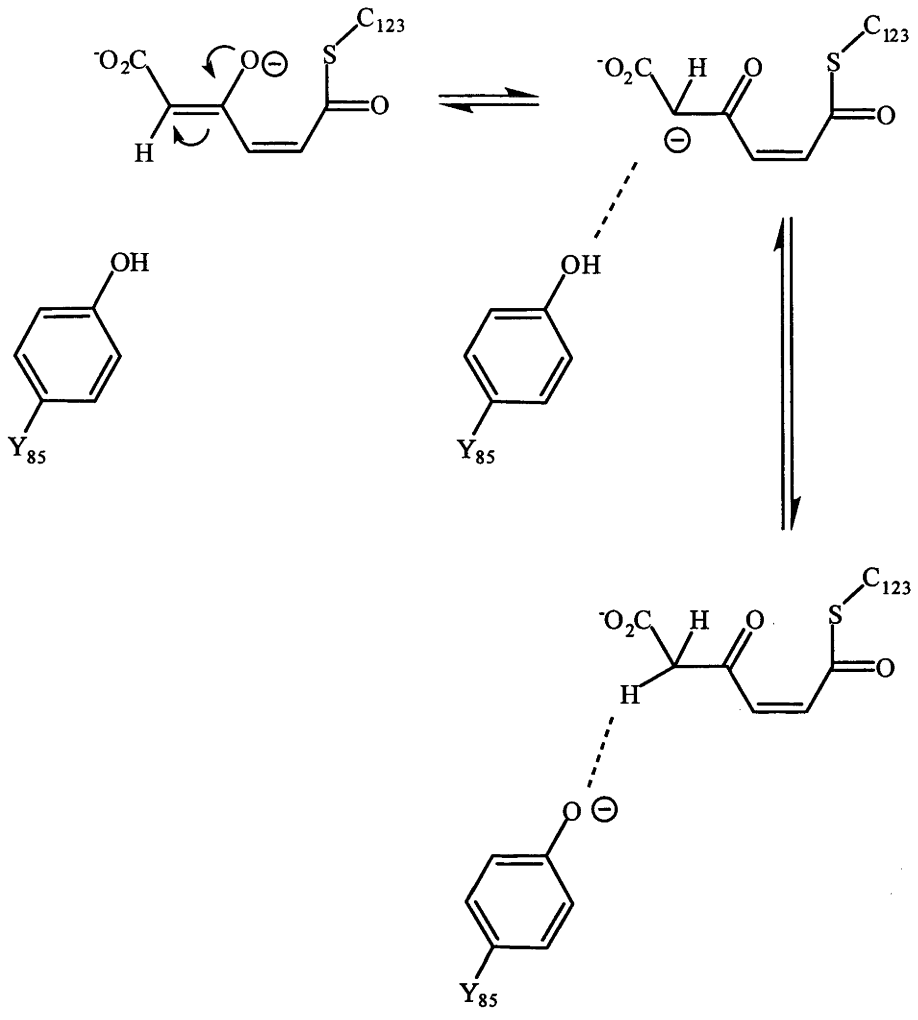

Figure 19. The possible role of Y85 in the hydrolysis of the *Z*-dienelactone.

As discussed in the Introduction, W88 is the only residue in close proximity to the substrate ring hydrogens and may contribute to the formation of the Michaelis complex. A schematic demonstrating the position of the inhibitor *Z*-dienelactam in the active site in the Michaelis complex is shown in Figure 20 (Cheah *et al.*, 1993a). In 3-dimensions, the tryptophan side chain is perpendicular to the plane of the page, at a 90 degree angle to what is illustrated. It is possible that the steric bulk of the tryptophan and the π-π interactions between the ring hydrogens of the inhibitor and the tryptophan side chain aid in positioning the inhibitor (or substrate) in the Michaelis complex. Therefore, the mutation of this residue (W88) to an alanine should reduce the affinity of the enzyme for the substrate. In agreement with this, the W88A mutant enzyme has a substantially increased K_m when compared to that of the wt enzyme. There was no substantial

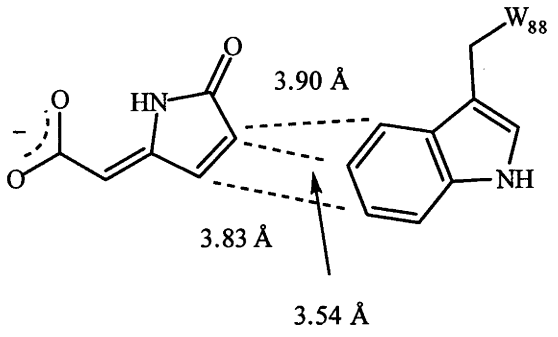

Figure 20. A schematic of the distance(s) that W88 is from the ring hydrogens of the lactam inhibitor *Z*-dienelactam in the C123S mutant enzyme (Cheah *et al.*, 1993a). These distances give an estimation of the corresponding distances for the substrate *Z*-dienelactone in the active site of the wt enzyme.

change in k_{cat}. It appears that this residue mainly functions to correctly position the substrate for the formation of the Michaelis complex and does not participate in the reaction of the *Z*-dienelactone once bound.

5.1.6 Summary of the hydrolysis of the *Z*-dienelactone by DLH mutant enzymes

The proposed hydrolytic mechanism of DLH as determined from X-ray crystallography has been studied by kinetic analysis of DLH mutant enzymes in solution. The proposed role that E36 has in the hydrolytic mechanism of DLH in the deprotonation of the active site cysteine (C123) is supported by the data presented here. Further support for the proposed hydrolytic mechanism of DLH is given by the role that R206 has in the formation of the Michaelis complex and in the reaction of the bound substrate. The function of R81 in the formation of the Michaelis complex is consistent with the proposed mechanism of DLH. Additionally, it has been demonstrated that R206 and R81 can be replaced with lysine without adversely affecting the formation of the Michaelis complex. However, the reaction of the bound substrate proceeds less efficiently with the R206K mutant suggesting that the ion-pair formed between R206 and E36 is very important in the hydrolysis of the *Z*-dienelactone. The roles of Y85 and W88 have not previously been reported in the literature. From the data presented here,

there is uncertainty as to the role of Y85. The Y85 residue may participate in the hydrolysis of the *Z*-dienelactone through acid catalysis. However, the data presented here do not confirm this proposed role. The major role of W88 appears to be to position the substrate in forming the Michaelis complex.

5.2 Hydrolysis of the *E*-dienelactone

The wt DLH and nine mutants were kinetically characterised with the *E*-dienelactone to investigate the catalytic mechanism. One mutant, E36Q, did not overexpress. The very low activity and the low expression level of this mutant protein made a full kinetic analysis impossible. The kinetic data characterising the interaction of the *E*-dienelactone with wt DLH and eight mutants are summarised in Table 14. Some of the kinetic data were shown in Chapter 4 but their contribution to the catalytic mechanism of DLH will be discussed in detail in this chapter. It should be noted that there was some deviation at low substrate concentrations from Michaelis-Menten kinetics which will be discussed later in more detail. Removal of the outlying data at low substrate concentration did not substantially affect the values obtained for k_{cat} and K_m when fitting the data of the substrate saturation curve directly to the Michaelis-Menten equation.

The data were collected under the same conditions as those for the *Z*-dienelactone. The hydrolysis of the *E*-dienelactone under these conditions by the wt enzyme shows a catalytic rate constant (k_{cat}) of 870 min^{-1} and a binding constant (K_m) of 184 ± 12 μM. Specific literature values have not been reported for the rate of hydrolysis of the *E*-dienelactone. The literature indicates that the rates of the hydrolysis of the *E*- and *Z*-dienelactones are "almost identical" (Schmidt and Knackmuss, 1980). A K_m value of 400 μM for the *E*-dienelactone was reported (Ngai *et al.*, 1987; Schmidt and Knackmuss, 1980). These data were obtained in 33 mM phosphate buffer at pH 6.5 and 25 °C and are in reasonable agreement with the present work.

Table 14. Kinetic data for the interaction of wt DLH and various active site mutants with the *E*-dienelactone.

	k_{cat}[a] (min^{-1})	K_m (μM)	Ratio k_{cat}/K_m wt:mutant
wt DLH	870	184 ± 12	
E36D	44	257 ± 11	28
R206A	6	238 ± 21	190
R81A	650	1550 ± 88	11
R206A/ R81A[b]	4	2910 ± 120	3440
R81K	940	213 ± 11	1.1
R206K	41	171 ± 13	20
Y85F	440	239 ± 11	2.6
W88A	270	1730 ± 81	30

[a] Non-linear regression of the kinetic data indicates that the error in the k_{cat} value is less than 5% except with the R206A/R81A double mutant where the error is 9%. The values obtained for k_{cat} and K_m assume Michaelis-Menten kinetics. [b] Data were fit to a sigmoidal curve (velocity *vs* log [S]) to reduce the error in k_{cat} and K_m.

5.2.1 **E36D mutant**

Mutation of E36 to an aspartate reduces the side chain length at position 36 by one methylene group. The E36D mutant enzyme shows a 20 fold decrease in the k_{cat} value to 44 min^{-1} when compared to that of the wt enzyme. The K_m value of 257 ± 11 μM for this mutant enzyme is similar to this value for the wt enzyme (184 ± 12 μM). Overall, these changes result in a reduction in k_{cat}/K_m of 28 fold, attributed mainly to the low k_{cat} value.

As discussed in the Introduction, the proposed catalytic mechanism of DLH is based only on the crystallographic results of the inhibitor *Z*-dienelactam soaked into the C123S mutant enzyme. To compensate for the lack of information for the hydrolysis of the *E*-dienelactone, this isomer was modelled into the active site of C123S (Cheah, 1991). This modelling predominantly maintained the ion-pairs of the R206 and R81 side chains with the substrate carboxylate. As mentioned above for the *Z*-dienelactone, these contacts are important for the formation of the Michaelis complex and for the substrate induced activation of C123 after the disruption of the R206-E36 ion-pair. The observed reduction in k_{cat} for the E36D mutant enzyme is consistent with the proposal of E36 participating in the reaction of the *E*-dienelactone once bound. Since D36 does not adequately activate C123, the distance between these two residues probably exceeds the maximum required for the deprotonation of C123.

It is evident from the K_m value of this mutant enzyme that the reduction of the side chain length by one methylene group has little affect on the affinity of the substrate for the enzyme. The results presented here for the hydrolysis of the *E*-dienelactone by the E36D mutant are consistent with those presented for the hydrolysis of the *Z*-dienelactone that suggest the catalytic triad of DLH cannot work independently of other residues within the active site.

5.2.2 **R206A, R81A and R206A/R81A mutants**

The R206A mutant enzyme displays a decrease in k_{cat} to only 6 min^{-1} with a K_m of 238 ± 21 μM. Compared to the wt enzyme this mutant enzyme shows a 145 fold decrease in k_{cat} with little change in the K_m value. Together, these values represent a 190 fold decrease in the k_{cat}/K_m value when compared to that of the wt enzyme.

As discussed above, modelling studies for the interaction of the *E*-dienelactone with DLH were used to indicate the positioning of this isomer in the active site for the formation of the Michaelis complex. Based on these studies the mechanism of catalytic

activation of C123 for the hydrolysis of the *E*-dienelactone was proposed to be same as for the *Z*-dienelactone. That is, the carboxylate of the *E*-dienelactone forms an ion-pair with R206 in the Michaelis complex. This interaction weakens the ion-pair between R206 and E36 which then rotates towards and deprotonates C123. Consistent with this hypothesis, the low k_{cat} for the R206A mutant enzyme in the reaction of the *E*-dienelactone once bound demonstrates the role this residue has in this catalytic process. However, the K_m value for the R206A mutant enzyme in the hydrolysis of the *E*-dienelactone is not consistent with this hypothesis. With the knowledge gained from the hydrolysis of the *Z*-dienelactone with the R206A mutant, it would also be expected that K_m would increase for the hydrolysis of the *E*-dienelactone with the R206A mutant enzyme as a reflection of the difficulties in forming the Michaelis complex. Clearly this does not occur. Therefore, binding of the *E*-dienelactone in the active site of DLH does not require the formation of the ion-pair between the substrate carboxylate and the guanidinium of R206, as was demonstrated with the *Z*-isomer. The importance of R206 in the catalytic mechanism of DLH for the hydrolysis of the *E*-dienelactone is directed towards its participation in the catalytic activation of C123 only and not substrate binding.

The catalytic rate constant (k_{cat}) for the hydrolysis of the *E*-dienelactone by the R81A mutant enzyme changed little (650 min^{-1}) when compared to that of the wt enzyme (870 min^{-1}). The binding constant (K_m) for this mutant enzyme was increased 6 fold to 1550 ± 88 μM with an overall decrease in the k_{cat}/K_m value of 11 fold.

As discussed above for the *Z*-dienelactone, the side chain of R81 is involved in the formation of the Michaelis complex only. The negligible reduction in k_{cat} for the R81A mutant enzyme indicates no substantial role for this arginine side chain during the reaction of the *E*-dienelactone after the substrate has bound. The decreased binding affinity of the mutant enzyme highlights the role that the R81 residue has in the formation of the Michaelis complex. This clearly demonstrates the distinct role that R81 has for the binding of the substrate and not in the reaction of the substrate once

bound.

The R206A/R81A double mutant enzyme displays a low k_{cat} (4 min^{-1}) which is 220 fold less than that of the wt enzyme. The K_m value shows a 16 fold increase to 2190 ± 120 μM when compared to that of the wt enzyme which results in an overall decrease in the k_{cat}/K_m value of 3440 fold. To reduce the error in the values generated for k_{cat} and K_m the data were fit to a sigmoidal curve (v versus log [S]).

This double mutant enzyme displays the importance of R81 for binding the *E*-dienelactone and R206 for the reaction of this substrate once bound. Removal of these guanidino side chains reduces the hydrolytic activity of DLH to an extent where it is practically non-functional as an enzyme.

5.2.3 **R81K and R206K mutants**

The R81K and R206K mutants were analysed to compare the effect of retaining a positively charged, although slightly shorter, residue at these positions. The R81K mutant shows little change in either k_{cat} (940 min^{-1}) or K_m (213 ± 11 μM) when compared to those values for the wt enzyme. Overall, the k_{cat}/K_m changed little (1.1 fold).

As discussed above for the hydrolysis of the *E*-dienelactone by the R81A mutant, an arginine at this position is important for the formation of the Michaelis complex and not the reaction of the substrate once bound. Consistent with this, the R81K mutation had little effect on k_{cat}. Additionally, for the hydrolysis of the *E*-dienelactone the formation of the Michaelis complex with the R81K mutant enzyme was little affected. It appears that a lysine side chain can replace the arginine side chain indicating that an arginine at position 81 is not an essential residue.

The R206K mutant enzyme displays a low k_{cat} value of 41 min^{-1} compared to that of

the wt enzyme (870 min^{-1}) with the K_m value little affected (171 ± 13 μM). Combining the effects of the k_{cat} and K_m values for the R206K mutation results in a 20 fold decrease in k_{cat}/K_m.

As discussed above for the R206A mutant, R206 is important for the reaction of the *E*-dienelactone once bound and not in the formation of the Michaelis complex. Consistent with this, the hydrolysis of the *E*-dienelactone with the R206K mutant enzyme only affected k_{cat} and not K_m. The discussion of the reduction of k_{cat} for the hydrolysis of the *Z*-dienelactone by the R206K mutant enzyme can be applied to the reduction seen in the k_{cat} for the hydrolysis of the *E*-dienelactone by this same mutation. That is, the concentration of charge of the lysine side chain may increase the ionic interaction of the lysine (K206) with E36. Even though the *E*-dienelactone does not bind the side chain of position 206, a strong interaction between E36 and K206 could affect the ability of E36 to deprotonate C123 for nucleophilic attack on the substrate once bound. This inability of E36 to deprotonate C123 would be reflected in the rate of the hydrolytic reaction, as shown here.

5.2.4 **Y85F mutant**

The contribution of the hydroxyl group of the tyrosine at position 85 in the hydrolysis of the *E*-dienelactone was determined by replacing the tyrosine with a phenylalanine (Y85F). The Y85F mutation did not substantially change k_{cat} (440 min^{-1}) or K_m (239 ± 11 μM). The overall decrease in k_{cat}/K_m was only 2.6 fold.

As discussed above for the Y85F mutation in the hydrolysis of the *Z*-dienelactone, the hydroxyl group of Y85 may act as an acid and donate its proton (H^+) to C5 of the substrate to stabilise the developing anion at this position after the formation of the enolate intermediate. It is possible that this effect would be reflected in the k_{cat} value. However, the k_{cat} value for the Y85F mutant enzyme is not substantially different from the value of this constant for the wt enzyme. Based on this information, it appears that

the hydroxyl group of Y85 does not participate in the reaction of the bound substrate, at least not before the rate-determining step of the reaction.

5.2.5 W88A mutant

The W88A mutation replaces the bulk of a tryptophan side chain with the small methyl group of an alanine. The W88A mutation reduced k_{cat} 3 fold to 270 min^{-1} with an increase in K_m of approximately 9 fold to 1730 ± 81 μM. An overall decrease in the k_{cat}/K_m value of 30 fold was observed for hydrolysis of the *E*-dienelactone.

As discussed above for the role of W88 in the hydrolysis of the *Z*-dienelactone, the bulky side chain of tryptophan 88 (W88) is important in the formation of the Michaelis complex. In agreement with this, the W88A mutation decreased the affinity (increased K_m) of the enzyme-substrate complex approximately 9 fold for the hydrolysis of the *E*-dienelactone. Replacement of the tryptophan residue with an alanine has a small affect on k_{cat} (3 fold decrease) in the hydrolysis of the *E*-dienelactone. Therefore, the correct positioning of the substrate by W88 is important for the formation of the Michaelis complex and for the reaction of the substrate once bound. However, it is clear that the major contribution of W88 in the hydrolysis of the *E*-dienelactone is in the formation of the Michaelis complex.

5.2.6 Summary of the hydrolysis of the *E*-dienelactone by DLH mutant enzymes

The proposed hydrolytic mechanism of DLH has been studied by kinetic analysis of the hydrolysis of the *E*-dienelactone by DLH mutant enzymes in solution. The proposed role of E36 in the reaction of the substrate once bound is supported by the data presented here. Additional support for the proposed hydrolytic mechanism of DLH is provided with the role of R206 in the reaction of this substrate once bound. However, the formation of the Michaelis complex does not require R206 as suggested by the

proposed mechanism. Formation of the Michaelis complex is dependent on R81 as proposed by X-ray crystallography. A lysine can substitute for arginine at position 81 for the formation of the Michaelis complex. A lysine at position 206 is less efficient than an arginine for the reaction of the *E*-dienelactone once bound. Proposed roles for Y85 and W88 have not appeared in the literature. The data presented here suggest a minimal role for Y85 in the hydrolytic mechanism of DLH, at least before the rate-determining step of the reaction. The W88 residue is important for the formation of the Michaelis complex with a minimal role in the reaction of the *E*-dienelactone once bound.

5.2.7 Active site conformational change in DLH for hydrolysing the *E*-dienelactone

The kinetic information obtained above from the site-directed mutant enzymes of DLH for the hydrolysis of the *E*- and *Z*-dienelactones illustrates a major difference between the coupling of binding of these substrates to the reaction of the substrates once bound. As mentioned above, the interaction of the *Z*-dienelactone with R206 in the Michaelis complex disrupts the ion-pair this residue has with E36 which then deprotonates C123. As shown above, the *E*-dienelactone does not interact with R206 in the Michaelis complex so the above mechanism cannot occur. Therefore, how does DLH couple binding of the *E*-dienelactone in the active site, which does not involve R206, to the deprotonation of C123? It is possible that for DLH to hydrolyse the *E*-isomer the enzyme undergoes a small but significant conformational change in the active site that couples substrate binding to the reaction of the substrate once bound. A deviation from Michaelis-Menten kinetics at low substrate concentrations observed for the hydrolysis of the *E*-dienelactone by DLH may be the result of the conformational change required in the active site.

Figure 21 shows the hydrolysis of the *E*-dienelactone at different concentrations by wt DLH in 20 mM HEPES buffer containing 1 mM EDTA, at pH 7.0 and 25 °C. In Figure 21a, the substrate saturation curve for the hydrolysis of the *E*-dienelactone by wt DLH

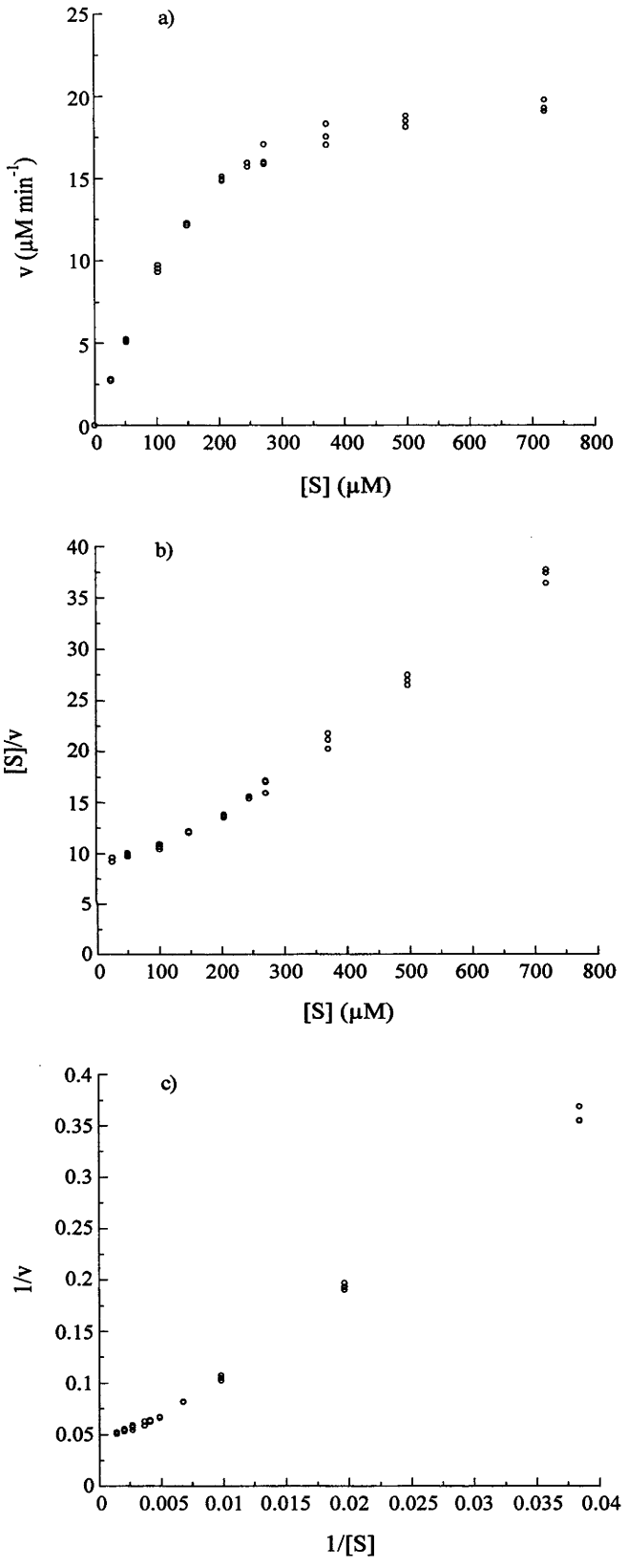

Figure 21. Demonstration of the deviation from Michaelis-Menten kinetics for the DLH hydrolysis of the *E*-dienelactone. a) Michaelis-Menten type kinetics and after transformation of this data into b) a Hanes plot and c) a Lineweaver-Burk plot. The data were collected in triplicate at each substrate concentration.

appears in good agreement with Michaelis-Menten type kinetics. However, upon linearisation of this data and replotting it according to the method of Hanes (Figure 21b) or Lineweaver-Burk (Figure 21c) it is evident that at low substrate concentrations a deviation from Michaelis-Menten type kinetics occurs. This deviation from linearity is not evident with the hydrolysis of the *Z*-dienelactone by DLH. The shapes of these linearised curves are indicative of an 'activation' process occurring (Shultz, 1994) that is dependent on substrate concentration. Substrate induced activation of enzymes with only one active site that turn over one substrate and release one product (monomeric cooperativity) must involve an active site conformational change (Cornish-Bowden and Cardenas, 1987). This cooperativity can be either positive or negative. The number of enzymes that exhibit monomeric cooperativity is relatively small and include the enzymes hexokinase L_I (Meunier *et al.*, 1974), δ-chymotrypsin (Ainslie and Neet, 1979) and acid phosphatase (Palma *et al.*, 1983). These enzymes demonstrate negative cooperativity while glucokinase (Storer and Cornish-Bowden, 1976) displays positive cooperativity, similar to the cooperativity shown here.

The appearance of non-Michaelian kinetics may result from micelle formation or other aggregation of the enzyme, impurities, ionic-strength effects, hysteretic effects, or non-linear instrument response. All these affects, except hysteretic effects, can be discounted as to the cause of the non-Michaelian kinetics observed with the *E*-dienelactone since the *Z*-isomer displays only Michaelis-Menten type kinetics. If this activity of DLH occurred with both isomers of dienelactone, further exploration of the above mentioned problems that can cause non-Michaelian type kinetics would need to be investigated.

It is possible that micelle formation or other aggregation of the *E*-dienelactone, may affect the availability of this substrate to the enzyme. The *E*-dienelactone can form micelles in solution due to the polar ($R\text{-}CO_2^-Na^+$) and non-polar (lactone ring) nature of the substrate. It is not expected that micelle formation was a problem with the *Z*-dienelactone as there was no deviation from Michaelis-Menten kinetics with this

substrate. The *E*-dienelactone may be different. Aggregation of the *E*-dienelactone would result in decreased enzyme activity as the substrate concentration is increased, since aggregation would increase. However, this did not occur. Impurities in the *E*-dienelactone substrate can also be eliminated as the cause of the non-Michaelian kinetics as this compound was pure by ^{1}H NMR and HPLC.

Hysteretic enzymes are enzymes that respond slowly to rapid changes in substrate concentration (Frieden, 1970). This type of reactivity was proposed by Rabin (1967) for a one-substrate one-product reaction that involved a slow transition or isomerisation between an active and a 'less' active conformation of an enzyme that was further developed by Frieden (1970). This model is based on the enzyme having two possible conformations in the free, substrate bound and catalytic states. An additional model based on these initial observations was proposed for the transition of the active site from one conformation to another, but with only one catalytic state, and this was termed a mnemonical transition (Meunier *et al.*, 1974; Ricard *et al.*, 1974; Ricard, 1978). Scheme 2 is a representation of the mnemonical model (Cornish-Bowden and Cardenas, 1987). In the absence of substrate the enzyme appears in the more stable conformation (E′) compared to an unstable conformation (E) with a slow transition between the two. Substrate (A) can bind to either conformation but it is the less stable conformation (EA) that proceeds on to the reaction of the bound substrate. If the substrate binds to the more stable enzyme species the enzyme undergoes a conformational change to the less stable form (EA) before catalysis proceeds. This change in conformation is substrate dependent. If the substrate concentration is low, and hence catalysis is low, the enzyme has time to revert back to the more stable enzyme species before another substrate molecule can bind into the active site. However, if there is sufficient substrate for the enzyme to work at a maximal or near-maximal catalytic rate, the enzyme has little time to relax and revert back to the stable enzyme species. It is possible that this phenomenon results in the non-Michaelian type kinetics demonstrated here for the hydrolysis of the *E*-dienelactone by DLH.

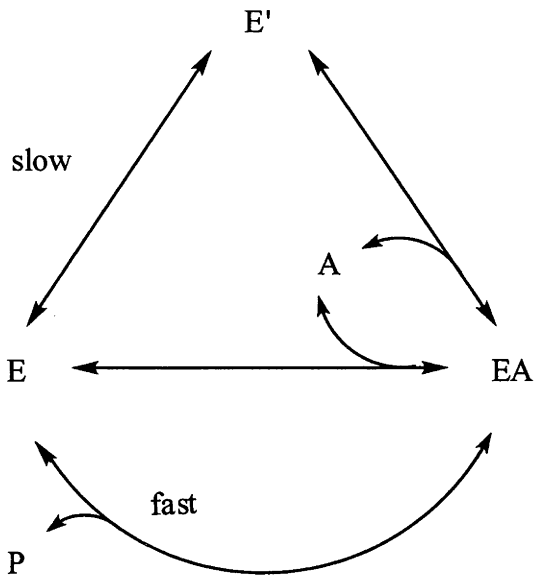

Scheme 2. The proposed mnemonical mechanism (Cornish-Bowden and Cardenas, 1987) for DLH. The enzyme appears in two conformations; as the more stable E' and the less stable E. Both forms of the enzyme can bind substrate (A) but only one form of the enzyme is catalytic (EA). Terminology used is that of Cornish-Bowden and Cardenas, 1987.

Regardless of the apparent mechanism, the data presented here suggests that an anomaly occurs during the hydrolysis of the *E*-dienelactone by DLH.

5.3 Hydrolysis of the *E*- and *Z*-dienelactones by S203 mutant enzymes

X-Ray crystallographic analysis of the C123S mutant of DLH bound with the *Z*-dienelactam inhibitor indicates that the serine hydroxyl of S203 is within hydrogen bonding distance (3.10 Å) of the inhibitor carboxylate (Cheah *et al.*, 1993a). The serine hydroxyl of S203 is also in close proximity to Nη2 of R206 (3.67 Å). To understand the extent of the interaction that S203 has with the substrate carboxylate in the hydrolysis of the *E*- and *Z*-dienelactones, this amino acid was mutated to 3 different residues and the kinetics of the mutant enzymes were analysed. The data for the *E*- and *Z*-dienelactones were collected in 20 mM HEPES buffer containing 1 mM EDTA, at pH 7.0 and 25 °C and the results are summarised in Table 15.

Table 15. Comparison of the kinetics of wt DLH with various mutants of the active site residue S203.

	Z-dienelactone			*E*-dienelactone		
	k_{cat}[a] (min^{-1})	K_m (μM)	Ratio k_{cat}/K_m wt:mutant	k_{cat} (min^{-1})	K_m (μM)	Ratio k_{cat}/K_m wt:mutant
wt DLH	1120	11 ± 0.5		870	184 ± 12	
S203A	815	2 ± 0.1	0.25	510	390 ± 12	4
S203H	450	160 ± 10	36	26[b]	6870 ± 71	1250
S203D	12	5065 ± 400	42980	4	6190 ± 275	7320

[a] Non-linear regression of the kinetic data indicates that the error in the k_{cat} values is less than 5%. [b] Data were fit to a sigmoidal curve (velocity *vs* log [S]) to reduce the error in k_{cat} and K_m.

5.3.1 **Hydrolysis of the *Z*-dienelactone**

5.3.1.1 *S203A mutant*

Site-directed mutagenesis of the serine at position 203 to an alanine (S203A) eliminates the hydrogen bonding capability of the hydroxyl side chain of S203. The S203A mutant has a k_{cat} value (815 min^{-1}) similar to that of the wt enzyme. The K_m value for the S203A mutant protein is reduced 5.5 fold to 2 ± 0.1 μM. This mutation has clearly increased the affinity of DLH for the *Z*-dienelactone resulting in an overall increase in k_{cat}/K_m of 4 fold.

As discussed above, the hydroxyl side chain of S203 could conceivably hydrogen bond to the substrate carboxylate in the Michaelis complex. It would be expected that replacing the serine at position 203 with a side chain incapable of hydrogen bonding to the carboxylate of the *Z*-dienelactone in the Michaelis complex would reduce binding.

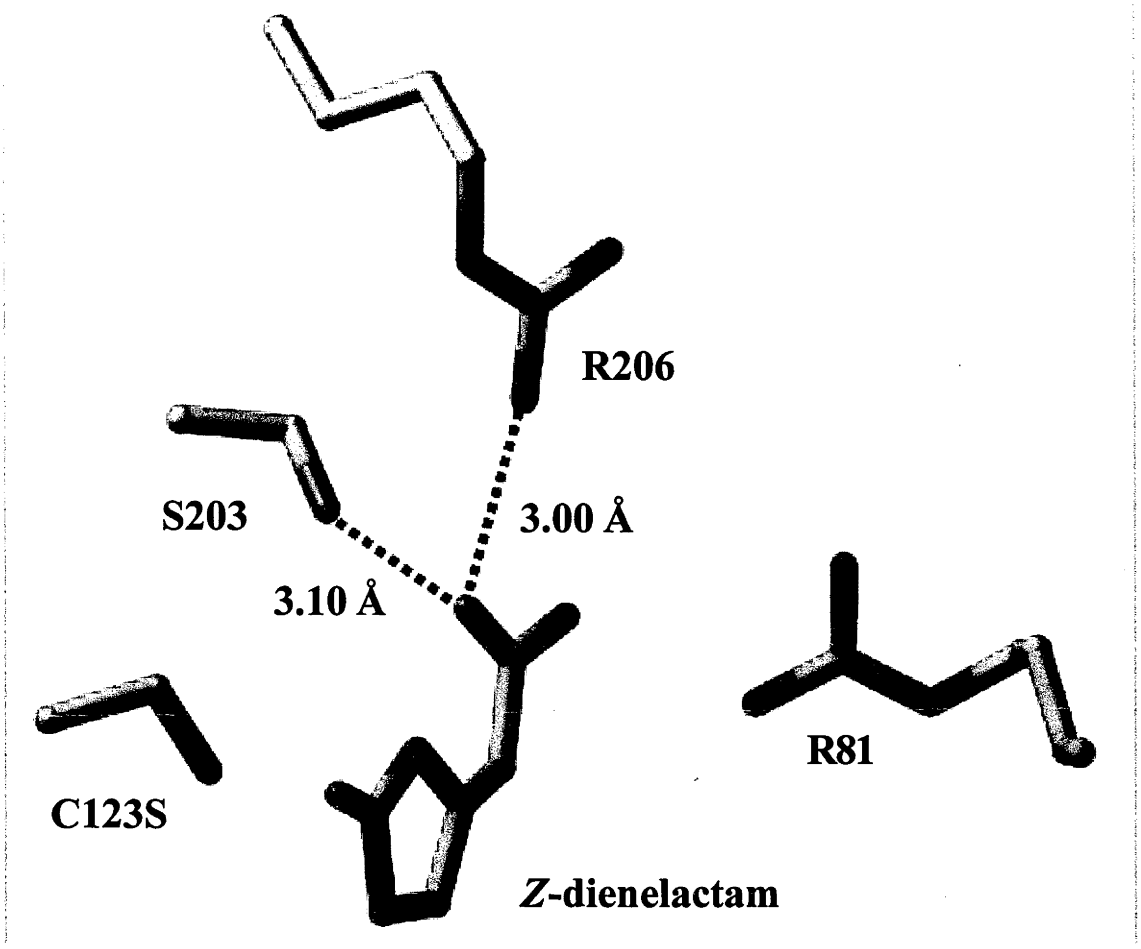

Figure 22. The distance in angstroms that S203 and R206 are from the carboxylate of the inhibitor *Z*-dienelactam (Cheah *et al.*, 1993a). Also shown are the R81 and the C123S residues.

This would not be expected to affect the reaction of the substrate once bound. Consistent with this proposal, the S203A mutation did not substantially change k_{cat}. However, the reduction of greater than 5 fold in the K_m value has produced a more proficient enzyme, inconsistent with the above proposal. Since S203 is in close spatial proximity to R206, the removal of the serine hydroxyl side chain (S203A) may expose the guanidinium of R206 and permit a more efficient binding of the *Z*-dienelactone (Figure 22).

5.3.1.2 *S203H mutant*

The serine to histidine mutation at position 203 replaces the relatively small side chain

of a serine with a bulkier side chain which might be expected to result in difficulties in substrate binding or in the reaction of the substrate once bound. The S203H mutation reduced k_{cat} to 450 min^{-1} from the rate observed for the wt enzyme (1120 min^{-1}) in the hydrolysis of the *Z*-dienelactone. The K_m value was substantially increased to 160 ± 10 μM, an approximate 15 fold increase. This results in an overall decrease in k_{cat}/K_m of 36 fold which is mainly attributed to a decrease in the enzyme-substrate affinity.

The observed change in k_{cat} with the S203H mutation (approximately 2.5 fold decrease) suggests that the size of the histidine side chain near the position of the substrate carboxylate does not substantially affect the reaction of the *Z*-dienelactone once bound. The substantial decrease in the stability of the Michaelis complex for the S203H enzyme is consistent with the proposal that a bulkier side chain at position 203 interferes with the formation of this complex.

5.3.1.3 *S203D mutant*

Replacing the S203 residue with an aspartate (S203D) by site-directed mutagenesis was used to determine what effect a negative charge would have at this position. The S203D mutant enzyme shows a substantial decrease in the k_{cat} value (12 min^{-1}) by 93 fold compared to that of the wt enzyme. The K_m value of the S203D mutant increased 460 fold to 5065 ± 400 μM from the K_m value (11 ± 0.5 μM) of the wt enzyme. Clearly, this mutation affects both the binding and the reaction of the substrate once bound, that when combined, correspond to an approximate 43000 fold decrease in the k_{cat}/K_m value.

If the serine at position 203 in the wt enzyme is within hydrogen bonding distance of the substrate carboxylate, as mentioned above, replacing this serine with an aspartate (S203D) would introduce a negative charge that would result in electrostatic repulsion between this side chain and the substrate carboxylate. In this regard, the S203D mutation can affect both the formation of the Michaelis complex and the reaction of the *Z*-dienelactone once bound. Consistent with this proposal, the low k_{cat} for the S203D

mutant demonstrates the problem associated with the reaction of the substrate once bound. The proposed close proximity of the substrate carboxylate to the carboxylate of D203 also results in a substantial increase in K_m for the S203D mutant, in agreement with the expected effects of an aspartate at position 203 on the stability of the Michaelis complex.

5.3.2 **Hydrolysis of the *E*-dienelactone**

5.3.2.1 *S203A mutant*

The S203A mutant has a k_{cat} value for the hydrolysis of the *E*-dienelactone of 510 min^{-1} which is less than a 2 fold decrease when compared to that of the wt enzyme. The K_m value (390 ± 12 μM) for this mutant protein is not substantially different from that of the wt enzyme (184 ± 12 μM). Further indication of the similarity of the hydrolysis of the *E*-dienelactone by the S203A mutant and the wt enzyme is that there is only a 4 fold difference in k_{cat}/K_m.

As discussed above, the mechanism for the hydrolysis of the *E*-dienelactone by DLH was determined only through modelling studies with the available X-ray crystallographic data. The k_{cat} and K_m values for the hydrolysis of the *E*-dienelactone by the S203A mutant are similar to those values for the wt enzyme. Therefore, the serine at position 203 in the wt enzyme is of little significance in the proposed mechanism for the hydrolysis of the *E*-dienelactone.

5.3.2.2 *S203H mutant*

The S203H mutant enzyme demonstrates a substantial reduction in k_{cat} of 33 fold to 26 min^{-1} compared to that of the wt enzyme. This mutation also substantially increased the K_m value by 37 fold to 6870 ± 71 μM compared to that of the wt enzyme. This results in an overall decrease in the k_{cat}/K_m value by 1250 fold. To reduce the error in

the values generated for k_{cat} and K_m the data were fit to a sigmoidal curve.

As discussed above, the bulk of a histidine side chain could result in a decrease in substrate binding and its reaction once bound. The data presented here for k_{cat} and K_m for the hydrolysis of the *E*-dienelactone by the S203H mutant enzyme support this proposal.

5.3.2.3 *S203D mutant*

The S203D mutant demonstrates a reduction in k_{cat} (4 min^{-1}) of 218 fold with a substantially increased K_m value (6190 ± 275 μM) of 34 fold when compared to those values of the wt enzyme. Overall, a decrease in k_{cat}/K_m by approximately 7300 fold is observed for the hydrolysis of the *E*-dienelactone.

As discussed above, replacing the serine with an aspartate at position 203 places a carboxylate side chain within a short distance of the substrate carboxylate. This can have an adverse effect on substrate binding and reaction of the substrate once bound. In agreement with this proposal, the affect of these two carboxylates being a close distance from one another is illustrated by the observed low k_{cat}. Additionally, K_m is substantially increased with this mutant protein suggesting that the aspartate carboxylate is too close to the carboxylate of the *E*-dienelactone when forming the Michaelis complex.

5.3.3 **Summary of the hydrolysis of the *E*- and *Z*-dienelactones by S203 mutant enzymes**

The proposed role that S203 has in DLH in the hydrolysis of dienelactone was studied using site-directed mutagenesis and kinetic analysis of the mutant proteins. Serine 203 is proposed to bind to the substrate carboxylate in forming the Michaelis complex. This role is not supported by the kinetic data presented here. The results presented here are

inconsistent with this proposal. It appears that mutation of the serine to an alanine exposes the R206 guanidinium that enhances binding of the *Z*-dienelactone. Binding of the *E*-dienelactone is not affected. The kinetic analysis of the S203 mutants does provide some insights into a difference in the positioning of the *E*- and *Z*-isomers in the enzyme active site. This is demonstrated by the large differences in the k_{cat} and K_m values for the hydrolysis of the dienelactone isomers by the S203H and S203D mutant proteins.

5.4 Conclusion

The results presented in this chapter have increased the understanding of the catalytic mechanism of DLH in the hydrolysis of both the natural substrates *E*- and *Z*-dienelactone. The kinetics of DLH in the hydrolysis of the *Z*-dienelactone are in general agreement with the mechanism proposed by X-ray crystallography. One notable exception is the role that S203 has in substrate hydrolysis where mutation of this side chain to an alanine produced a more efficient enzyme for the hydrolysis of the *Z*-dienelactone. The important catalytic residues identified in the hydrolysis of the *Z*-dienelactone are also utilised in the hydrolysis of the *E*-dienelactone by DLH. However, it is not completely clear how the binding of this substrate in the active site is related to reaction of this substrate once bound given that the *E*-isomer does not interact with R206 in the Michaelis complex; the key residue that couples substrate binding to the reaction of the *Z*-dienelactone once bound. It may be that the active site undergoes a conformational change after binding of the *E*-dienelactone so that the enzyme can proceed through to the catalytic step of the reaction and hydrolyse this substrate.

Chapter 6

Kinetic analysis of the reactions of the *E*- and *Z*-dienelactones catalysed by C123S and C123D mutant enzymes

The kinetic analysis of the wt and DLH mutant proteins described in Chapter 5 has increased the understanding of the catalytic mechanism of DLH. These proteins retained the cysteine nucleophile. As discussed in the Introduction, the C123S mutant enzyme was mainly used for the elucidation of the catalytic mechanism of DLH in the X-ray crystal structure bound with the *Z*-dienelactam. In the literature it has been reported that this mutant protein interacts with the *E*-dienelactone at approximately 20% of the k_{cat} value of the wt enzyme (Pathak *et al.*, 1991). This amount of activity is unusual since nucleophilic substitution in enzymes normally results in a 10^5 to 10^6 fold reduction in their activity toward normal ester and amide substrates (Higaki *et al.*, 1989; Neet and Koshland, 1966; Polgár and Bender, 1966; Yokosawa, 1977). The purpose of the work described in the first part of this chapter was to investigate the kinetics of the interactions of the *E*- and *Z*-dienelactones with C123S and site-directed mutants, and in the second part to investigate the interaction of the *E*-dienelactone with C123D, in order to probe the catalytic mechanism of these active site mutants.

6.1 Observation of isomerase and not hydrolase activity by the C123S mutant enzyme

The general procedure for monitoring the activity of DLH is by the rate of the decrease in the absorbance of the lactone substrates against time. Monitoring the time course for the reaction of the *E*-dienelactone with the C123S mutant enzyme by UV spectroscopy shows a decrease in absorbance. This is in agreement with the hydrolysis of either dienelactone to form the product, maleylacetate. When using the *Z*-dienelactone as substrate, the change in absorbance was close to negligible at the substrate concentration

(500 μM) and enzyme concentration (1μM) initially used (similar to that for the reaction of the *E*-dienelactone). An approximately 10 fold increase in the substrate and C123S concentrations resulted in a clear difference in the absorbance change between that expected for hydrolysis of the *Z*-dienelactone and the reaction that was occurring here. Instead of observing the expected decrease in the absorbance over time with this substrate, there was an increase. This is in contrast to that presented for the *E*-dienelactone.

To examine this unusual and unexpected behaviour, the reaction of the *Z*-dienelactone with the C123S mutant enzyme was then followed by thin layer chromatography. This technique showed that in addition to the substrate (*Z*-dienelactone) the reaction product contained a component with an R_f value which corresponded to the *E*-dienelactone. To further clarify this result, the reaction was followed by reverse-phase HPLC using a diode array detector. A comparison of the retention times of the substrate and the product formed in the reaction with those of the *E*- and *Z*-dienelactone standards confirmed the appearance of the *E*-dienelactone as the product. A similar experiment using the *E*-dienelactone as the substrate was followed and showed that the product formed was the *Z*-dienelactone. Appropriate control experiments established that the reaction was being catalysed by the C123S mutant enzyme and was not from the spontaneous isomerisation of the lactones. Further confirmation of the isomerase activity by the C123S mutant was by ^{1}H NMR spectroscopy. Using the *E*-dienelactone as substrate, the observed chemical shifts in the spectrum of the product were consistent with the formation of the *Z*-dienelactone as the product. These three techniques used for the analysis of the reaction of dienelactone with C123S provide unequivocal evidence for the isomerase activity of this protein, which may therefore be called dienelactone isomerase (DLI), and not a hydrolase as previously assumed (Pathak *et al.*, 1991)

6.2 Kinetic analysis of the isomerase activity of DLI by HPLC

The isomerase activity by the C123S mutant enzyme (dienelactone isomerase) of the *E*- and *Z*-dienelactones was further characterised using HPLC and the results are shown in Figure 23. The hydrolysis of the lactones by wt DLH is illustrated in Figure 24. The data were collected in 20 mM HEPES buffer containing 1 mM EDTA, at pH 7.0 and 25 °C. At designated time periods, an aliquot of the reaction mix was injected onto a reverse-phase column and the eluent was monitored at 210 nm and 280 nm in 10% acetonitrile (ACN) and 0.1% trifluoroacetic acid (TFA) in water. TFA is used to protonate the substrate carboxylate.

As shown, an equilibrium is obtained for the interconversion of the dienelactones by dienelactone isomerase (DLI), in a ratio of 53:47 (*E*:*Z*) with little, if any, hydrolysis of either substrate. The reaction of the *E*- and *Z*-dienelactones with wt DLH shows only their hydrolysis to the product maleylacetate.

As discussed in the Introduction, it is proposed that DLH reacts with dienelactone to form a thioester intermediate. This intermediate is hydrolysed with release of the product, as shown in Scheme 3. In principle, DLI could react in quite a different manner, by reversible Michael addition of the enzyme's active site serine to the enolic carbon (C4) of the lactones, with isomerisation. However, this mechanism seems implausible, since a similar process involving the thiolate of DLH would be more likely to lead to isomerisation if that was the case, and the distance between the serine oxygen of DLI and the enolic carbon of the lactone substrates is likely to be too great. The crystal structure of the *Z*-dienelactam bound in the active site of DLI indicates this distance is 4.2 Å (Cheah *et al.*, 1993a).

The lack of hydrolysis of the acyl enzyme by DLI may indicate that water is not available, at least in the correct orientation, in the active site. Alternatively, it could be due to non-productive collapse of the second tetrahedral intermediate (Wilke *et al.*,

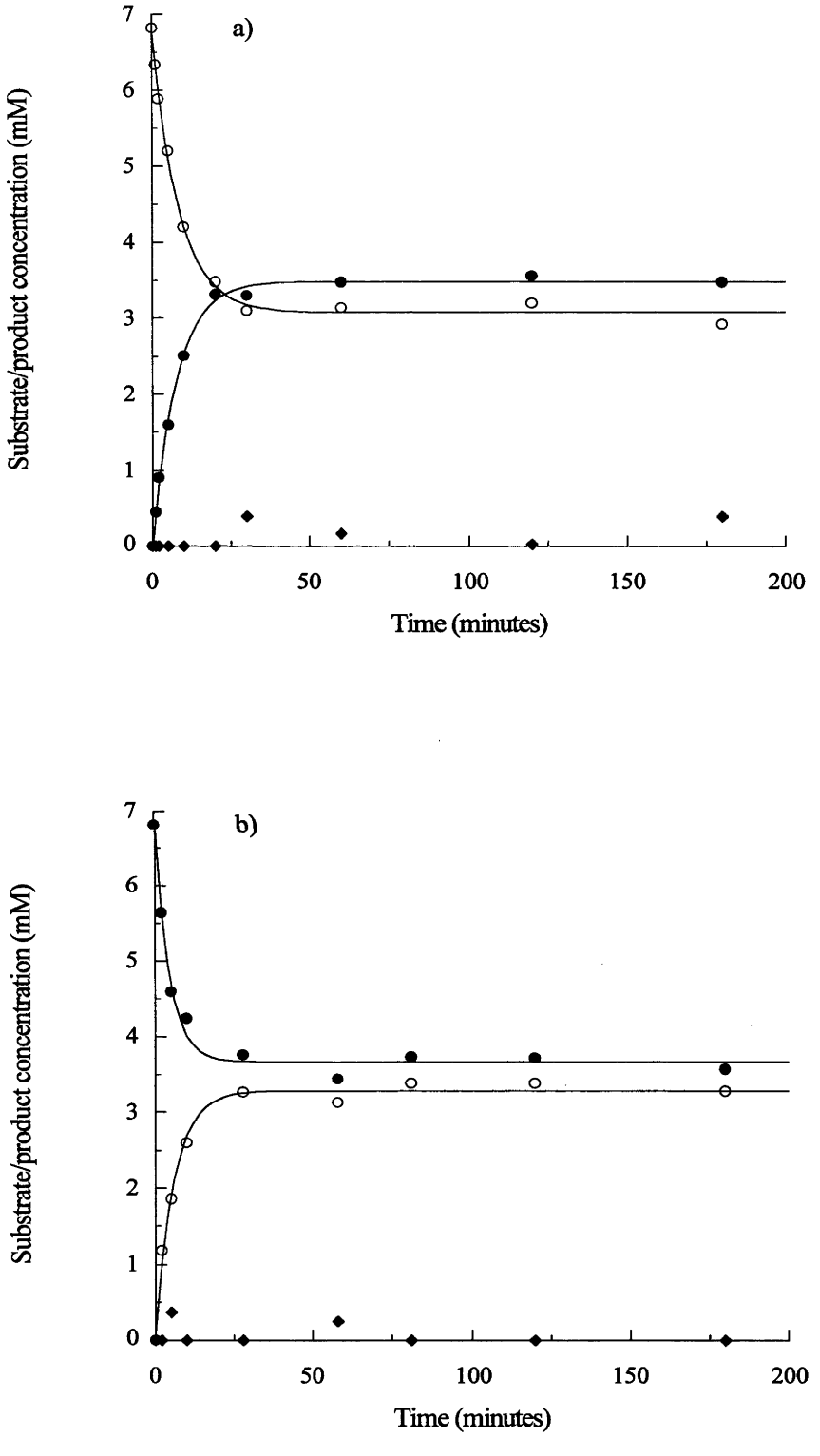

Figure 23. Concentrations of the *Z*-dienelactone (○), the *E*-dienelactone (●) and the hydrolytic product (◆) after reaction of a) the *Z*-dienelactone and b) the *E*-dienelactone with DLI (10.7 μM), as determined by HPLC.

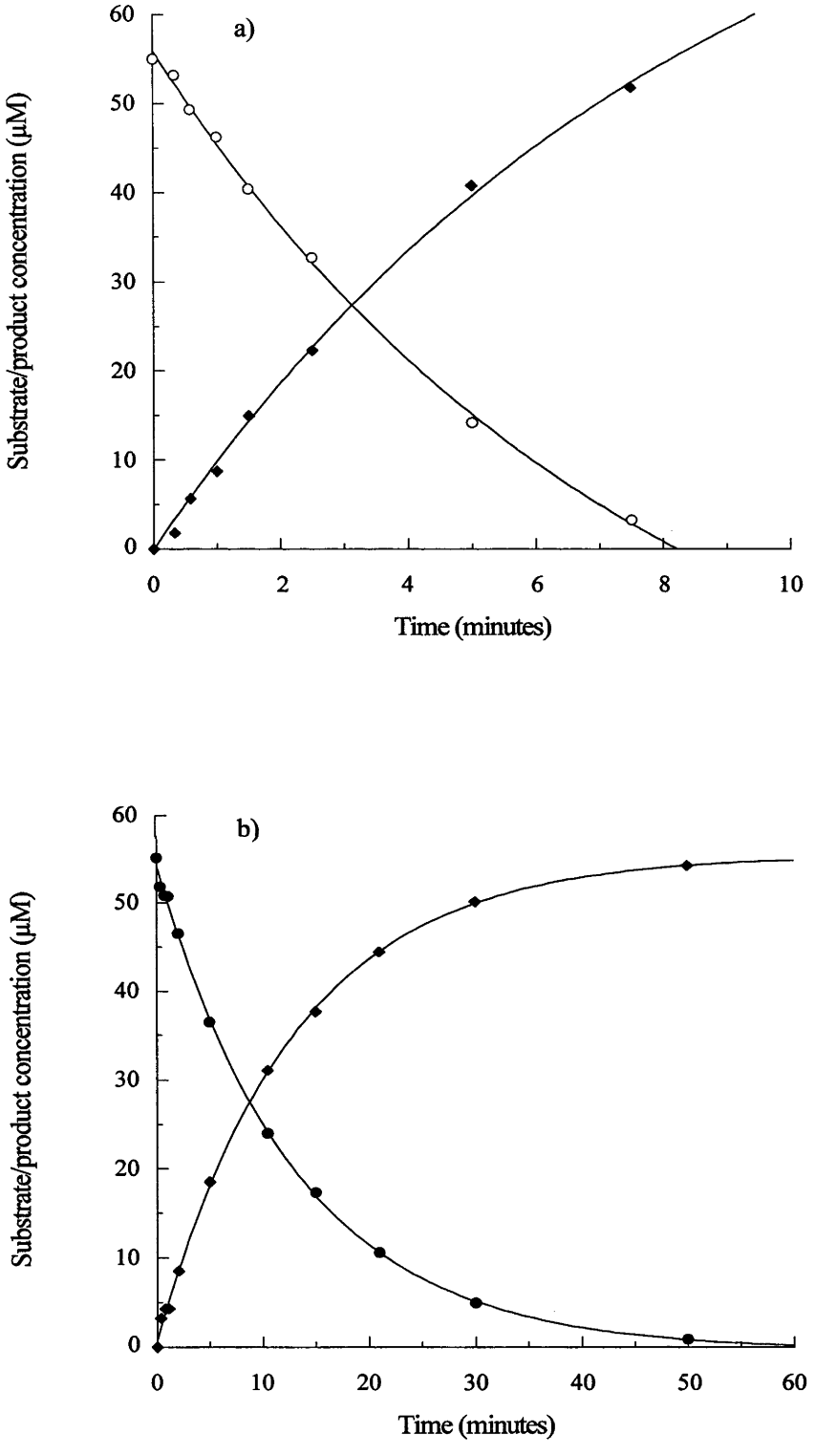

Figure 24. Concentrations of the *Z*-dienelactone (○), the *E*-dienelactone (●) and the hydrolytic product (◆) after reaction of a) the *Z*-dienelactone with DLH (12 nM) and b) the *E*-dienelactone with DLH (20 nM), as determined by HPLC.

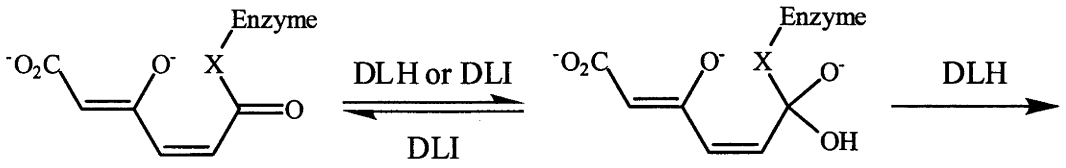

Scheme 3. Formation and collapse of the second tetrahedral intermediate. DLH, X = S; DLI, X = O.

1991). Whereas the second tetrahedral intermediate of DLH will readily collapse with loss of the thiolate group, this intermediate in DLI should most readily lose hydroxide and revert to the acyl enzyme intermediate which could then recyclise (Scheme 3). Irrespective of the mechanism, it is clear there is a difference between the catalytic reaction of the dienelactones by DLH and DLI.

6.3 Kinetic analysis of the isomerisation of the *E*- and *Z*-dienelactones by DLI using UV spectroscopy

The kinetic data characterising the interaction of the *E*- and *Z*-dienelactones with DLI are summarised in Table 16. The data were collected in 20 mM HEPES buffer containing 1 mM EDTA, at pH 7.0 and 25 °C. It should be noted that there was deviation from Michaelis-Menten kinetics at low substrate concentrations for the isomerisation of the *E*-dienelactone. This deviation resulted in a sigmoidal-shaped and not the typical hyperbolic-shaped curve. This will be discussed later in more detail.

6.3.1 Isomerisation of the *Z*-dienelactone

The active site C123S mutant protein (DLI) isomerised the *Z*-dienelactone to the *E*-isomer with a k_{cat} value of 11 ± 0.2 min^{-1} and a binding constant (K_m) of 2.6 ± 0.1 mM.

A comparison of the k_{cat} value for the isomerisation of the *Z*-dienelactone to the *E*-isomer by DLI with that for the hydrolysis of the *Z*-dienelactone by DLH is not

Table 16. Kinetic data for the isomerisation of the *E*- and *Z*-dienelactones by DLI.

	Z-dienelactone		*E*-dienelactone[#]	
	k_{cat} (min^{-1})	K_m (mM)	k_{cat} (min^{-1})	$K^h_{0.5}$ (mM)
DLI	11 ± 0.2	2.6 ± 0.1	38 ± 1	4.4 ± 0.2

[#] These data were best fit to the Hill equation (Hill, 1910) by non-linear regression to give the best estimates of the V_{max} and $K^h_{0.5}$ values.

sensible because of the different reactions that these two proteins catalyse. A comparison can be made with the K_m values which represent substrate binding in each case. The K_m value of DLI (2.6 ± 0.1 mM) is increased substantially by 236 fold compared to that of DLH (11 ± 0.5 μM).

As mentioned above, DLI was used for X-ray crystallography to help elucidate the catalytic mechanism of DLH. No catalytic activity of the mutant protein with the *Z*-dienelactone has previously been reported. In the crystal structure of this protein without inhibitor the hydroxyl group of S123 was shown to be in the proposed active conformation ready to acylate the incoming substrate (Cheah *et al.*, 1993a; Cheah *et al.*, 1993b). In the C123S mutant protein bound with the *Z*-dienelactam inhibitor, the distances between the serine side chain Oγ and the acyl carbon (2.5 Å) and Oγ and the carbonyl oxygen (2.3 Å) are approximately 0.3 Å below the ideal van der Waals separations for these atoms (Cheah *et al.*, 1993a). The short distances between S123 and the substrate may explain the substantial increase in the K_m value of DLI compared to that of DLH.

6.3.2 **Isomerisation of the *E*-dienelactone**

The kinetic data for the isomerisation of the *E*-dienelactone to the *Z*-isomer were fit to the Michaelis-Menten equation by non-linear regression using the modification of Hill (Hill, 1910) and are shown in Figure 25. In Equation 6, V_{max} retains its usual meaning of

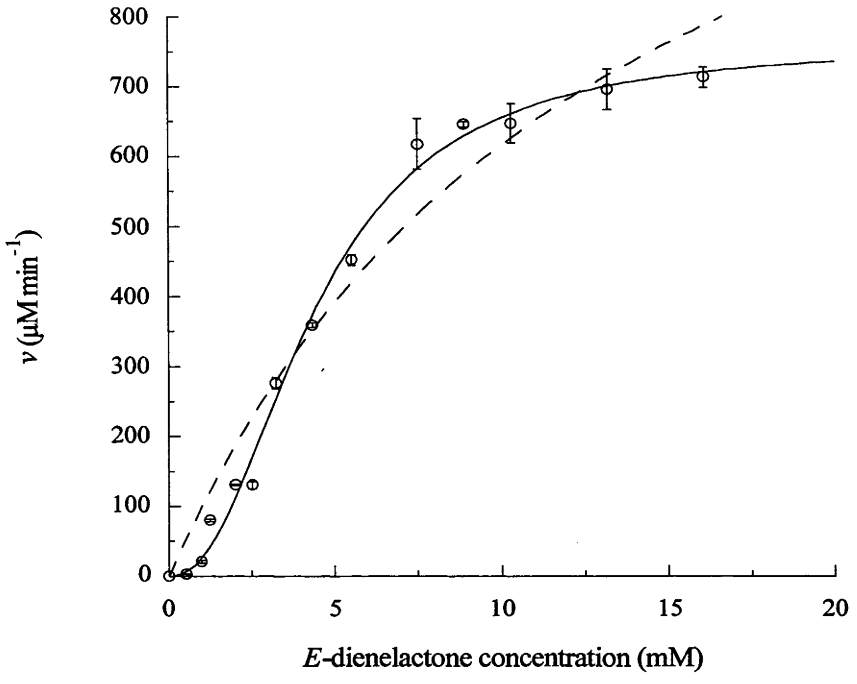

Figure 25. Isomerisation of the *E*-dienelactone by DLI. Shown is the theoretical fit of the data to the Hill equation (—) and to the Michaelis-Menten equation (---). The data points shown at each substrate concentration are the average and standard deviation of 3 replicates.

$$v = \frac{V_{max} \times s^h}{K^h_{0.5} + s^h} \qquad (6)$$

defining the limiting rate of the catalytic reaction. Although $K^h_{0.5}$ equates to 0.5 x V_{max}, its concentration is dependent on the power h and therefore cannot be considered to represent the same value as K_m (Cornish-Bowden, 1995).

DLI isomerised the *E*-dienelactone to the *Z*-isomer with a k_{cat} of 38 ± 1 min^{-1}. The $K^h_{0.5}$ value is 4.4 ± 0.2 mM which is approximately 24 fold higher than the K_m value of DLH (Table 16).

A comparison of the literature k_{cat} value (Pathak *et al.*, 1991) with that obtained here is not sensible because the literature value for the C123S mutant assumed hydrolysis of the *E*-dienelactone and not isomerisation. The literature 'K_m' value for the interaction of

DLI with the *E*-dienelactone is reported to be 9.9 ± 2.3 mM (Pathak *et al.*, 1991). This value is more than 2 fold higher than that obtained here. It is possible that the presence of a sigmoidal-shaped curve was not observed earlier resulting in the higher value (and the correspondingly high error) in the literature than that obtained here.

As discussed above, steric interactions in the active site of DLI with the *Z*-dienelactone may result in the substantially increased K_m value compared to that of DLH. It is possible that similar interactions occur with the *E*-dienelactone. The high binding constant of the *E*-dienelactone with DLI compared to that of DLH may reflect similar steric interactions.

6.3.2.1 *Active site conformational change when isomerising the E-dienelactone*

In Chapter 5 it was proposed that a conformational change in the active site of DLH is required for the hydrolysis of the *E*-dienelactone. It is shown here that the isomerisation of the *E*-dienelactone to the *Z*-isomer shows a clear deviation from Michaelis-Menten kinetics (Figure 25). It is likely that an active site conformational change also occurs in DLI when interacting with the *E*-dienelactone.

6.3.3 Summary of the isomerase activity of DLI with the *E*- and *Z*-dienelactones

The interaction of the *E*- and *Z*-dienelactones with DLI has been studied by kinetic analysis in solution. It is clearly shown that DLI catalyses the interconversion of the lactones and not their hydrolysis, as previously assumed. There is little, if any, hydrolysis of the dienelactones. The binding constants for the *E*- and *Z*-dienelactones with DLI are substantially higher than those of DLH, possibly as a result of steric interactions of the substrates with the serine nucleophile in the Michaelis complex. There is a non-linear dependence of DLI for reaction with the *E*-dienelactone. It may be that the active site undergoes a conformational change on binding the *E*-dienelactone so

that DLI can proceed through to the catalytic step of the reaction and isomerise this substrate.

6.4 Kinetic analysis of the reactions of the *E*- and *Z*-dienelactones catalysed by DLI mutants

To further characterise the isomerase activity of DLI, selected mutants were used to assess the contribution of specific side chain residues to this behaviour.

6.4.1 Reaction of the *Z*-dienelactone analysed using HPLC

The interactions of DLI R206A and DLI R81A with the *Z*-dienelactone were characterised using HPLC and the results are shown in Figures 26 and 27. The data were collected in 20 mM HEPES buffer containing 1 mM EDTA, at pH 7.0 and 25 °C, and the reactions were monitored by HPLC, as described above for DLI.

It is evident that the isomerase activity of the DLI R206A and R81A mutants occurs in conjunction with hydrolysis.

6.4.2 Reaction of the *Z*-dienelactone analysed using UV spectroscopy

The kinetic data characterising the isomerisation and hydrolysis of the *Z*-dienelactone by DLI mutants are summarised in Table 17. The data were collected in 20 mM HEPES buffer containing 1 mM EDTA, at pH 7.0 and 25 °C. The rates of isomerisation and hydrolysis were determined from the difference in the absorbance of the reaction mixtures *vs* time and the extinction coefficients of the reactants and products, as well as the ratio of product formation as determined by HPLC. It should be noted that the R206A and R81A mutants displayed a burst when isomerising the *Z*-dienelactone to the *E*-isomer which will be discussed later in more detail. The kinetic data presented in Table 17 were derived from the steady-state portion of the progress curve only.

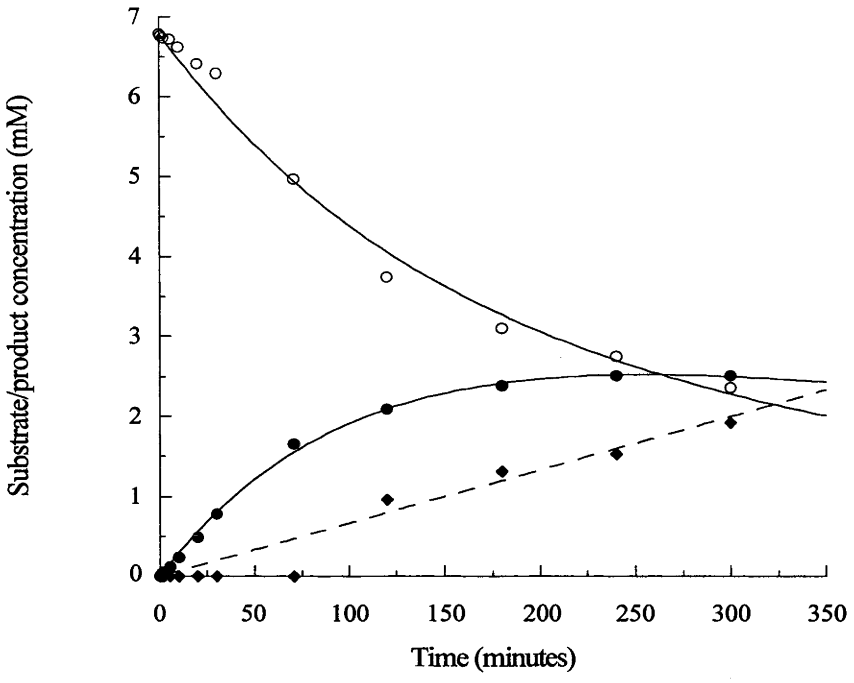

Figure 26. Concentrations of the *Z*-dienelactone (○), the *E*-dienelactone (●) and the hydrolysis product (◆) after reaction of the *Z*-dienelactone with DLI R206A (80.0 μM), as determined by HPLC.

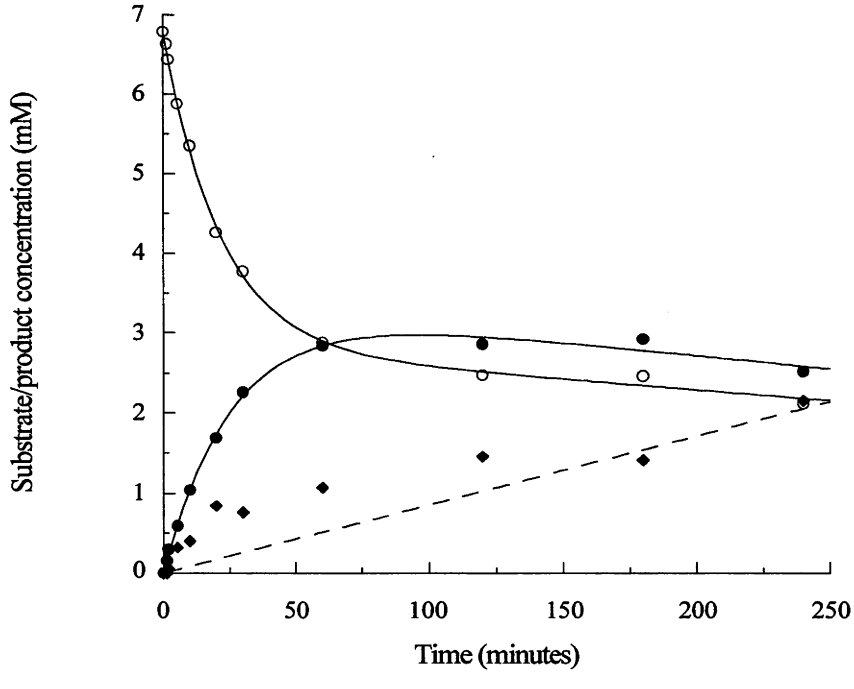

Figure 27. Concentrations of the *Z*-dienelactone (○), the *E*-dienelactone (●) and the hydrolysis product (◆) after reaction of the *Z*-dienelactone with DLI R81A (59.7 μM), as determined by HPLC.

Table 17. Kinetic data for the interaction of DLI R206A and DLI R81A with the *Z*-dienelactone.

	Z-dienelactone		
	Isomerisation k_{cat} (min^{-1})	Hydrolysis k_{cat} (min^{-1})	K_m (mM)
DLI	11 ± 0.2	≤0.01	2.6 ± 0.1
DLI R206A	1.4 ± 0.1	0.4 ± 0.1	36.2 ± 3.5
DLI R81A	4.6 ± 0.3	0.4 ± 0.3	8.6 ± 1.5

6.4.2.1 *DLI R206A mutant*

The DLI R206A mutant enzyme shows a substantial reduction in the k_{cat} value (1.4 ± 0.1 min^{-1}) for isomerisation by approximately 8 fold compared to that of the parent protein (DLI). The k_{cat} for hydrolysis is estimated to be 0.4 ± 0.1 min^{-1}. The K_m value (36.2 ± 3.5 mM) was increased substantially by approximately 14 fold when compared to that value of DLI.

As discussed in Chapter 5, the R206A DLH mutant enzyme has a substantially increased K_m value when compared to that of the wt enzyme suggesting the importance of R206 for binding the *Z*-dienelactone. This effect parallels the effect seen here for DLI R206A and DLI where a substantial increase in the K_m value is evident for the double mutant. This suggests that the side chain of R206 is also important for binding the *Z*-dienelactone in DLI.

As discussed in the Introduction, during the hydrolysis of the *Z*-dienelactone by wt DLH it is proposed that the enolate formed after the breakdown of the first tetrahedral intermediate participates in the hydrolysis of the acyl enzyme. As mentioned above, the isomerase activity of DLI may result from the water molecule used in deacylation not being in the correct orientation for hydrolysis or that there is non-productive

collapse of the second tetrahedral intermediate with loss of hydroxide. It is possible that the role of R206 in the reaction of the *Z*-dienelactone once bound may be to secure the position of the acyl enzyme intermediate, and hence the enolate, through the ionic interaction it has with the substrate carboxylate (Figure 28). If the enolate is not correctly held in position by this ionic interaction, the enolate may be too far away to attack the acyl carbon of the ester. This would effectively increase the life-time of the acyl enzyme intermediate and, therefore increase the probability of hydrolysis with DLI R206A.

6.4.2.2 *DLI R81A mutant*

The k_{cat} value (4.6 ± 0.3 min^{-1}) for the isomerisation of the *Z*-dienelactone to the *E*-isomer by the DLI R81A mutant is decreased slightly (2.4 fold) compared to that value for DLI. The k_{cat} for the hydrolysis is estimated to be 0.4 ± 0.3 min^{-1}. The K_m value (8.6 ± 1.5 mM) has increased by 3.3 fold compared to that of the parent protein (DLI).

As discussed in Chapter 5, the side chain of R81 is proposed to bind the carboxylate of the *Z*-dienelactone when forming the Michaelis complex. The increase observed here for the K_m value from the R81A mutation is consistent with this role of R81. The presence of some hydrolysis of the *Z*-dienelactone with the R81A mutant suggests that R81 is also involved in securing the position of the enolate in the acyl enzyme intermediate probably *via* an ionic interaction with the substrate carboxylate (Figure 28).

It appears that the results presented above for DLI R206A and DLI R81A compared to those of DLI indicate some important trends. The substantial increase in K_m (14 fold) for DLI R206A parallels a large decrease in k_{cat} for isomerisation (8 fold). A competing hydrolysis reaction occurs that is 3.5 fold less fast than the rate for isomerisation. This is in contrast to DLI R81A where a moderate increase in K_m parallels a moderate decrease in k_{cat} for isomerisation with a competing hydrolysis reaction that is 11.5 fold less fast than the rate for isomerisation. It is clear that when R206 is mutated to an

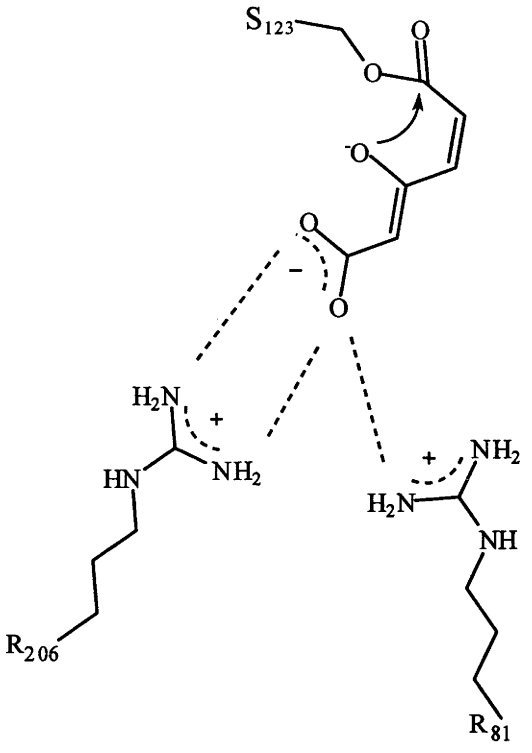

Figure 28. Securing the position of the enolate in the acyl enzyme intermediate by ionic interactions with R206 and R81.

alanine the ability of DLI to secure the position of the enolate in the acyl enzyme intermediate is decreased more than that of the R81 mutation. This effect is reflected in the ratio of isomerisation to hydrolysis for the two mutant proteins.

6.4.2.3 *Observation of a burst with the arginine mutants of DLI when reacting with the Z-dienelactone*

As mentioned above, the reactions of the *Z*-dienelactone when using the DLI R206A and DLI R81A mutants result in the observation of burst kinetics.

As discussed above, interconversion of the lactones probably occurs *via* the ring-opened acyl enzyme intermediate. In this case, the observed burst does not correspond to the formation of the acyl enzyme intermediate because this intermediate is expected to have

negligible absorbance in the wavelength region used in this study (Schlömann *et al.*, 1990). The burst, then, probably relates to the formation of the *E*-dienelactone from the *Z*-isomer. At low substrate concentrations the burst size approximates to the concentration of enzyme and it is proposed that this burst corresponds to the rapid stoichiometric formation of the *E*-dienelactone product. The steady-state region of the progress curve is proposed to be the rate-determining release of product from the enzyme.

Therefore, to relate the above burst kinetics to the reaction of the *Z*-dienelactone with DLI R206A and DLI R81A, Scheme 4 is proposed. In this scheme k_2 represents the rate of formation of the *E*-dienelactone product (EP) with k_3 representing the rate of product release from the enzyme. It is assumed that k_1 and k_{-1} are rapid compared to k_2 and k_3. The reversible nature of the isomerisation reaction necessitates the addition of two further rates (k_{-2} and k_{-3}) which are assumed in the burst phase to be unimportant compared to k_2 and k_3.

$$E + S \underset{k_{-1}}{\overset{k_1}{\rightleftharpoons}} ES \underset{k_{-2}}{\overset{k_2}{\rightleftharpoons}} EP \underset{k_{-3}}{\overset{k_3}{\rightleftharpoons}} E + P$$

Scheme (4)

The kinetic data characterising the interaction of the *Z*-dienelactone with DLI R206A and DLI R81A during the burst and steady-state phases are summarised in Table 18. The data were collected as described above. In the examples shown, the reactions were carried out at concentrations of the *Z*-dienelactone that approximated the K_m value for both the DLI R206A and DLI R81A mutants. The data were normalised to the maximum catalytic rate (that is, to the estimated k_{cat} value, as determined above).

The rate of k_2 for the isomerisation of the *Z*-dienelactone to the *E*-isomer is estimated to

Table 18. Estimation of the rate constants for the isomerisation of the *Z*-dienelactone to the *E*-isomer by the arginine mutants of DLI.

	k_2 (min^{-1})	k_3 (min^{-1})	k_2/k_3
DLI R206A	370 ± 83	1.62 ± 0.02	228
DLI R81A	152 ± 32	2.91 ± 0.11	52

be 370 ± 83 min^{-1} for the DLI R206A mutant. The rate of k_3 (1.62 ± 0.02 min^{-1}) is in good agreement with the k_{cat} value (1.4 ± 0.1 min^{-1}) obtained above from the full kinetic analysis of this mutant protein. The rate of k_2 is 228 fold greater than that of k_3.

The rate constant for the isomerisation of the *Z*-dienelactone to the *E*-isomer (k_2) by the DLI R81A mutant is 152 ± 32 min^{-1}. The rate of k_3 for this mutant is 2.91 ± 0.11 min^{-1} which is slightly lower than the rate determined above for k_{cat} (4.6 ± 0.3 min^{-1}). The rate of k_2 is 52 fold greater than that of k_3.

It is clear that the rate of formation of the *E*-dienelactone from the *Z*-isomer exceeds that of its release. It could be that the enzyme undergoes a conformational change to release the product but there is no direct evidence for or against this hypothesis.

6.4.3 **Reaction of the *E*-dienelactone analysed using HPLC**

The interactions of three mutants of DLI with the *E*-dienelactone were analysed using HPLC, as described above, and the results are shown in Figures 29 and 30. The data were collected in 20 mM HEPES buffer containing 1 mM EDTA, at pH 7.0 and 25 °C. It is clearly shown that the mutants of DLI isomerise the *E*-dienelactone to the *Z*-isomer with competitive hydrolysis.

The kinetic data characterising the reactions of the *E*-dienelactone (6.82 mM) with DLI and mutants determined using HPLC, as described above, are summarised in Table 19. The rate of isomerisation of the *E*-dienelactone by DLI, from Figure 23b above, is

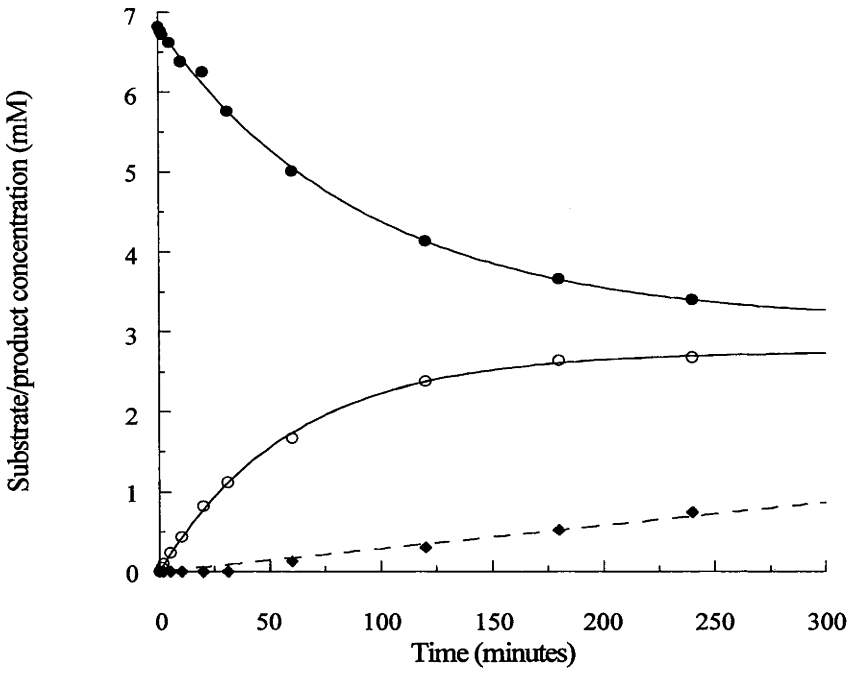

Figure 29. Concentrations of the *Z*-dienelactone (○), the *E*-dienelactone (●) and the hydrolytic product (◆) after reaction of the *E*-dienelactone with DLI R206A (80.0 μM), as determined by HPLC.

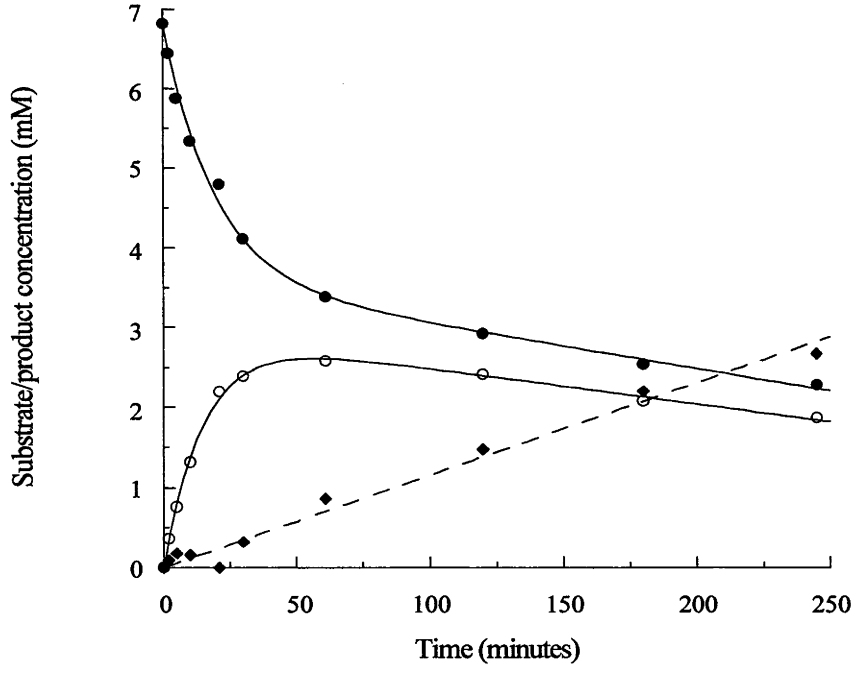

Figure 30. Concentrations of the *Z*-dienelactone (○), the *E*-dienelactone (●) and the hydrolytic product (◆) after reaction of the *E*-dienelactone with DLI R81A (59.7 μM), as determined by HPLC.

shown as a comparison. A full kinetic analysis of the DLI R206A and DLI R81A mutant proteins by UV spectroscopy could not be done because the solubility limit of the *E*-dienelactone was reached (approximately 22 mM) before V_{max} was approached. This limit is substantially below that of the *Z*-dienelactone where V_{max} could be determined for these mutants. Therefore, the reaction of the DLI mutants with the *E*-dienelactone was analysed by HPLC at one substrate concentration (6.82 mM) and the rates of reaction compared relative to that of DLI at the same substrate concentration.

6.4.3.1 *DLI*

The rate of isomerisation of the *E*-dienelactone to the *Z*-isomer by DLI was 4.3 ± 0.72 mM min^{-1} mg^{-1}, as determined from Figure 23b.

6.4.3.2 *DLI R206A mutant*

The DLI R206A mutant isomerised the *E*-dienelactone to the *Z*-isomer at a rate of 0.08 ± 0.002 mM min^{-1} mg^{-1}. This rate is 54 fold less than that of DLI. The rate of hydrolysis increased by at least 6 fold to 0.006 ± 0.0001 mM min^{-1} mg^{-1} compared to that of DLI. The rate of hydrolysis by DLI R206A is approximately 13 fold less than that of isomerisation.

As discussed in Chapter 5, the R206A mutation of DLH did not substantially change the value of K_m when reacting with the *E*-dienelactone. As shown here, the low rate of isomerisation of the *E*-dienelactone by DLI R206A illustrates the importance of R206 for the partitioning of isomerisation from hydrolysis. With the knowledge gained from the reaction of the *Z*-dienelactone catalysed by DLI R206A once bound, it is possible that reaction of DLI R206A with the *E*-dienelactone, once bound, is similar. That is, in the reaction of the bound *E*-dienelactone, the competitive hydrolysis reaction probably occurs as a result of the difficulties in securing the position of the enolate in the acyl enzyme intermediate. Although K_m could not be determined, an ionic interaction

Table 19. Kinetic data for the interaction of DLI and various active site mutants with the *E*-dienelactone.

	Isomerisation ($mM\ min^{-1}\ mg^{-1}$)	Hydrolysis ($mM\ min^{-1}\ mg^{-1}$)	Ratio[#] I:H
DLI	4.3 ± 0.72	≤0.001	≥4310
DLI R206A	0.08 ± 0.002	0.006 ± 0.0001	13
DLI R81A	0.36 ± 0.021	0.03 ± 0.001	12

[#] Ratio of isomerisation to hydrolysis.

between R206 and the substrate carboxylate during the reaction of the substrate once bound probably occurs.

6.4.3.3 *DLI R81A mutant*

The rate of isomerisation by the DLI R81A mutant decreased 12 fold to 0.36 ± 0.021 $mM\ min^{-1}\ mg^{-1}$ from that of the parent protein (DLI). The hydrolysis rate (0.03 ± 0.001 $mM\ min^{-1}\ mg^{-1}$) is at least 30 fold greater than that of DLI. The rate of isomerisation is approximately 12 fold greater than that of hydrolysis.

As discussed in Chapter 5, R81 is important for the formation of the Michaelis complex with the *E*-dienelactone. As mentioned above, no K_m value could be determined here. As discussed above for the *Z*-dienelactone, R81 is important for the reaction of the substrate once bound by partitioning the reaction between isomerisation and hydrolysis. This effect is comparative to that shown here for the reaction of DLI R81A with the *E*-dienelactone. The likely contribution that R81 has in the isomerase activity of DLI with the *E*-dienelactone is to secure the position of the enolate of the acyl enzyme intermediate by an ionic interaction with the substrate carboxylate, as discussed above.

6.4.4. Summary of the reaction of the *E*- and *Z*-dienelactones by DLI mutant enzymes

The R206 and R81 residues are important for the reactions of the *E*- and *Z*-dienelactones where their removal partitions the reactions between isomerisation and hydrolysis. It is proposed that the arginine side chains secure the position of the enolate in the acyl enzyme intermediate so that isomerisation proceeds in preference to the competing hydrolysis reaction.

6.5 Reaction of the *E*- and *Z*-dienelactone *tert*-butyl esters catalysed by DLI analysed using HPLC

As discussed above, the isomerisation of the *E*- and *Z*-dienelactones by DLI and mutants showed that these isomers approached an equilibrium of 53:47 (*E*:*Z*). The precursors to the *E*- and *Z*-dienelactones, in their chemical synthesis, are the *E*- and *Z*-dienelactone *tert*-butyl esters (Figure 31). These esters are formed together in the same reaction mix in a ratio of approximately 26:1 (*E*:*Z*) (Massy-Westropp and Price, 1980). Attempts were made to isomerise the *E*-dienelactone *tert*-butyl ester to the *Z*-isomer (Massy-Westropp and Price, 1980). The reaction proceeded *via* a ring-opened intermediate on treatment with sodium methoxide or sodium ethoxide. Recyclisation of the ring-opened intermediate on silica gel for 17 hours gave the *E*-dienelactone *tert*-butyl ester (21%), the *Z*-dienelactone *tert*-butyl ester (27%) and side products (52%). To assess the chemical versatility of the isomerase activity of DLI, the interaction of the *E*- and *Z*-dienelactone *tert*-butyl esters with DLI was analysed.

The interactions of the *E*- and *Z*-dienelactone *tert*-butyl esters with DLI were analysed using HPLC and the results are shown in Figures 32 and 33. The data were collected in 20 mM HEPES buffer containing 1 mM EDTA, 10% ACN (to solubilise the substrate esters), at pH 7.0 and 25 °C. At designated time periods, an aliquot of the reaction mix was injected onto a reverse-phase column and the eluent was monitored at 210 nm and

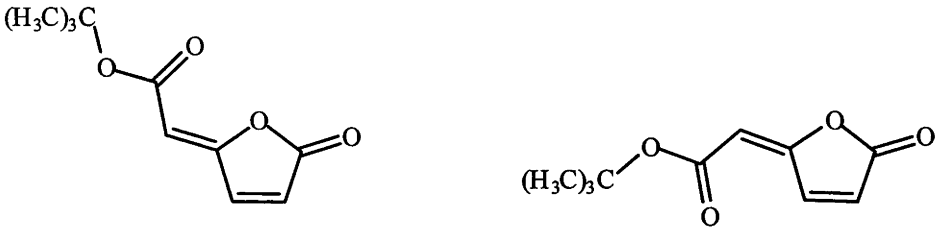

Figure 31. The *tert*-butyl esters of dienelactone.

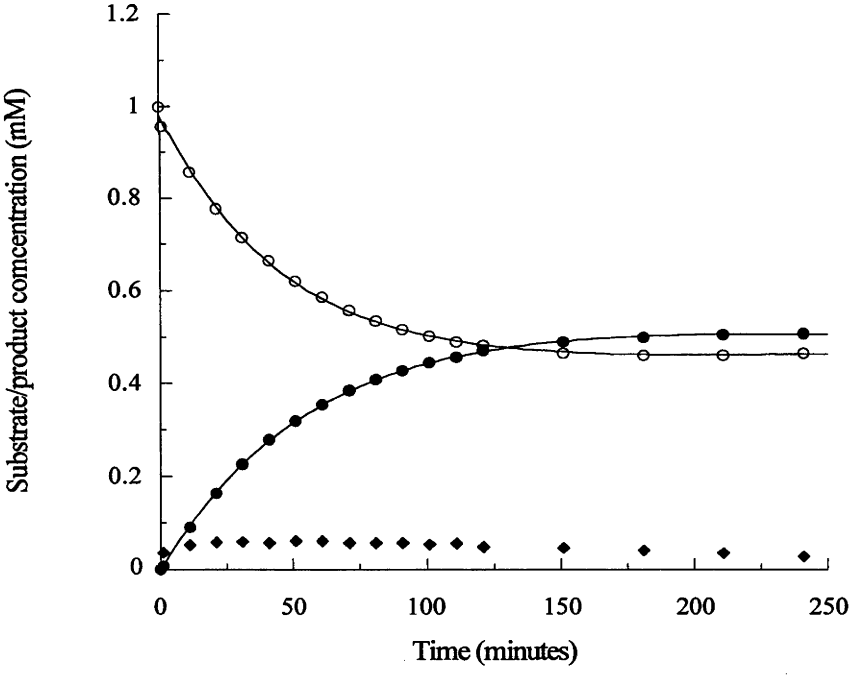

Figure 32. Concentrations of the *Z*-dienelactone *tert*-butyl ester (○), the *E*-dienelactone *tert*-butyl ester (●) and the hydrolysis product (◆) after reaction of the *Z*-dienelactone *tert*-butyl ester with DLI (270 nM), as determined by HPLC.

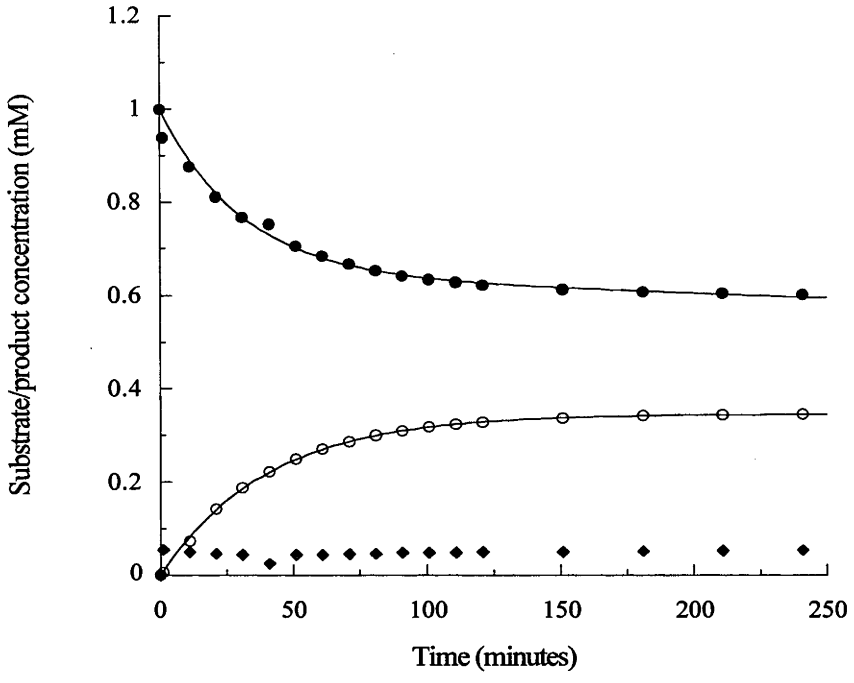

Figure 33. Concentrations of the *Z*-dienelactone *tert*-butyl ester (○), the *E*-dienelactone *tert*-butyl ester (●) and the hydrolysis product (◆) after reaction of the *E*-dienelactone *tert*-butyl ester with DLI (324 nM), as determined by HPLC.

280 nm in 50% ACN in water. It is clearly shown that DLI isomerises the *E*-dienelactone *tert*-butyl ester to the *Z*-isomer.

As shown in Figure 32, the interaction of the *Z*-dienelactone *tert*-butyl ester with DLI results in a ratio of 52:48 for the *E*- and *Z*-isomers, respectively. In Figure 33, the interaction of the *E*-dienelactone *tert*-butyl ester with DLI results in a ratio of 64:36 for the *E*- and *Z*-isomers, respectively. It is clear that an equilibrium for the interconversion of the esters is not obtained. Preliminary studies indicated that enzyme activity is sensitive to ACN concentration. Therefore, it is possible that the enzyme slowly denatured during the reaction of either ester with DLI resulting in an equilibrium not being reached. It is not expected that hydrolysis of either substrate occurred because the level of this product did not increase over the time course of the reaction. In contrast to the above chemical isomerisation, no side products were formed by the enzyme catalysed reaction.

6.5.1 Reaction of the *E*-dienelactone *tert*-butyl ester with DLH analysed using HPLC

The ability of DLI to interconvert the *tert*-butyl esters of dienelactone is unusual given the steric bulk of the *tert*-butyl group. This suggests that the active site of DLI is able to accommodate and react with sterically bulky substrates. With this knowledge about the accessibility of the active site by the *E*- and *Z*-dienelactone *tert*-butyl esters, the interaction of the *E*-dienelactone *tert*-butyl ester with DLH was examined.

The interaction of the *E*-dienelactone *tert*-butyl esters with DLH was analysed using HPLC, as described above for DLI, and the results are shown in Figure 34. The data were collected in 20 mM HEPES buffer containing 1 mM EDTA, 10% ACN (to solubilise the substrate ester), at pH 7.0 and 25 °C. It is clear that DLH interacts with the *E*-dienelactone *tert*-butyl ester.

The identity of the product from the interaction of DLH with the *E*-dienelactone *tert*-butyl ester was uncertain. Treatment of the *E*-dienelactone *tert*-butyl ester with NaOH (17 mM) and analysis of the reaction by HPLC, as above, showed that the retention time for this product corresponded to that of the DLH catalysed reaction. To further identify the product formed from the interaction of the *E*-dienelactone *tert*-butyl ester with DLH, it was extracted from the reaction mix and analysed by ^{1}H NMR spectroscopy. Using an authentic maleylacetate standard (by reacting DLH with the *E*-dienelactone), the observed chemical shifts in the spectrum were consistent with the formation of the *tert*-butyl ester of maleylacetate. To further confirm the structure of this hydrolysis product it was analysed by ESI-MS. The molecular mass of the hydrolysis product corresponded to that of the *tert*-butyl ester of maleylacetate. It is clear, then, that DLH is able to hydrolyse the *E*-dienelactone *tert*-butyl ester to the *tert*-butyl ester of maleylacetate (Figure 35). There was no isomerase activity.

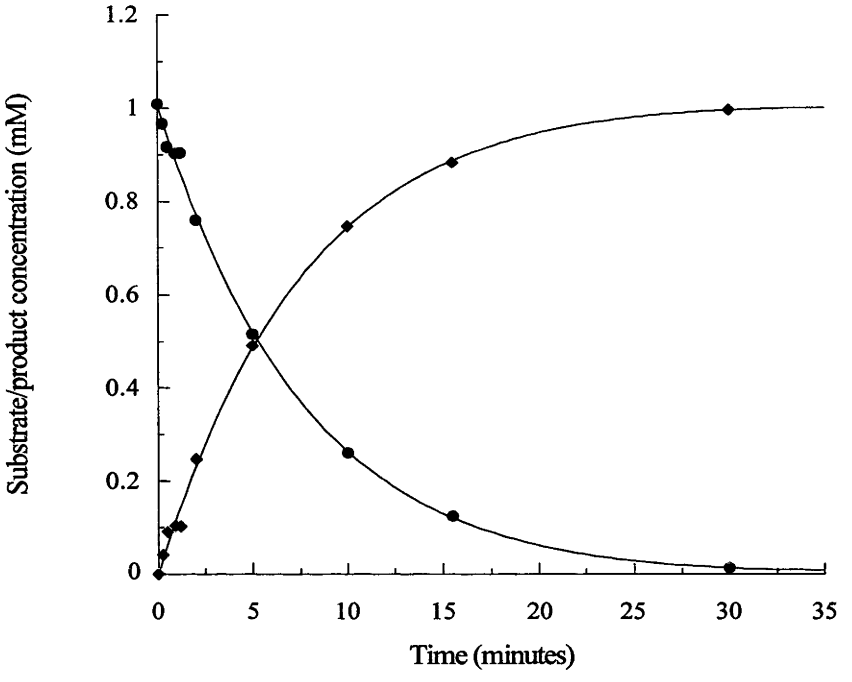

Figure 34. Concentrations of the *E*-dienelactone *tert*-butyl ester (●) and the hydrolytic product (◆) after reaction with DLH (998 nM), as determined by HPLC.

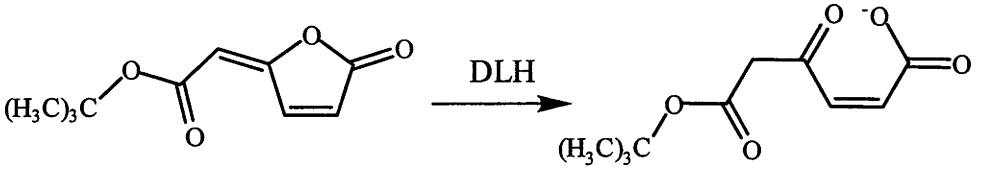

Figure 35. DLH hydrolysis of the *E*-dienelactone *tert*-butyl ester to the *tert*-butyl ester of maleylacetate.

6.6 Kinetic analysis of the C123D mutant

As discussed in the Introduction, DLH is from the α/β hydrolase family of proteins that have a common topology that functions to align the catalytic triad. These triads comprise a nucleophile (C, S, or D), a histidine and an acid (D or E). The catalytic triad of DLH comprises a C, H and a D while in DLI the nucleophile is replaced with a serine (S, H, D). As discussed above, replacement of the cysteine nucleophile of DLH to a serine (DLI) completely changes the catalytic reaction that these two proteins perform. To further investigate the versatility of replacing the nucleophile of DLH to that of another of the α/β hydrolase proteins, the cysteine nucleophile of DLH was mutated to an aspartate (D, H, D catalytic triad).

6.6.1 Reaction of the *E*-dienelactone analysed using HPLC

The interaction of DLH C123D with the *E*-dienelactone was analysed using HPLC, as described above for DLI, and is shown in Figure 36. The data were collected in 20 mM HEPES buffer containing 1 mM EDTA, at pH 7.0 and 25 °C. It is clear that C123D catalyses the isomerisation of the *E*-dienelactone to the *Z*-isomer.

For DLI, the most probable reasons for the isomerase activity are that water is not available, at least in the correct orientation, for hydrolysis of the acyl enzyme or that non-productive collapse of the second tetrahedral intermediate occurs with subsequent reclosure of the lactone ring. This mechanism could also be relevant for the isomerase activity shown by C123D. Alternatively, the reaction of the aspartate of C123D with dienelactone could occur *via* general base hydrolysis by activating a nearby water molecule. Whatever mechanism prevails, it is clear that C123D isomerises the *E*-dienelactone to the *Z*-isomer.

The C123D mutant enzyme isomerised the *E*-dienelactone to the *Z*-isomer at a rate of 3.3 ± 0.2 μM min^{-1} mg^{-1}. Within experimental error, it appears that C123D does not

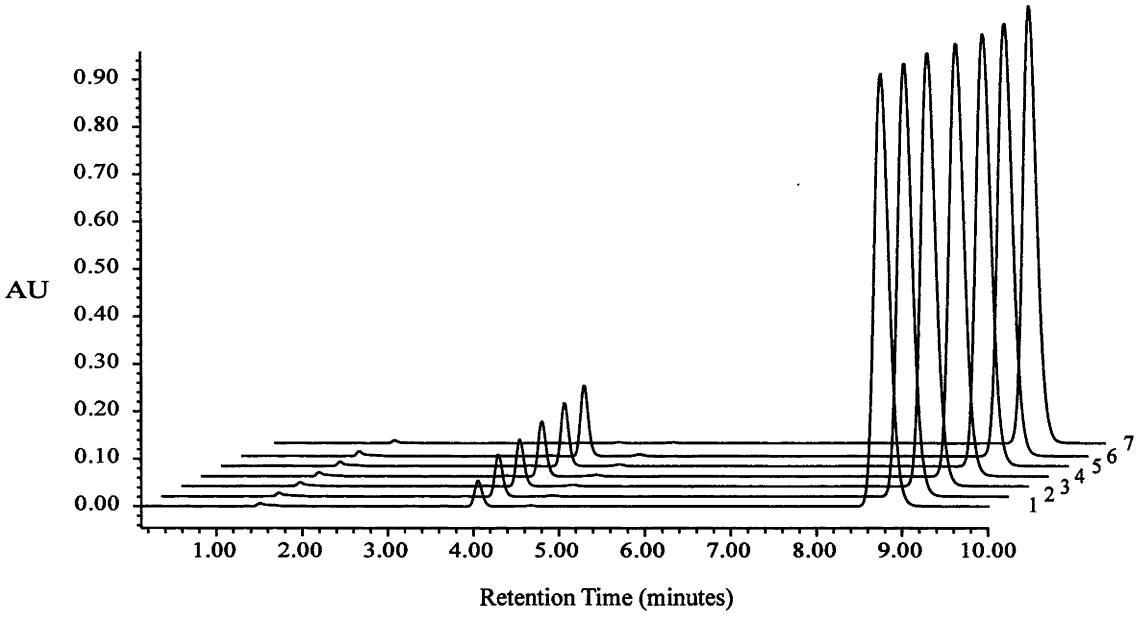

Figure 36. Isomerisation of the *E*-dienelactone (2.01 mM) to the *Z*-isomer by C123D (21.8 μM). The retention time for the *E*-dienelactone is approximately 9 minutes and that of the *Z*-dienelactone is approximately 4 minutes. The overlayed traces are from the HPLC analysis of the enzyme reaction over different time periods (1-6). The time periods correspond to the injection of an aliquot of the reaction mix at 30 minute intervals for 180 minutes after the start of the reaction. The reaction proceeded for 300 minutes. The final trace (7) is the reaction without enzyme after 180 minutes.

catalyse the hydrolysis of the *E*-dienelactone. It is clear that the relatively poor aspartate nucleophile is able to react with the natural substrate of DLH (*E*-dienelactone) and the fact that C123D shows any catalytic activity at all is extraordinary.

6.6.2 Hydrolysis of *p*-nitrophenyl acetate by C123D analysed using UV spectroscopy

Previously, it has been shown that DLH and DLI hydrolyse the activated ester *p*-nitrophenyl acetate (Pathak *et al.*, 1991). In this study, DLI showed burst kinetics when hydrolysing *p*-nitrophenyl acetate (*p*-NPA) and it was suggested that deacylation was the rate-determining step in the reaction (Pathak *et al.*, 1991). No burst was observable with DLH. To investigate the versatility of C123D as an enzyme, it was treated with *p*-NPA to obtain the kinetic data shown in Table 20. The data for the

Table 20. Kinetic data for the interaction of C123D, DLH and DLI with *p*-nitrophenyl acetate.

	k_{cat} (min^{-1})	K_m (mM)	Ratio[#] k_{cat}/K_m
C123D	0.13 ± 0.01	3.9 ± 0.6	
DLH	37 ± 0.8	1.6 ± 0.1	690
DLI	0.77 ± 0.11	0.023 ± 0.001	1000

[#] Ratio of the k_{cat}/K_m value of DLH or DLI to C123D.

hydrolysis of *p*-NPA by DLH and DLI are shown for comparison. The data were collected in 20 mM HEPES buffer, 2% ACN (to solubilise the substrate ester) containing 1 mM EDTA, at pH 7.0 and 25 °C and the rates corrected for background hydrolysis. The extinction coefficient used for the rate of product formation was that of Pathak *et al.* (1991).

As shown, it is clear that C123D reacts with *p*-NPA. The trend shown for k_{cat} with C123D, DLH and DLI may parallel the nucleophilicity of the active site residue at position 123. For substrate binding, the size or position of the nucleophile may dictate the value of K_m. It appears that the steric bulk of an aspartate side chain or its position in C123D interferes with the formation of the Michaelis complex. As discussed in the Introduction, the cysteine thiolate of DLH is proposed to rotate about its Cα-Cβ bond into the active site from its position in the resting state. It is apparent that DLH hydrolyses *p*-NPA at a substantial rate. For DLH to hydrolyse *p*-NPA it is expected that the cysteine rotates into the active site to react with this substrate. This rotation may sterically interfere with the binding of *p*-NPA resulting in the high K_m for this enzyme. As discussed in the Introduction, the side chain of S123 in DLI is proposed to be positioned only in the 'active conformation'. As shown by the low K_m, the position of this serine side chain may result in little steric interference with the binding substrate.

6.7 Conclusion

The results presented in this chapter have provided clear evidence that the C123S mutant protein (DLI) catalyses a different reaction (isomerisation) to that of DLH (hydrolysis). DLI catalyses the interconversion of the *E*- and *Z*-dienelactones with little, if any, hydrolysis. An active site conformational change in DLI may occur after binding the *E*-dienelactone. It is proposed that this conformational change is needed so that the enzyme can proceed through to the catalytic step of the reaction and isomerise this substrate. Active site residues of DLH that are important for binding the *E*- and *Z*-dienelactones, as determined in Chapter 5, also have this role in DLI. Additionally, these residues (R206 and R81) are critical for the reaction of the substrate once bound by partitioning the isomerase activity of DLI from hydrolase activity, possibly by securing the position of the enolate formed in the acyl enzyme intermediate. The arginine mutants of DLI show burst kinetics when reacting with the *Z*-dienelactone. It is proposed that this burst represents the rapid formation of the *E*-dienelactone product with its release from the enzyme being rate-determining. The versatility of the isomerase activity of DLI was shown where this protein isomerised the *tert*-butyl esters of dienelactone with no apparent hydrolysis. The C123D mutant isomerises the *E*-dienelactone to the *Z*-isomer and is also catalytically active toward simple activated esters.

References

Ainslie, G.R. and Neet, K.E. (1979) Cooperativity and the slow isomerization of δ-chymotrypsin. *Molecular and Cellular Biochemistry*. **24**:183-191.

Arad, D., Langridge, R., Kollman, P.A. (1990) A simulation of the sulfur attack in the catalytic pathway of papain using molecular mechanics and semiempirical quantum mechanics. *Journal of the American Chemical Society*. **112**:491-502.

Armarego, W.L.F. and Perrin, D.D. (1996) *Purification of laboratory chemicals*. 4th ed. Butterworth-Heinemann Publishing, Oxford. pp. 529.

Baker, E.N. (1980) Structure of actinidin, after refinement at 1.7 Å resolution. *Journal of Molecular Biology*. **141**:441-484.

Bender, M.L. and Kézdy, F.J. (1964) The current status of the α-chymotrypsin mechanism. *Journal of the American Chemical Society*. **86**:3704-3714.

Beveridge, A.J. and Ollis, D.L. (1995) A theoretical study of substrate-induced activation of dienelactone hydrolase. *Protein Engineering*. **8**:135-142.

Chatterjee, D.K. and Chakrabarty, A.M. (1982) Genetic rearrangements in plasmids specifying total degradation of chlorinated benzoic acids. *Molecular and General Genetics*. **188**:279-285.

Chatterjee, D.K., Chakrabarty, A.M. (1983) Genetic homology between independently isolated chlorobenzoate-degradative plasmids. *Journal of Bacteriology*. **153**:532-534.

Cheah, U. E. (1991) Dienelactone hydrolase: structure, function and evolution. PhD Dissertation. Northwestern University, Evanston, Illinois.

Cheah, E., Ashley, G.W., Gary, G., Ollis, D. (1993a) Catalysis by dienelactone hydrolase: a variation on the protease mechanism. *Proteins:Structure, Function, and Genetics*. **16**:64-78.

Cheah, E., Austin, C., Ashley, G.W., Ollis, D. (1993b) Substrate-induced activation of dienelactone hydrolase: an enzyme with a naturally occurring cys-his-asp triad. *Protein Engineering*. **6**:575-583.

Cornish-Bowden, A. (1995) *Fundamentals of enzyme kinetics*. Portland Press Ltd, London. pp 343.

Cornish-Bowden, A. and Cardenas, M.L. (1987) Co-operativity in monomeric enzymes. *Journal of Theoretical Biology*. **124**:1-23.

Dorn, E., Hellwig, M., Reineke, W., Knackmuss, H.-J. (1974) Isolation and characterisation of a 3-chlorobenzoate degrading pseudomonad. *Archives of Microbiology*. **99**:61-70.

Drenth, J., Kalk, K.H., Swen, H.M. (1976) Binding of chloromethyl ketone substrate analogues to crystalline papain. *Biochemistry*. **15**:3731-3738.

van Duijnen, P.T., Thole, B.T., Hol, W.G.J. (1979) On the role of the active site helix in papain, an ab initio molecular orbital study. *Biophysical Chemistry*. **9**:273-280.

Ellis, K.J., and Morrison, J.F. (1987) Buffers of constant ionic strength for studying pH-dependent processes. *Methods in Enzymology*. **87**:405-426.

Eulberg, D., Kourbatova, E.M., Golovleva, L.A., Schlömann, M. (1998) Evolutionary relationship between chlorocatechol catabolic enzymes from *Rhodococcus opacus* 1CP and their counterparts in proteobacteria: sequence divergence and functional

convergence. *Journal of Bacteriology*. **180**:1082-1094.

Evans, W.C., Smith, B.S.W., Moss, P., Fernley, H.N. (1971) Bacterial metabolism of 4-chlorophenoxyacetate. *Biochemical Journal*. **122**:509-517.

Fastrez, J. and Fersht, A.R. (1973) Mechanism of chymotrypsin: structure, reactivity, and nonproductive binding relationships. *Biochemistry*. **12**:1067-1074.

Frantz, B., Ngai, K.-I., Chatterjee, D.K., Ornston, L.N., Chakrabarty, A.M. (1987) Nucleotide sequence and expression of *clc*D, a plasmid-borne dienelactone hydrolase gene from *Pseudomonas* sp. strain B13. *Journal of Bacteriology*. **169**:704-709.

Frieden, C. (1970) Kinetic aspects of regulation of metabolic processes: the hysteretic enzyme concept. *The Journal of Biological Chemistry*. **245**:5788-5799.

Gill, S.C. and von Hippel, P.H. (1989) Calculation of protein extinction coefficients from amino acid sequence data. *Analytical Biochemistry*. **182**:319-326.

Glasoe, P.K. and Long, F.A. (1960) Use of glass electrodes to measure acidities in deuterium oxide. *Journal of Physical Chemistry*. **64**:188-190.

Hartnett, G.B. and Ornston, L.N. (1994) Acquisition of apparent DNA slippage structures during extensive evolutionary divergence of pcaD and catD genes encoding identical catalytic activities in *Acinetobacter calcoaceticus*. *Gene*. **142**:23-29.

Harwood, C.S. and Parales, R.E. (1996) The β-ketoadipate pathway and the biology of self-identity. *Annual Review of Microbiology*. **50**:553-590.

Henderson, R. (1970) Structure of crystalline α-chymotrypsin. IV. The structure of

indoleacryloyl-α–chymotrypsin and its relevance to the hydrolytic mechanism of the enzyme. *Journal of Molecular Biology*. **54**:341-354.

Higaki, J.N., Evnin, L.B., Craik, C.S. (1989) Introduction of a cysteine protease active site into trypsin. *Biochemistry*. **28**:9256-9263.

Hill, A.V. (1910) The possible effects of the aggregation of the molecules of haemoglobin on its dissociation curves. *Journal of Physiology*. **40**:iv-vii.

Hol, W.G.J., van Duijnen, P.T., Berendsen, H.J.C. (1978) The α–helix dipole and the properties of proteins. *Nature*. **273**:443-446.

Howard, A.E. and Kollman, P.A. (1988) OH^- versus SH^- nucleophilic attack on amides: dramatically different gas-phase and solvation energies. *Journal of the American Chemical Society*. **110**:7195-7200.

Hwang, C-C. and Cook, P.F. (1998) Multiple isotope effects as a probe of proton and hydride transfer in the 6-phosphogluconate dehydrogenase reaction. *Biochemistry*. **37**:15698-15702.

Jefferies, C. (1998) Enzyme engineering: active site modifications of dienelactone hydrolase. Honours Dissertation. Australian National University, Canberra, ACT.

Kamphuis, I.G., Kalk, K.H., Swarte, B.A., Drenth, J. (1984) Structure of papain refined to 1.65 Å resolution. *Journal of Molecular Biology*. **179**:233-256.

Lewis, S.D., Johnson, F.A., Shafer, J.A. (1981) Effect of cysteine-25 on the ionisation of histidine-159 in papain as determined by proton nuclear magnetic resonance spectroscopy. Evidence for a his-159–cys-25 ion pair and its possible role in catalysis. *Biochemistry*. **20**:48-51.

Love, C.A., Lilley, P.E., and Dixon, N.E. (1996) Stable high-copy-number bacteriophage λ promoter vectors for overproduction of protein in *Escherichia coli*. *Gene*. **176**:49-53.

Massy-Westropp, R.A. and Price, M.F. (1980) The synthesis of 5-oxo-2,5-dihydrofuran-2-ylideneacetic acids. *Australian Journal of Chemistry*. **33**:333-341.

Meuneir, J.-C., Buc, J., Navarro, A., Ricard, J. (1974) Regulatory behavior of monomeric enzymes. 2. A wheat-germ hexokinase as a mnemonical enzyme. *European Journal of Biochemistry*. **49**:209-223.

Ménard, R., Khouri, H.E., Plouffe, C., Laflamme, P., Dupras, R., Vernet, T., Tessier, D.C., Thomas, D.Y., Storer, A.C. (1991) Importance of hydrogen-bonding interactions involving the side chain of Asp158 in the catalytic mechanism of papain. *Biochemistry*. **30**:5531-5538.

Migliorini, M. and Creighton, D.J. (1986) Active-site ionisations of papain: an evaluation of the potentiometric difference titration method. *European Journal of Biochemistry*. **156**:189-192.

Ngai, K.-L., Schlömann, M., Knackmuss, H.-J., Ornston, L.N. (1987) Dienelactone hydrolase from *Pseudomonas* sp. strain B13. *Journal of Bacteriology*. **169**:699-703.

Neet, K.E. and Koshland, D.E. (1966) The conversion of serine at the active site of subtilisin to cysteine: a "chemical mutation". *Proceedings of the National Academy of Science*. **56**:1606-1611.

Ollis, D.L., Cheah, E., Cygler, M., Dijkstra, B., Frolow, F., Franken, S.M., Harel, M., Remington, S.J., Silman, I., Schrag, J., Sussman, J.L., Verschueren, K.H.G., Goldman, A. (1992) The α/β hydrolase fold. *Protein Engineering*. **5**:197-211.

Ornston, L.N (1966) The conversion of catechol and protocatechuate to β-ketoadipate by *Pseudomonas putida*. III. Enzymes of the catechol pathway. *Journal of Biological Chemistry*. **241**:3795-3799.

Palma, M.S., Teno, A.M., Rossi, A. (1983) Acid phosphatase from maize scutellum: negative co-operativity suppression by glucose. *Phytochemistry*. **22**:1899-1901.

Papworth, C., Bauer, J.C., Braman, J., Wright, D.A. (1996) Site-directed mutagenesis in one day with >80% efficiency. *Strategies*. **9**:3-4.

Parsek, M.R., McFall, S.M., Shinabarger, D.L., Chakrabarty, A.M. (1994) Interaction of two lysR-type regulatory proteins catR and clcR with heterologous promoters: functional and evolutionary implications. *Proceedings of the National Academy of Science*. **91**:12393-12397.

Pathak, D. and Ollis, D. (1990) Refined structure of dienelactone hydrolase at 1.8 Å. *Journal of Molecular Biology*. **214**:497-525.

Pathak, D., Ashley, G., Ollis, D. (1991) Thiol protease-like active site found in the enzyme dienelactone hydrolase: localisation using biochemical, genetic, and structural tools. *Proteins:Structure, Function, and Genetics*. **9**:267-279.

Pathak, D., Ngai, K.L., Ollis, D. (1988) X-ray crystallographic structure of dienelactone hydrolase at 2.8 Å. *Journal of Molecular Biology*. **204**:435-445.

Polgar, L. (1974) Mercaptide-imidazolium ion-pair: the reactive nucleophile in papain catalysis. *FEBS Letters*. **47**:15-18.

Polgár, L. and Asóbth, B. (1986) The basic difference in the catalyses by serine and

cysteine proteinases resides in charge stabilisation in the transition state. *Journal of Theoretical Biology*. **121**:323-326.

Polgár, L. and Bender, M.L. (1966) A new enzyme containing a synthetically formed active site: thiol-subtilisin. *Journal of the American Chemical Society*. **88**:3153-3154.

Rabin, B.R. (1967) Co-operative effects in enzyme catalysis: a possible kinetic model based on substrate-induced conformational isomerisation. *Biochemical Journal*. **102**:22c-23c.

Reineke, W. and Knackmuss, H.-J. (1988) Microbiol degradation of haloaromatics. *Annual Review of Microbiology*. **42**:263-287.

Ricard, J. (1978) Generalised microscopic reversibility, kinetic co-operativity of enzymes and evolution. *Biochemical Journal*. **175**:779-791.

Ricard, J., Meunier, J.-C., Buc, J. (1974) Regulatory behavior of monomeric enzymes. 1. The mnemonical enzyme concept. *European Journal of Biochemistry*. **49**:195-208.

Robinson, A. (1998) Protein engineering of dienelactone hydrolase. PhD Dissertation. Australian National University, Canberra, ACT.

Rullmann, J.A.C., Bellido, M.N., van Duijnen, P.T. (1989) The active site of papain: all-atom study of interactions with protein matrix and solvent. *Journal of Molecular Biology*. **206**:101-118.

Schlömann, M. (1994) Evolution of chlorocatechol catabolic pathways: conclusions to be drawn from comparisons of lactone hydrolases. *Biodegradation*. **5**:301-321.

Schlömann, M., Schmidt, E., Knackmuss, H.-J. (1990) Different types of dienelactone

hydrolase in 4-fluorobenzoate-utilising bacteria. *Journal of Bacteriology*. **172**:5112-5118.

Schlömann, M., Ngai, K.-L., Ornston, L.N., Knackmuss, H.-J. (1993) Dienelactone hydrolase from *Pseudomonas cepacia*. *Journal of Bacteriology*. **175**:2994-3001.

Schmidt, E. and Knackmuss, H.-J. (1980) Chemical structure and biodegradability of halogenated aromatic compounds: conversion of chlorinated muconic acids into maleoylacetic acid. *Biochemical Journal*. **192**:339-347.

Seltzer, S. and Stevens, K.D. (1968) The preparation of *cis*-β-acetylacrylic acid. *The Journal of Organic Chemistry*. **33**:2709-2711.

Shultz, A.R. (1994) *Enzyme kinetics: from diastase to multi-enzyme systems*. Cambridge University Press. pp 246.

Stevens, L. (1992) Buffers and the determination of protein concentrations. In *Enzyme Assays: a practical approach*. R. Eisenthal and M.J. Danson (Ed.). Oxford University Press. p317-335.

Storer, A.C. and Cornish-Bowden, A. (1976) Kinetics of rat glucokinase: cooperative interactions with glucose at physiologically significant concentrations. *Biochemical Journal*. **159**:7-14.

Tipton, K.F. and Dixon, H.B.F. (1979) Effect of pH on enzymes. *Methods in Enzymology*. **63**:183-234.

Venkatasubban, K.S. and Schowen, R.L. (1984) The proton inventory technique. *Critical Reviews in Biochemistry*. **17**:1-44.

Warshel, A. (1978) Energetics of enzyme catalysis. *Proceedings of the National Academy of Science*. **75**:5250-5254.

Wilke, M.E., Higaki, J.N., Craik, C.S., Fletterick, R.J. (1991) Crystal structure of rat trypsin S195C at -150 °C: analysis of low activity of recombinant and semisynthetic thiol proteases. *Journal of Molecular Biology*. **219**:511-523.

Xu, Y., Kakhniashvili, D.A., Gremse, D.A., Wood, D.O., Mayor, J.A., Walters, D.E., Kaplan, R.S. (2000) The yeast mitochondrial citrate transport protein: probing the roles of cysteines, arg181, and arg189 in transport function. *The Journal of Biological Chemistry*. **275**:7117-7124.

Yokosawa, H., Ojima, S., Ishii, S. (1977) Thioltrypsin: chemical transformation of the active site serine residue of *Streptomyces griseus* trypsin to a cysteine residue. *Journal of Biochemistry* (Japan). **82**:869-876.

Appendix 1

Synthesis of the *E*- and *Z*-dienelactams

As discussed in the Introduction, the catalytic mechanism of DLH is based on the information provided by a crystal structure using the *Z*-dienelactam only. The need for a crystal structure using the *E*-dienelactam is evident. Synthesis of the *Z*-dienelactam followed the procedure of Cheah *et al.* (1993a), with some modifications. In this procedure the *E*-dienelactam was also produced in a ratio of 1:1.3 (*E*:*Z*), but the *E*-isomer was not previously observed (Cheah *et al.*, 1993a).

To 1.0 g (0.0051 mol) of (4b) in a round-bottom flask suspended in a dry ice/acetone bath equipped with a dry ice/acetone condenser was added 50 ml of liquid ammonia with stirring. The orange solution that developed was stirred for 1 hour before the cooling bath was removed and the solution allowed to reflux for 2 hours. The ammonia was then removed and the resulting orange precipitate dried under vacuum overnight. The precipitate was dissolved in dry benzene (50 ml) and was heated at reflux under a nitrogen atmosphere with *p*-toluenesulfonic acid (0.38 g, 0.0022 mol) for 6 hours. Removal of the solvent under reduced pressure afforded a brown precipitate which showed two spots by t.l.c. (R_F 0.14 and 0.21; 80:20:2 diethyl ether/hexane/acetic acid) in addition to baseline material. Separation of *p*-toluenesulfonic acid from the lactam isomers was *via* reverse-phase HPLC with a 250 mm x 10 mm (i.d.) C18 column (ODS-AQ, 120A; YMC Co., Ltd., Japan) of 5 micron particle size in 33% ACN and 0.1% TFA in water at a flow rate of 4 ml/minute and monitored at 280 nm. The solvent system was then changed to 10% ACN in water with 0.1% TFA at the same flow rate to separate the isomers. The *E*-isomer eluted first with a R_t of 8.7 minutes (λ_{280}), 0.072 g (10.2%); mp no lit value; ^{1}H NMR (CD_3OD) δ = 8.07 (d, J = 6.3 Hz, C2-H), 6.33 (d, J = 3.8 Hz, C3-H), 5.64 (s, C5-H), 4.94 (s, NH); ^{13}C NMR (CD_3OD) δ = 173.9, 168.9, 152.2, 137.3, 129.2, 102.3; MS (ESI) *m/z* $[M-H]^-$ 138.1, HRMS (EI) Found: M^+, 139.026505. $C_6H_5NO_3$ requires M^+, 139.026943; mp. 165-168 °C. The *Z*-isomer eluted

with a R_t of 10.7 minutes, 0.095 g (13.4%); ^{1}H NMR (CD_3OD) δ = 7.26 (d, J = 5.8 Hz, C2-H), 6.34 (d, J = 5.6 Hz, C3-H), 5.48 (s, C5-H), 4.93 (s, NH); mp. 185-186 °C, lit 187-188 °C.

Protein Crystallography

The previous procedure for crystallisation of DLH was that of Pathak *et al.* (1988). Data collection was at room temperature. To potentially improve the resolution of the data set, conditions for low temperature data collection on DLH was investigated.

New conditions for the crystallisation of DLH was determined in this lab by Dr Jian-Wei Liu. Briefly, crystals were grown at 4 °C from a hanging drop in 0.1 M sodium citrate, at pH 6.25 or pH 6.50 with 1.0 M or 1.2 M ammonium sulfate as the precipitant. Crystals grew after 1 to 2 weeks.

After crystal growth, they were prepared for cryo data collection (100 K) by increasing the ammonium sulfate concentration (2.0 M final) and by gradually introducing glycerol (25% final). The protocol is shown in Table 1.

Table 1. Protocol used for preparation of crystals for the C123S mutant of DLH for cryo X-ray crystallography.

Time Duration (minutes)	Glycerol concentration (%)	AS[a] concentration (M)
0[b]	0	1.2
60	5	1.2
120	10	1.2
150	20	1.2
o/n[c]	20	2.0
360	25	2.0

[a], ammonium sulfate. [b], the crystal growth conditions were 0.1 M sodium citrate pH 6.5 (or pH 6.25), 1.2 M ammonium sulfate. [c], crystals soaked overnight.

Appendix 2

Kinetic data used in Chapter 3

The activity of DLH after incubation in increasing concentrations of β-ME.

[β-ME] (mM)	v (μM min^{-1})	[β-ME] (mM)	v (μM min^{-1})
0.000	42.39	1.500	29.40
0.000	39.72	1.500	31.30
0.000	39.37	1.500	28.91
0.1250	38.61	2.000	29.89
0.1250	34.66	2.000	30.17
0.1250	36.00	2.000	30.87
0.2500	39.68	5.000	25.66
0.2500	38.41	5.000	24.54
0.2500	39.32	5.000	23.90
0.5000	38.23	10.00	15.99
0.5000	39.92	10.00	17.39
0.5000	39.70	10.00	18.45
0.7500	35.52	20.00	8.127
0.7500	33.75	20.00	9.817
0.7500	36.36	20.00	8.056
1.000	36.67		
1.000	34.63		
1.000	35.82		

The effects of NaCl concentration on the activity of wt DLH hydrolysing the *E*-dienelactone.

[NaCl] (mM)	v (μM min^{-1})
0.000	4.070
30.00	3.740
80.00	3.140
130.0	2.640
180.0	2.170
210.0	1.926

Comparison of the kinetics of hydrolysis by wt DLH without and in the presence of 100 mM NaCl.

		100 mM NaCl	
[S] (μM)	v (μM min^{-1})	[S] (μM)	v (μM min^{-1})
0.0000	0.0000	0.0000	0.0000
6.6700	0.61765	7.1800	0.40120
6.6700	0.57000	7.1800	0.36410
6.6700	0.65290	7.1800	0.42180
13.200	1.1529	13.180	0.80590
13.200	1.1588	13.180	0.75880
13.200	1.1529	13.180	0.77060
20.080	1.7588	19.590	1.1706
20.080	1.7000	19.590	1.1824
20.080	1.7941	19.590	1.0824
26.040	2.3412	26.370	1.5941
26.040	2.3706	26.370	1.5412
26.040	2.2941	26.370	1.5412
55.510	4.7059	53.330	2.9118
55.510	4.4824	53.330	2.9118
55.510	4.5529	53.330	2.8588
108.75	7.5636	108.25	5.0853
108.75	7.5528	108.25	5.3213
108.75	7.8210	108.25	5.2140
147.00	8.7977	143.77	6.7223
147.00	9.0232	143.77	6.2260
147.00	8.8653	143.77	6.6998
198.21	10.941	200.09	7.9856
198.21	10.647	200.09	8.6172
198.21	10.512	200.09	8.6849
312.71	12.583	313.75	10.673
312.71	12.375	313.75	10.880
506.51	15.158	313.75	10.008
506.51	14.369	518.27	12.334
506.51	13.704	518.27	12.292
		518.27	12.168

Appendix 3

Kinetic data used in Chapter 4

pH 5.0

[S] (μM)	v (μM min^{-1})	[S] (μM)	v (μM min^{-1})
0.0000	0.0000	202.74	8.868
7.7653	0.614	202.74	9.298
7.7653	0.516	202.74	9.298
7.7653	0.626	242.66	8.673
12.224	0.872	242.66	8.604
12.224	0.841	242.66	7.632
12.224	1.001	279.71	8.395
28.629	2.142	279.71	8.188
28.629	2.113	279.71	9.020
28.629	2.241	318.42	9.436
58.453	4.177	318.42	10.526
58.453	4.001	318.42	9.575
58.453	4.353	395.84	11.032
99.864	5.786	395.84	8.395
99.864	5.009	395.84	8.882
99.864	5.703	810.66	12.005
154.84	7.285	810.66	10.756
154.84	6.141		
154.84	7.563		
177.59	8.188		
177.59	8.395		
177.59	7.979		

pH 5.15

[S] (μM)	v (μM min^{-1})	[S] (μM)	v (μM min^{-1})
0.0000	0.0000	251.09	6.5234
24.110	1.2879	251.09	6.9624
24.110	1.3770	251.09	6.8997
24.110	1.3503	325.05	7.1507
50.940	2.8428	325.05	7.1507
50.940	2.8162	325.05	6.7116
50.940	2.9228	408.19	7.7152
99.110	4.0582	408.19	8.4051
99.110	4.6290	504.59	8.7188
99.110	3.7133	504.59	8.7188
167.50	5.5387	504.59	9.1579
167.50	5.4947		
167.50	5.4508		

pH 5.25

[S] (μM)	v (μM min^{-1})	[S] (μM)	v (μM min^{-1})
0.0000	0.0000	145.81	2.8550
6.0587	0.15058	145.81	2.6102
6.0587	0.15058	145.81	3.0342
6.0587	0.18526	172.62	2.8909
9.9627	0.28509	172.62	2.4190
9.9627	0.27324	172.62	2.9208
9.9627	0.29185	205.75	3.9600
15.275	0.44751	205.75	3.1955
15.275	0.42213	205.75	3.2672
15.275	0.41282	249.28	2.7057
19.648	0.53803	249.28	3.9481
19.648	0.49657	249.28	2.9744
19.648	0.55241	333.48	3.5341
25.451	0.81211	333.48	4.2763
25.451	0.75628	333.48	3.0104
25.451	0.74105	376.41	3.7032
49.301	1.4804	376.41	3.3448
49.301	1.3028	376.41	4.1093
49.301	1.2774		
93.689	2.7296		
93.689	2.0308		
93.689	2.1025		

pH 5.4

[S] (μM)	v (μM min^{-1})	[S] (μM)	v (μM min^{-1})
0.0000	0.0000	252.15	9.5197
25.170	1.5409	252.15	7.6498
25.170	1.4687	252.15	8.3298
25.170	1.5409	330.92	9.3497
50.470	3.1541	330.92	10.143
50.470	3.1541	330.92	8.6698
50.470	2.7849	403.83	9.5197
97.450	5.1906	403.83	9.2365
97.450	5.6666	403.83	9.8030
97.450	5.5418		
173.37	7.3665		
173.37	7.3665		
173.37	6.6298		

pH 5.5

[S] (μM)	v (μM min^{-1})	[S] (μM)	v (μM min^{-1})
0.0000	0.0000	170.36	4.8763
5.9500	0.21769	170.36	5.0588
5.9500	0.24901	170.36	4.9980
5.9500	0.21925	196.26	6.3580
9.7900	0.42441	196.26	6.1921
9.7900	0.40170	196.26	5.9710
9.7900	0.40561	254.10	5.9710
24.430	1.1354	254.10	6.2474
24.430	1.1824	254.10	5.7498
24.430	1.1824	325.35	6.7450
49.620	2.3021	325.35	7.5743
49.620	2.2160	325.35	6.6897
49.620	2.3178	397.80	7.4084
101.97	3.6102	397.80	6.8556
101.97	4.3013	397.80	6.9661
101.97	3.9420	493.15	6.6344
150.02	5.9710	493.15	6.5238
150.02	6.0815	493.15	7.6849
150.02	5.2634		

pH 6.0

[S] (μM)	v (μM min^{-1})	[S] (μM)	v (μM min^{-1})
0.0000	0.0000	173.07	7.4279
5.5893	0.24597	173.07	7.1140
5.5893	0.19485	173.07	6.8525
5.5893	0.28746	198.83	8.0033
10.112	0.52379	198.83	7.3233
10.112	0.48156	198.83	7.8987
10.112	0.52009	249.44	8.8402
25.323	1.4151	249.44	8.3694
25.323	1.5373	249.44	8.4218
25.323	1.3632	321.89	10.043
50.752	3.0153	321.89	10.853
50.752	2.6893	321.89	10.880
50.752	2.7338	489.98	11.874
96.551	5.0478	489.98	10.828
96.551	3.9284	489.98	11.665
96.551	4.2946	677.06	11.246
150.78	7.5325	677.06	10.409
150.78	6.5386	677.06	11.090
150.78	6.8002		

pH 6.5

[S] (μM)	v (μM min^{-1})	[S] (μM)	v (μM min^{-1})
0.0000	0.0000	201.54	6.8213
5.9947	0.25690	201.54	6.8729
5.9947	0.24006	201.54	6.8213
5.9947	0.24080	249.74	8.4750
9.9627	0.46769	249.74	7.8031
9.9627	0.52624	249.74	7.6482
9.9627	0.49843	317.67	8.8884
24.725	1.3979	317.67	8.3199
24.725	1.3394	317.67	8.3716
24.725	1.3613	400.21	9.7668
50.325	2.8325	400.21	9.0434
50.325	2.7373	400.21	9.1984
50.325	2.5983	498.87	10.439
96.099	4.7284	498.87	9.2501
96.099	3.9378	498.87	8.8884
96.099	3.8395	659.14	10.955
151.98	6.0978	659.14	10.180
151.98	5.6844	659.14	10.180
151.98	6.2529		
178.34	6.5112		
178.34	6.2529		
178.34	6.5112		

pH 7.0

[S] (μM)	v (μM min^{-1})	[S] (μM)	v (μM min^{-1})
0.0000	0.0000	173.07	5.7840
11.300	0.58500	173.07	4.7890
11.300	0.60400	173.07	5.3770
11.300	0.57200	248.53	6.8680
23.573	1.2410	248.53	6.5070
23.573	1.2410	248.53	7.2750
23.573	1.2670	331.22	8.2690
50.858	2.7200	331.22	7.9070
50.858	2.6490	331.22	7.9530
50.858	2.6170	407.29	9.2630
101.82	5.0150	407.29	8.3140
101.82	5.6030	407.29	9.0370
101.82	5.0610	496.76	9.8960
125.32	5.8740	496.76	9.3990
125.32	4.9250	496.76	8.7210
125.32	5.6930	698.30	9.8960
145.80	5.6480	698.30	8.9470
145.80	5.4670	698.30	9.3080
145.80	5.4220		

pH 7.5

[S] (μM)	v (μM min^{-1})	[S] (μM)	v (μM min^{-1})
0.0000	0.0000	165.84	7.5915
5.8667	0.29568	165.84	6.9589
5.8667	0.29888	165.84	6.2811
5.8667	0.32517	201.99	7.5915
10.997	0.54080	201.99	8.3597
10.997	0.52096	201.99	6.1907
10.997	0.52224	311.19	8.1789
23.488	1.4336	311.19	8.2693
23.488	1.4144	311.19	7.4108
23.488	1.6000	389.37	9.6249
49.077	2.6432	389.37	9.6701
49.077	2.5984	389.37	8.1338
49.077	2.6176	453.23	9.9413
97.605	4.5639	453.23	8.6760
97.605	4.5052	453.23	9.6701
97.605	4.9706	650.70	10.303
141.93	6.0551	650.70	9.8961
141.93	5.7840	650.70	10.032
141.93	6.1907		

pH 8.0

[S] (μM)	v (μM min^{-1})	[S] (μM)	v (μM min^{-1})
0.0000	0.0000	233.17	12.743
24.000	2.9312	233.17	12.562
24.000	2.7456	233.17	12.607
24.000	2.8416	304.56	15.183
52.030	5.1827	304.56	13.195
52.030	5.0867	304.56	14.776
52.030	5.1059	388.61	14.686
89.020	7.2752	388.61	15.319
89.020	7.0041	388.61	14.686
89.020	7.3204	467.24	17.171
138.73	10.890	467.24	15.770
138.73	9.7153	467.24	15.725
138.73	10.800	784.46	18.527
163.13	11.116	784.46	19.024
163.13	9.8509	784.46	16.990
163.13	11.116		
207.96	11.613		
207.96	11.794		
207.96	12.201		

pH 8.5

[S] (μM)	v (μM min^{-1})	[S] (μM)	v (μM min^{-1})
0.0000	0.0000	248.13	8.0434
25.024	2.2848	248.13	7.9530
25.024	2.1504	248.13	8.1789
25.024	2.2528	316.77	8.0886
50.304	3.9232	316.77	8.5404
50.304	3.7504	316.77	7.4108
50.304	3.6736	407.59	8.9019
90.375	5.9648	407.59	9.2634
90.375	5.1966	407.59	8.1789
90.375	5.7388	535.02	9.4894
159.51	6.8685	535.02	8.9019
159.51	7.1396	535.02	8.4049
159.51	7.0493	700.41	10.529
173.52	7.7271	700.41	9.5526
173.52	6.1907	700.41	9.9141
173.52	6.2359		
206.96	7.3656		
206.96	7.7271		
206.96	6.9589		

pH 9.0

[S] (μM)	v (μM min^{-1})	[S] (μM)	v (μM min^{-1})
0.0000	0.0000	244.92	5.9196
24.512	2.0480	244.92	5.5129
24.512	2.0096	244.92	5.1966
24.512	2.0032	348.40	6.0551
47.616	3.2768	348.40	6.3263
47.616	3.2448	348.40	5.6033
47.616	3.1232	411.21	5.2418
103.93	4.5188	411.21	5.3773
103.93	4.6543	411.21	5.8292
103.93	3.9855	519.20	7.1848
144.60	5.0610	519.20	6.9137
144.60	4.1075	519.20	7.1848
144.60	4.0624	696.34	6.7329
168.55	5.4225	696.34	6.9137
168.55	4.9254	696.34	7.4108
168.55	4.6091		
195.66	4.9254		
195.66	4.6543		
195.66	4.8803		

pH 9.5

[S] (μM)	v (μM min^{-1})	[S] (μM)	v (μM min^{-1})
0.0000	0.0000	265.70	6.9137
25.088	2.5088	265.70	7.7271
25.088	2.6368	265.70	7.0944
25.088	2.5024	315.86	7.6819
47.810	3.9744	315.86	7.2300
47.810	3.7824	315.86	7.4559
47.810	3.7312	399.01	8.2241
105.74	5.0158	399.01	8.5404
105.74	4.2793	399.01	7.8174
105.74	4.5639	501.58	8.5404
152.73	5.9196	501.58	8.9923
152.73	5.6484	501.58	8.8116
152.73	5.9196	736.10	7.9078
173.97	5.7388	736.10	9.3086
173.97	4.7447	736.10	9.3086
173.97	5.0610		
195.66	6.5522		
195.66	6.1455		
195.66	6.2359		

pH 10.0

[S] (μM)	v (μM min^{-1})	[S] (μM)	v (μM min^{-1})
0.0000	0.0000	246.72	9.4894
28.864	3.4368	246.72	9.8057
28.864	3.0720	246.72	9.3538
28.864	3.5200	319.48	9.5346
48.840	4.9408	319.48	8.4953
48.840	4.9088	319.48	10.709
48.840	4.8512	406.24	11.478
111.93	6.8685	406.24	11.071
111.93	5.9648	406.24	11.116
111.93	6.4166	502.49	13.692
153.64	7.9530	502.49	12.110
153.64	7.5915	502.49	12.246
153.64	8.1338	683.69	12.201
174.44	6.6426	683.69	13.511
174.44	7.5011	683.69	13.421
174.44	7.6819		
200.63	9.3538		
200.63	8.8586		
200.63	8.7212		

Summary of pH kinetic parameters.

pH	V_{max} ($\mu M\ min^{-1}$)	K_m (μM)	k_{cat} (min^{-1})	[Enzyme] (nM)	k_{cat}/K_m ($M^{-1}\ min^{-1}$)
5.00	13.139	126.63	131.38	100.01	1.037e+06
5.15	11.592	179.99	115.91	100.01	6.439e+05
5.25	5.089	129.23	101.77	50.003	7.875e+05
5.40	13.739	161.79	137.38	100.01	8.491e+05
5.50	9.389	130.49	187.95	50.003	1.440e+06
6.00	15.443	199.40	308.84	50.003	1.548e+06
6.50	13.777	202.18	459.23	30.000	2.271e+06
7.00	12.058	168.74	401.93	30.000	2.382e+06
7.50	12.758	162.07	425.26	30.000	2.624e+06
8.00	22.033	170.96	440.66	50.000	2.577e+06
8.50	10.809	92.988	216.18	50.000	2.324e+06
9.00	7.813	102.01	104.17	75.000	1.021e+06
9.50	11.049	150.89	53.79	205.40	3.564e+05
10.00	16.676	189.99	33.35	500.03	1.755e+05

pD 5.0

[S] (μM)	v ($\mu M\ min^{-1}$)	[S] (μM)	v ($\mu M\ min^{-1}$)
0.0000	0.0000	259.98	3.5599
25.620	0.87375	259.98	4.0249
25.620	0.84721	259.98	3.1990
25.620	0.95238	331.07	4.9964
48.600	1.6119	331.07	4.9755
48.600	1.4251	331.07	4.9755
48.600	1.5529	488.33	5.0936
94.890	2.0055	488.33	5.3364
94.890	2.4983	488.33	3.7681
94.890	2.0124	628.26	4.3093
141.44	3.1921	628.26	3.9833
141.44	2.8105	628.26	3.8792
141.44	2.8036		
203.19	3.0603		
203.19	3.2546		
203.19	3.2893		

pD 5.5

[S] (μM)	v (μM min^{-1})	[S] (μM)	v (μM min^{-1})
0.0000	0.0000	201.08	3.5494
27.710	0.62330	255.01	3.7374
27.710	0.64366	255.01	2.8307
27.710	0.63035	255.01	3.5384
49.620	1.3547	368.43	3.6931
49.620	1.0963	368.43	3.4057
49.620	1.1276	368.43	3.7429
104.92	2.1925	511.07	4.6275
104.92	2.0124	511.07	4.4948
104.92	2.0829	511.07	4.3732
149.72	2.1728	733.39	5.5288
149.72	2.2281	733.39	4.3179
201.08	2.8030	733.39	4.9205
201.08	2.4271		

pD 6.0

[S] (μM)	v (μM min^{-1})	[S] (μM)	v (μM min^{-1})
0.0000	0.0000	238.59	6.2248
27.200	1.3039	238.59	6.0679
27.200	1.2521	238.59	6.3817
27.200	1.2224	342.97	7.7940
49.150	2.0003	342.97	7.4802
49.150	1.9929	342.97	7.3233
49.150	1.9559	506.40	8.5264
88.420	3.5204	506.40	8.6309
88.420	2.9136	506.40	8.8926
88.420	3.6668	565.45	8.1079
143.55	4.6136	565.45	9.5202
143.55	4.5614	565.48	7.6895
143.55	4.1272	577.95	8.9449
200.78	6.2248	577.95	9.0494
200.78	5.2310		
200.78	5.5971		

pD 6.6

[S] (μM)	v (μM min^{-1})	[S] (μM)	v (μM min^{-1})
0.0000	0.0000	186.93	4.5694
34.130	1.2505	186.93	4.0530
34.130	1.0457	186.93	3.9601
34.130	1.1846	242.81	5.6794
64.110	1.9086	242.81	5.0650
64.110	1.8428	242.81	5.3696
64.110	1.9817	335.89	5.8860
100.17	3.3509	335.89	5.3180
100.17	3.3612	335.89	5.0547
100.17	3.2166	466.49	6.4023
160.57	4.4762	466.49	5.6278
160.57	4.0686	466.49	4.5849
160.57	4.3886		

pD 7.0

[S] (μM)	v (μM min^{-1})	[S] (μM)	v (μM min^{-1})
0.0000	0.0000	195.96	4.5639
27.290	1.0624	195.96	4.4284
27.290	1.1200	195.96	4.3877
27.290	1.0752	240.40	4.9254
50.170	2.0800	240.40	4.8803
50.170	1.9328	240.40	4.4555
50.170	1.7664	347.04	6.0551
51.310	1.9328	347.04	6.1907
51.310	1.8432	347.04	6.1003
51.310	1.8240	490.74	6.7329
94.140	3.0682	490.74	6.6436
94.140	2.9372	490.74	5.9196
94.140	3.1722	699.35	6.5522
158.01	3.7325	699.35	5.9196
158.01	3.9675	699.35	6.6426
158.01	3.9268		

pD 7.5

[S] (μM)	v (μM min^{-1})	[S] (μM)	v (μM min^{-1})
0.0000	0.0000	242.66	4.1844
34.110	1.1200	242.66	4.1979
34.110	1.1136	242.66	3.5201
34.110	1.0368	333.94	4.4916
51.500	1.6320	333.94	4.5052
51.500	1.4272	333.94	4.1844
51.500	1.4272	509.26	5.1966
102.73	2.7745	509.26	5.3773
102.73	2.6977	509.26	5.6033
102.73	3.2354	730.08	4.9706
149.42	3.5834	730.08	4.9254
149.42	3.4026	730.08	5.1062
149.42	3.4071		
195.96	3.7235		
195.96	3.6647		
195.96	4.3286		

pD 8.0

[S] (μM)	v (μM min^{-1})	[S] (μM)	v (μM min^{-1})
0.0000	0.0000	269.02	11.252
27.560	1.9904	269.02	9.2183
27.560	2.0864	269.02	9.2634
27.560	2.1248	399.76	12.788
48.620	3.4304	399.76	10.800
48.620	3.1936	399.76	11.839
48.620	3.2768	542.25	12.698
95.350	5.8744	542.25	11.523
95.350	5.5129	542.25	11.568
95.350	5.6033	722.55	14.008
154.69	8.0434	722.55	12.246
154.69	6.6426	722.55	11.884
154.69	7.5915		
217.20	10.212		
217.20	9.0827		
217.20	8.6308		

pD 8.5

[S] (μM)	v (μM min^{-1})	[S] (μM)	v (μM min^{-1})
0.0000	0.0000	266.00	7.4559
26.010	1.8176	266.00	7.4108
26.010	1.7088	266.00	6.5974
26.010	1.6960	358.34	7.7271
47.150	2.9248	358.34	8.4501
47.150	2.8544	358.34	8.1789
47.150	2.7840	494.20	9.3390
97.910	4.8803	494.20	8.5404
97.910	4.1934	494.20	8.0886
97.910	5.1062	734.15	9.7153
154.54	6.2359	734.15	9.7605
154.54	6.0099	734.15	9.0375
154.54	6.1455		
202.74	7.0041		
202.74	7.4559		
202.74	6.8685		

pD 9.0

[S] (μM)	v (μM min^{-1})	[S] (μM)	v (μM min^{-1})
0.0000	0.0000	267.51	9.1731
23.910	2.4384	267.51	9.9864
23.910	2.2912	361.20	8.6760
23.910	2.2976	361.20	9.4894
47.360	4.0192	361.20	9.8509
47.360	4.0384	521.92	12.201
47.360	3.9616	521.92	11.794
98.510	6.8233	521.92	10.845
98.510	6.5974	743.64	13.466
98.510	6.1907	743.64	13.737
160.42	8.4049	743.64	12.562
160.42	7.7271		
160.42	7.4559		
215.39	8.4953		
215.39	9.0827		
215.39	9.0375		

pD 9.5

[S] (μM)	v (μM min^{-1})	[S] (μM)	v (μM min^{-1})
0.0000	0.0000	216.60	5.8744
24.410	2.1056	216.60	5.3321
24.410	1.9840	273.99	5.7162
24.410	2.0608	273.99	5.3999
46.200	3.2960	273.99	5.4451
46.230	2.9696	366.77	6.1003
46.230	3.2512	366.77	5.1062
98.960	3.9087	366.77	5.4225
98.960	3.8771	509.87	6.5522
98.960	5.1062	509.87	5.1966
155.60	5.0610	509.87	5.3321
155.60	4.6543	727.97	7.6819
155.60	5.1966	727.97	5.9648
216.60	5.6936		

pD 10.0

[S] (μM)	v (μM min^{-1})	[S] (μM)	v (μM min^{-1})
0.0000	0.0000	125.17	3.9288
22.600	2.0672	125.17	4.0172
22.610	1.6640	165.54	4.3742
22.610	2.1632	165.54	3.7415
40.580	3.0144	165.54	3.3348
40.580	2.7328	215.24	4.4397
40.580	2.8224	215.24	4.0782
90.070	4.0172	215.24	3.7619
90.070	3.3168	238.74	4.3945
90.070	3.7460	238.74	3.7845
125.17	4.2883	238.74	3.8974

pD 10.4

[S] (μM)	v (μM min^{-1})	[S] (μM)	v (μM min^{-1})
0.0000	0.0000	197.32	2.6435
29.180	1.5936	197.32	2.4627
29.180	1.5360	197.32	2.3723
29.180	1.6320	277.90	2.9914
54.310	2.3680	277.90	3.0818
54.310	2.1952	277.90	2.6751
54.310	2.2400	342.82	2.5486
114.48	2.7144	342.82	2.1871
114.48	2.0696	342.82	2.1871
114.48	2.2820		
150.78	2.2910		
150.78	2.7429		
150.78	1.8400		

Summary of pD kinetic parameters.

pH	V_{max} (μM min^{-1})	K_m (μM)	k_{cat} (min^{-1})	[Enzyme] (nM)	k_{cat}/K_m (M^{-1} min^{-1})
5.0000	5.7032	134.04	22.813	250.00	1.701e+05
5.5000	6.5209	249.24	52.167	125.00	2.093e+05
6.0000	12.738	252.15	127.38	100.00	5.051e+05
6.6000	7.8273	150.31	130.46	60.000	8.679e+05
7.0000	8.3785	169.81	139.64	60.000	8.223e+05
7.5000	6.3120	133.67	126.24	50.000	9.444e+05
8.0000	16.079	171.73	153.13	105.00	8.917e+05
8.5000	11.096	130.55	110.96	100.00	8.499e+05
9.0000	14.666	137.87	97.730	150.07	7.088e+05
9.5000	6.6597	52.958	26.639	250.00	5.030e+05
10.000	4.6147	26.363	11.537	400.00	4.376e+05
10.500	2.7169	17.150	4.5434	597.99	2.649e+05

k_{cat}/K_m profiles for wt DLH and E36D mutant at 0.3 x K_m.

wt DLH		E36D	
pH	k_{cat}/K_m (M^{-1} min^{-1})	pH	k_{cat}/K_m (M^{-1} min^{-1})
5.1600	7.0918e+05	5.0500	30415
5.4700	9.9076e+05	5.2600	46845
5.6600	1.1345e+06	5.4900	64826
5.8300	1.3565e+06	5.7500	86523
5.9800	1.5434e+06	5.9900	97670
6.1300	1.7238e+06	6.2100	1.1289e+05
6.2500	1.7978e+06	6.5200	1.2555e+05
6.4000	1.8462e+06	6.6800	1.3229e+05
6.5100	1.9384e+06	6.9800	1.2704e+05
6.6800	1.9466e+06	7.1100	1.3068e+05
6.8700	1.9502e+06	7.2600	1.2876e+05
7.0200	1.9475e+06	7.3400	1.2975e+05
7.2600	1.9303e+06	7.6700	1.2674e+05
7.4700	1.8679e+06	7.9700	1.1816e+05
7.6200	1.7851e+06	8.2600	1.0236e+05
7.8000	1.8005e+06	8.5200	87555
7.9500	1.6875e+06	8.6300	71559
8.2000	1.4295e+06	9.0400	44205
8.5400	1.0827e+06	9.3100	26677
8.7900	7.3663e+05	9.5600	12827
8.9900	5.4600e+05	9.7100	8130.2
9.2000	1.7964e+05		
9.6500	1.0970e+05		
9.9100	86463		

k_{cat}/K_m profiles for R206A and R81A mutants at 0.3 x K_m.

R206A		R81A	
pH	k_{cat}/K_m (M^{-1} min^{-1})	pH	k_{cat}/K_m (M^{-1} min^{-1})
5.0000	1237.0	5.0200	1.4806e+05
5.1700	2269.1	5.1600	1.7681e+05
5.3800	5565.6	5.3900	2.1719e+05
5.6300	6290.5	5.6000	2.6697e+05
5.8300	8111.9	5.8300	2.9873e+05
5.9700	8175.0	6.0500	3.2955e+05
6.1200	8556.8	6.3700	3.3689e+05
6.4400	10336	6.7000	3.4133e+05
6.5600	11996	6.9600	3.2271e+05
6.7000	12273	7.2000	3.3906e+05
6.9700	13802	7.4700	3.1084e+05
7.3500	14505	7.7300	3.2404e+05
7.5600	13084	7.9900	3.2150e+05
7.7600	14454	8.2000	2.7712e+05
7.9600	14078	8.4700	2.4609e+05
8.4900	12691	8.6100	2.1730e+05
8.7100	12038	9.0400	1.8165e+05
9.0100	9954.0	9.3000	1.3889e+05
9.2700	7520.0	9.4800	1.1331e+05
9.4300	7060.0	9.7800	65555
9.6300	5307.0		

Appendix 4

Kinetic data used in Chapter 5

Z-dienelactone

wt DLH (5.0 nM)

[S] (μM)	v (μM min^{-1})	[S] (μM)	v (μM min^{-1})
0.0000	0.0000	25.070	3.9168
7.3400	2.3520	25.070	3.9808
7.3400	2.4480	25.070	3.8720
7.3400	2.4840	33.370	4.6272
8.7300	2.5080	33.370	4.3200
8.7300	2.4240	33.370	4.2752
8.7300	2.5200	66.300	4.6400
10.350	2.6720	66.300	4.6720
10.350	2.8160	66.300	4.6720
10.350	2.7360	130.53	5.2052
11.880	2.8320	130.53	5.1770
11.880	2.8000	169.34	5.5216
11.880	2.8800	169.34	5.0915
17.750	3.1920	169.34	5.2501
17.750	3.3520		
17.750	3.2560		

E36D (52.96 nM)

[S] (μM)	v (μM min^{-1})	[S] (μM)	v (μM min^{-1})
0.0000	0.0000	23.020	1.5488
7.4000	0.72320	23.020	1.5488
7.4000	0.72320	23.020	1.4208
7.4000	0.76160	33.750	1.8624
8.7900	0.81920	33.750	1.7856
8.7900	0.90880	33.750	1.8432
8.7900	0.85120	66.690	2.1842
10.410	0.97280	66.690	2.2033
10.410	0.92160	66.690	2.1142
10.410	1.0240	98.180	2.2570
12.310	1.0240	98.180	2.3558
12.310	1.0880	98.180	2.3981
12.310	1.1264	157.29	2.2570
16.920	1.3184	157.29	2.3487
16.920	1.2992	157.29	2.2147
16.920	1.3632		

R206A (993.59 nM)

[S] (μM)	v (μM min^{-1})	[S] (μM)	v (μM min^{-1})
0.0000	0.0000	1765.1	32.133
148.35	8.8157	1765.1	29.871
148.35	9.2698	1765.1	30.889
148.35	8.8963	1845.4	31.005
287.79	15.968	1845.4	31.568
287.79	16.416	3031.6	31.229
287.79	16.032	3031.6	34.057
599.89	24.000	3031.6	35.302
599.89	24.832	3348.1	32.037
599.89	24.608	3348.1	32.037
951.24	29.419	3348.1	30.490
951.24	28.565		
951.24	27.789		
1237.8	29.192		
1237.8	29.418		
1237.8	31.342		

R81A (15.54 nM)

[S] (μM)	v (μM min^{-1})	[S] (μM)	v (μM min^{-1})
0.0000	0.0000	207.54	9.0588
16.810	1.5488	207.54	9.5449
16.810	1.5104	207.54	8.9704
16.810	1.4528	310.50	10.782
34.600	2.8800	310.50	10.804
34.600	2.8416	310.50	11.224
34.600	2.8352	403.89	11.931
63.530	4.5760	403.89	11.887
63.530	4.5440	403.89	11.533
63.530	4.6720	535.57	12.726
98.650	6.1081	535.57	12.616
98.650	6.1504	535.57	12.815
98.650	6.2914		
130.44	7.7444		
130.44	7.6739		
130.44	7.3635		

R206A/R81A (3.0 μM)

[S] (μM)	v (μM min^{-1})	[S] (μM)	v (μM min^{-1})
0.0000	0.0000	288.83	1.1567
62.510	0.35392	288.83	1.1849
62.510	0.35712	619.03	2.3275
62.510	0.34624	619.03	2.4686
125.88	0.50360	619.03	2.5215
125.88	0.52830	2269.1	3.8886
125.88	0.53750	2269.1	3.8224
236.16	1.1264		
236.16	1.2032		

R81K (6.06 nM)

[S] (μM)	v (μM min^{-1})	[S] (μM)	v (μM min^{-1})
0.0000	0.0000	33.490	5.0112
6.9970	2.1931	33.490	5.1712
6.9970	2.2528	33.490	5.1264
6.9970	2.2357	63.890	6.0416
10.220	2.9952	63.890	5.8624
10.220	3.0592	63.890	5.8368
10.220	3.1104	99.260	6.7146
12.030	3.3536	99.260	6.7146
12.030	3.2640	99.260	6.5595
12.030	3.3152	130.30	6.8698
17.050	4.1472	130.30	6.7852
17.050	3.9936	130.30	6.8134
17.050	3.9424	249.23	7.0453
25.170	4.4928	249.23	7.3585
25.170	4.4608	249.23	6.7889
25.170	4.5184		

R206K (63.75 nM)

[S] (μM)	v (μM min^{-1})	[S] (μM)	v (μM min^{-1})
0.0000	0.0000	98.840	5.1911
7.4400	1.3312	98.840	5.0924
7.4400	1.4592	98.840	5.0078
7.4400	1.3568	130.72	5.4451
10.370	1.8304	130.72	5.0614
10.370	1.8688	130.72	5.7413
10.370	1.9200	170.00	5.0464
16.640	2.3936	170.00	4.9785
16.640	2.4576	170.00	5.3179
16.640	2.3296	205.78	5.6121
24.850	2.9824	205.78	5.3632
24.850	2.9760	205.78	5.7479
24.850	3.1168	232.03	5.3858
34.650	3.5648	232.03	5.2953
34.650	3.4688	232.03	5.2501
34.650	3.5840		
66.710	4.4352		
66.710	4.5312		
66.710	4.4160		

Y85F (59.87 nM)

[S] (μM)	v (μM min^{-1})	[S] (μM)	v (μM min^{-1})
0.0000	0.0000	59.180	7.8720
6.1120	2.4576	59.180	7.6800
6.1120	2.5856	59.180	7.8720
9.8100	3.2000	112.29	8.8729
9.8100	3.2256	112.29	8.6472
9.8100	3.2000	112.29	8.6049
18.090	4.8000	201.70	9.2479
18.090	4.5184	201.70	9.1273
18.090	4.6464	201.70	9.0066
28.330	6.3616	320.06	9.3686
28.330	6.1440	320.06	9.0820
28.330	6.2720	320.06	9.5798

W88A (73.78 nM)

[S] (μM)	v (μM min^{-1})	[S] (μM)	v (μM min^{-1})
0.0000	0.0000	369.72	26.337
33.280	4.3520	369.72	27.221
33.280	4.1344	369.72	27.265
33.280	4.3008	556.19	33.186
66.770	6.9760	556.19	32.435
66.770	7.3600	556.19	32.435
66.770	7.4880	730.41	34.196
128.27	13.782	730.41	32.396
128.27	13.458	730.41	32.677
128.27	13.472	980.88	38.470
282.08	23.535	980.88	36.839
282.08	23.308	980.88	37.852

S203A (6.44 nM)

[S] (μM)	v (μM min^{-1})	[S] (μM)	v (μM min^{-1})
0	0	16.94	4.6464
1.706	2.304	16.94	4.672
1.706	2.24	16.94	4.6336
3.3	3.1269	24.73	4.8192
3.3	3.0537	24.73	4.6144
3.3	3.2	24.73	4.5696
5.071	3.9863	33.66	5.1392
5.071	3.8766	33.66	4.9536
5.071	3.9497	33.66	5.0176
6.98	4.352	65.73	5.088
6.98	4.1984	65.73	5.0304
6.98	4.096	65.73	4.9344
10.16	4.6848	95.69	5.1559
10.16	4.3008	95.69	5.2405
10.16	4.4288	95.69	5.0994
12.48	4.5312		
12.48	4.5184		
12.48	4.5184		

S203H (30.11 nM)

[S] (μM)	v (μM min^{-1})	[S] (μM)	v (μM min^{-1})
0.0000	0.0000	285.43	8.7124
27.040	1.8944	285.43	9.0066
27.040	1.7984	285.43	9.2102
57.960	3.4880	399.03	9.9426
57.960	3.4432	399.03	9.8100
57.960	3.4432	399.03	10.318
117.08	5.8259	537.93	10.362
117.08	5.6284	537.93	10.782
117.08	5.6708	537.93	11.003
171.31	6.9246	748.03	11.417
171.31	7.0604	748.03	10.517
171.31	6.9925	748.03	10.349

S203D (51.97 μM)

[S] (mM)	v (μM min^{-1})	[S] (mM)	v (μM min^{-1})
0.0000	0.0000	6.0610	357.05
0.60700	75.904	6.0610	361.76
0.60700	76.672	6.0610	370.01
1.1940	119.97	7.5700	344.21
1.1940	125.80	7.5700	364.45
1.1940	124.10	7.5700	385.83
2.3460	197.93	9.2760	400.45
2.3460	190.39	9.2760	422.95
3.4810	235.68	9.2760	408.32
3.4810	239.21	11.560	416.20
3.4810	237.44	11.560	423.70
4.6150	287.23	11.560	437.20
4.6150	300.49		
4.6150	293.86		

E-dienelactone

wt DLH (30.32 nM)

[S] (μM)	v (μM min^{-1})	[S] (μM)	v (μM min^{-1})
0.0000	0.0000	236.86	15.823
52.390	5.5412	236.86	16.294
52.390	5.2824	236.86	15.353
52.390	5.7588	530.98	19.482
26.790	3.0412	530.98	19.871
26.790	3.0412	530.98	19.200
143.43	10.618	626.67	20.647
143.43	11.941	626.67	19.941
143.43	11.294	626.67	20.118

E36D (500.36 nM)

[S] (μM)	v (μM min^{-1})	[S] (μM)	v (μM min^{-1})
0.0000	0.0000	281.15	11.798
27.530	1.8882	281.15	11.460
27.530	1.9176	281.15	11.640
27.530	1.8882	373.75	12.417
53.960	3.4176	373.75	14.286
53.960	3.5118	373.75	13.040
53.960	3.5706	492.25	14.369
66.160	4.1941	492.25	14.161
66.160	4.3294	492.25	14.161
66.160	4.2235	755.40	17.193
101.81	6.3839	755.40	15.988
101.81	6.2711	755.40	16.985
101.81	6.2711	912.65	16.196
154.30	8.3916	912.65	18.148
154.30	8.0984	912.65	17.816
154.30	8.0532	1146.7	17.411
200.24	10.286	1146.7	18.058
200.24	9.9707	1146.7	17.087
200.24	9.5195		

R206A (198.72 nM)

[S] (μM)	v (μM min^{-1})	[S] (μM)	v (μM min^{-1})
0.0000	0.0000	293.60	0.67276
27.980	0.099412	293.60	0.64784
27.980	0.097059	293.60	0.63538
27.980	0.094118	376.27	0.75728
52.670	0.18882	376.27	0.65372
52.670	0.19059	376.27	0.67314
52.670	0.18353	588.78	0.88673
106.14	0.36155	588.78	0.84142
106.14	0.35189	588.78	0.75081
106.14	0.34653	749.40	0.91262
205.20	0.59328	749.40	0.86084
205.20	0.54365	749.40	0.84142
205.20	0.56846		

R81A (100.40 nM)

[S] (mM)	v (μM min^{-1})	[S] (mM)	v (μM min^{-1})
0.0000	0.0000	0.75870	21.769
0.025100	0.94706	0.75870	21.769
0.025100	0.87647	0.75870	20.302
0.025100	0.95882	1.0497	22.784
0.050150	1.8294	1.0497	23.460
0.050150	1.7471	1.2735	27.358
0.10081	3.7550	1.2735	26.660
0.10081	3.7871	1.6189	38.800
0.10081	3.6477	1.6189	37.559
0.12590	4.7598	1.6189	37.108
0.12590	4.6921	2.5837	40.379
0.12590	4.5342	2.5837	43.875
0.19971	7.3314	2.5837	43.650
0.19971	6.9253	3.0453	46.921
0.19971	7.5795	3.0453	45.342
0.27215	9.1362	3.0453	44.552
0.27215	8.7219	3.8137	44.435
0.27215	8.9701	3.8137	45.266
0.34427	12.002	4.4255	49.419
0.34427	10.631	4.4255	47.342
0.34427	11.711	4.4255	46.789
0.40061	12.251	5.0304	47.342
0.40061	11.835	5.0304	46.096
0.40061	11.296	5.0304	46.927
0.56077	17.151		
0.56077	17.608		
0.56077	17.193		
0.69536	20.712		
0.69536	20.000		
0.69536	18.900		

R206A/R81A (21.48 μM)

[S] (mM)	v (μM min^{-1})
0.0000	0.0000
0.56157	12.059
0.56157	12.882
0.56157	12.000
1.1426	28.001
1.1426	29.825
1.1426	27.036
2.0744	43.312
2.0742	43.988
3.4029	68.351
3.4029	68.802
6.0777	85.437
6.0777	97.087
6.0777	93.851
10.708	90.615
10.708	106.15
10.708	98.964

R81K (30.27 nM)

[S] (μM)	v (μM min^{-1})	[S] (μM)	v (μM min^{-1})
0.0000	0.0000	308.14	17.483
26.570	2.8941	308.14	16.861
26.570	2.9294	308.14	16.944
26.570	2.8412	399.50	19.726
53.490	5.2118	399.50	18.812
53.490	5.2118	399.50	19.269
53.490	5.0059	606.69	19.806
109.33	9.2037	606.69	19.547
109.33	9.2714	606.69	20.356
109.33	9.1586	770.23	22.071
154.52	12.452	770.23	22.427
154.52	11.730	770.23	22.411
154.52	11.775		
215.58	14.595		
215.58	15.001		
215.58	14.167		

R206K (254.99 nM)

[S] (μM)	v (μM min^{-1})
0.0000	0.0000
28.200	1.1941
28.200	1.2471
28.200	1.2882
51.670	2.2176
51.670	2.1706
51.670	2.2588
102.45	3.8529
102.45	3.6765
102.45	3.6765
142.84	4.7353
142.84	5.1471
142.84	4.9706
217.06	6.2353
217.06	6.5294
348.53	7.2353
348.53	7.1647
472.35	7.3059
472.35	6.8824
730.20	8.5059
730.20	8.3824
730.20	8.5059

Y85F (59.866 nM)

[S] (μM)	v (μM min^{-1})	[S] (μM)	v (μM min^{-1})
0.0000	0.0000	313.93	14.426
19.650	1.7118	313.93	15.068
19.650	1.7176	313.93	14.940
19.650	1.6588	391.41	17.409
38.410	3.1235	391.41	17.951
38.410	2.9118	391.41	16.952
38.410	3.0353	1045.0	20.384
90.920	6.4275	1045.0	20.694
90.920	6.7643	1045.0	21.128
90.920	6.4422	1496.0	22.739
156.52	10.293	1496.0	22.243
156.52	10.293	1496.0	21.685
156.52	10.527		
213.32	12.293		
213.32	11.957		
213.32	12.069		

W88A (329.39 nM)

[S] (μM)	v (μM min^{-1})	[S] (μM)	v (μM min^{-1})
0.0000	0.0000	627.49	24.806
26.410	1.4235	627.49	24.945
26.410	1.2765	627.49	24.336
26.410	1.4000	782.31	28.263
52.900	2.5529	782.31	28.479
52.900	2.6118	782.31	27.918
52.900	2.6988	1203.8	33.160
102.71	4.9177	1203.8	34.648
102.71	5.1658	1203.8	32.754
102.71	4.7372	1581.3	44.394
138.14	6.5418	1581.3	43.853
138.14	6.4967	2472.4	52.785
138.14	6.3839	2472.4	51.973
219.41	9.8353	2943.0	58.803
219.41	9.8353	2943.0	56.810
219.41	9.7677	2943.0	58.803
439.09	19.968	4017.9	60.796
439.09	17.497	4017.9	60.547
439.09	17.830		

S203A (64.363 nM)

[S] (μM)	v (μM min^{-1})	[S] (μM)	v (μM min^{-1})
0.0000	0.0000	308.28	14.348
26.120	1.7824	308.28	14.389
26.120	1.8529	308.28	14.784
26.120	1.8529	388.70	16.861
50.160	3.3765	388.70	16.300
50.160	3.4941	388.70	16.445
50.160	3.4412	560.73	19.644
102.71	6.4967	560.73	19.417
102.71	6.7674	560.73	20.000
102.71	6.5644	757.28	22.654
154.90	9.4518	757.28	22.136
154.90	9.0007	757.28	22.686
154.90	9.2263	1338.6	24.879
219.26	12.136	1338.6	24.578
219.26	12.091	1338.6	25.361
219.26	11.866		

S203H (7.61 μM)

[S] (mM)	v (μM min^{-1})	[S] (mM)	v (μM min^{-1})
0.0000	0.0000	6.2584	94.118
0.77980	18.528	6.2584	104.49
0.77980	18.635	6.2584	100.00
0.77980	17.463	8.0000	137.72
1.5041	32.504	9.5709	153.29
1.5041	34.479	9.5709	161.25
1.5041	31.772	9.5709	149.13
3.1022	61.430	11.322	153.98
3.1022	59.289	11.322	154.67
3.1022	57.149	11.322	150.17
4.8116	96.533		
4.8116	100.39		

S203D (51.97 μM)

[S] (mM)	v (μM min^{-1})	[S] (mM)	v (μM min^{-1})
0.0000	0.0000	9.6450	133.00
1.3200	41.288	9.6450	132.18
1.3200	40.410	9.6450	137.96
1.3200	41.874	12.110	153.66
2.6090	65.204	12.110	148.70
2.6090	65.920	12.110	146.84
2.6090	68.339	16.815	159.85
5.0570	98.887	16.815	166.05
5.0570	100.60	16.815	167.91
5.0570	101.46		
7.3910	128.03		
7.3910	121.11		
7.3910	117.65		

Appendix 5

Kinetic data used in Chapter 6

HPLC: DLI (10.7 μM) and *Z*-dienelactone

Time (minutes)	*Z*-lactone (mM)	*E*-lactone (mM)	Product (mM)
0.0000	6.8200	0.0000	0.0000
1.0000	6.3400	0.45000	0.0000
2.0000	5.8850	0.90500	0.0000
5.0000	5.2000	1.6000	0.0000
10.000	4.2000	2.5100	0.0000
20.000	3.4800	3.3100	0.0000
30.000	3.1000	3.3000	0.39000
60.000	3.1400	3.4800	0.17000
120.00	3.2000	3.5600	0.030000
180.00	2.9200	3.4800	0.39000

HPLC: DLI (10.7 μM) and *E*-dienelactone

Time (minutes)	*E*-lactone (mM)	*Z*-lactone (mM)	Product (mM)
0.0000	6.8200	0.0000	0.0000
2.0000	5.6400	1.1800	0.0000
5.0000	4.5900	1.8600	0.37000
10.000	4.2400	2.6000	0.0000
28.000	3.7600	3.2700	0.0000
58.000	3.4400	3.1300	0.25000
81.000	3.7300	3.3800	0.0000
120.00	3.7200	3.3800	0.0000
180.00	3.5700	3.2800	0.0000

HPLC: DLH (12 nM) and *Z*-dienelactone

Time (minutes)	*Z*-lactone (μM)	Product (μM)
0.0000	55.000	0.0000
0.33000	53.200	1.8000
0.58000	49.330	5.6700
1.0000	46.280	8.7200
1.5000	40.400	14.960
2.5000	32.690	22.310
5.0000	14.230	40.770
7.5000	3.2600	51.740

HPLC: DLH (20 nM) and *E*-dienelactone

Time (minutes)	*E*-lactone (μM)	Product (μM)
0.0000	55.070	0.0000
0.33000	51.790	3.2800
0.75000	50.810	4.2600
1.0800	50.760	4.3100
2.0000	46.530	8.5400
5.0000	36.510	18.560
10.500	24.000	31.070
15.000	17.350	37.720
21.000	10.620	44.450
30.000	4.9600	50.110
50.000	0.87700	54.193

UV: DLI (19.65 μM) and *Z*-dienelactone

[S] (mM)	v (μM min^{-1})	[S] (mM)	v (μM min^{-1})
0.0000	0.0000	3.2171	117.25
0.25572	18.517	3.2171	119.48
0.25572	16.842	5.1031	142.93
0.25572	19.262	5.1031	152.70
0.48781	30.397	5.1031	147.12
0.48781	30.025	9.2426	166.56
0.48781	30.583	9.2426	163.77
0.97560	55.521	9.2426	160.24
0.97560	57.506	12.497	174.75
0.97560	57.072	12.497	183.68
1.5936	76.675	12.497	180.89
1.5936	72.581	14.932	173.45
1.5936	79.280	14.923	187.97
2.2647	102.36	14.923	173.26
2.2647	110.42		
2.2647	105.77		

UV: DLI (20.01 μM) and *E*-dienelactone

[S] (mM)	v (μM min^{-1})	[S] (mM)	v (μM min^{-1})
0.0000	0.0000	4.3272	362.27
0.52181	2.8445	4.3272	355.66
0.52181	3.8009	5.5219	448.29
0.52181	3.0162	5.5219	460.70
0.97629	19.903	5.5219	447.47
0.97629	22.694	7.5016	643.19
1.2445	78.775	7.5106	592.12
1.2445	81.153	8.8824	643.19
1.2444	82.045	8.8824	650.19
2.0077	130.79	8.8824	644.57
2.0077	131.19	10.289	651.44
2.0077	130.40	10.289	672.86
2.5182	135.26	10.289	616.71
2.5182	131.39	13.185	724.95
2.5182	125.15	13.185	694.53
3.2350	282.26	13.185	666.65
3.2350	279.16	16.076	717.35
3.2350	267.37	16.076	697.07
4.3272	358.14	16.076	724.95

HPLC: DLI R206A (80.0 μM) and *Z*-dienelactone

Time (minutes)	*Z*-lactone (mM)	*E*-lactone (mM)	Product (mM)
0.0000	6.7900	0.0000	0.0000
1.0000	6.7600	0.030000	0.0000
2.0000	6.7400	0.050000	0.0000
5.5000	6.7200	0.12000	0.0000
10.000	6.6200	0.24000	0.0000
20.000	6.4100	0.49000	0.0000
30.000	6.2900	0.78000	0.0000
71.000	4.9700	1.6600	0.16000
120.00	3.7400	2.0900	0.96000
180.00	3.1000	2.3800	1.3100
240.00	2.7500	2.5100	1.5300
300.00	2.3600	2.5100	1.9200

HPLC: DLI R81A (59.7 μM) and *Z*-dienelactone

Time (minutes)	*Z*-lactone (mM)	*E*-lactone (mM)	Product (mM)
0.0000	6.8200	0.0000	0.0000
1.0000	6.7650	0.050600	0.0044000
2.0000	6.7205	0.099500	0.0000
5.0000	6.6240	0.24200	0.0000
10.000	6.3820	0.44100	0.0000
20.000	6.2540	0.82100	0.0000
31.000	5.7600	1.1180	0.0000
60.000	5.0110	1.6760	0.13300
120.00	4.1330	2.3820	0.30500
180.00	3.6600	2.6380	0.52200
240.00	3.3990	2.6790	0.74200

UV: DLI R206A (61.52 μM) and *Z*-dienelactone

[S] (mM)	v (μM min^{-1})
0.0000	0.0000
1.8054	3.0800
1.8054	3.8617
4.7657	9.3052
4.7657	9.3672
4.7657	9.4293
12.235	23.201
12.235	21.464
12.235	21.712
16.324	28.291
18.480	31.988
18.480	30.574
21.930	35.115
27.382	38.580
27.382	38.028
40.449	45.722

UV: DLI R81A (30.0 μM) and *Z*-dienelactone

[S] (mM)	v (μM min^{-1})
0.0000	0.0000
1.0232	6.2705
1.0232	7.0697
1.0232	5.9570
4.6907	51.161
4.6907	52.171
4.6907	55.893
14.552	86.849
14.552	88.089
14.552	89.330
22.070	95.238
22.070	98.861
22.070	103.00

HPLC: DLI R206A (80.0 μM) and *E*-dienelactone

Time (minutes)	*E*-lactone (mM)	*Z*-lactone (mM)	Product (mM)
0.0000	6.8200	0.0000	0.0000
1.0000	6.7650	0.050600	0.0044000
2.0000	6.7205	0.099500	0.0000
5.0000	6.6240	0.24200	0.0000
10.000	6.3820	0.44100	0.0000
20.000	6.2540	0.82100	0.0000
31.000	5.7600	1.1180	0.0000
60.000	5.0110	1.6760	0.13300
120.00	4.1330	2.3820	0.30500
180.00	3.6600	2.6380	0.52200
240.00	3.3990	2.6790	0.74200

HPLC: DLI R81A (59.7 μM) and *E*-dienelactone

Time (minutes)	*E*-lactone (mM)	*Z*-lactone (mM)	Product (mM)
0.0000	6.8200	0.0000	0.0000
2.0000	6.4500	0.36600	0.094000
5.0000	5.8800	0.76000	0.18000
10.000	5.3400	1.3200	0.16000
21.000	4.7900	2.2000	0.0000
30.000	4.1100	2.3900	0.32000
61.000	3.3800	2.5800	0.86000
120.00	2.9200	2.4200	1.4800
180.00	2.5400	2.0800	2.2000
245.00	2.2800	1.8700	2.6700

HPLC: DLI Y85F (19.9 μM) and *E*-dienelactone

Time (minutes)	*E*-lactone (mM)	*Z*-lactone (mM)	Product (mM)
0.0000	6.8200	0.0000	0.0000
1.0000	5.7040	1.1160	0.0000
2.0000	5.1120	1.6710	0.037000
5.0000	4.2720	2.5440	0.0040000
10.000	3.8160	2.9990	0.0050000
20.000	3.6750	3.2160	0.0000
30.000	3.5870	3.1870	0.046000
60.000	3.5450	3.1600	0.11500
120.00	3.4160	3.0530	0.35100
180.00	3.4160	2.9920	0.41200

HPLC: DLI (270 nM) and *Z*-dienelactone *tert*-butyl ester

Time (minutes)	*Z*-ester (mM)	*E*-ester (mM)	Product (mM)
0.0000	1.0000	0.0000	0.0000
1.0000	0.95630	0.0074000	0.036300
11.000	0.85594	0.090835	0.053230
21.000	0.77700	0.16400	0.059000
31.000	0.71480	0.22600	0.059200
41.000	0.66395	0.27875	0.057300
51.000	0.62000	0.31880	0.061200
61.000	0.58520	0.35380	0.061000
71.000	0.55745	0.38445	0.058100
81.000	0.53445	0.40805	0.057500
91.000	0.51575	0.42685	0.057400
101.00	0.50190	0.44410	0.054000
111.00	0.48875	0.45535	0.055900
121.00	0.48100	0.47040	0.048600
151.00	0.46485	0.48825	0.046900
181.00	0.46005	0.49925	0.040700
211.00	0.46030	0.50410	0.035600
241.00	0.46500	0.50660	0.028400

HPLC: DLI (324 nM) and *E*-dienelactone *tert*-butyl ester

Time (minutes)	*Z*-ester (mM)	*E*-ester (mM)	Product (mM)
0.0000	0.0000	1.0000	0.0000
1.0000	0.0067300	0.93821	0.055060
11.000	0.073950	0.87595	0.050100
21.000	0.14250	0.81100	0.046500
31.000	0.18805	0.76695	0.045000
41.000	0.22245	0.75245	0.025100
51.000	0.24950	0.70570	0.044800
61.000	0.27085	0.68455	0.044600
71.000	0.28720	0.66730	0.045500
81.000	0.29990	0.65340	0.046700
91.000	0.30980	0.64220	0.048000
101.00	0.31760	0.63380	0.048600
111.00	0.32385	0.62765	0.048500
121.00	0.32805	0.62165	0.050300
151.00	0.33725	0.61235	0.050400
181.00	0.34150	0.60630	0.052200
211.00	0.34365	0.60345	0.052900
241.00	0.34535	0.60105	0.053600

HPLC: DLH (998 nM) and *E*-dienelactone *tert*-butyl ester

Time (minutes)	*E*-ester (mM)	Product (mM)
0.0000	1.0091	0.0000
0.25000	0.96660	0.041560
0.50000	0.91690	0.090810
0.92000	0.90330	0.10407
1.1700	0.90420	0.10296
2.0000	0.75980	0.24717
5.0000	0.51600	0.49128
10.000	0.26110	0.74718
15.500	0.12530	0.88340
30.000	0.013000	0.99610

HPLC: C123D (21.8 μM) and *E*-dienelactone

Time (minutes)	*E*-lactone (mM)	*Z*-lactone (mM)	Product (mM)
0.0000	2.0110	0.0000	0.0000
1.0000	2.0102	0.00081200	0.0000
30.000	1.9931	0.017940	0.0000
60.000	1.9768	0.034160	0.0000
90.000	1.9618	0.049220	0.0000
120.00	1.9471	0.063880	0.0000
150.00	1.9317	0.076580	0.0026900
180.00	1.9138	0.087640	0.0095400
210.00	1.9023	0.097860	0.010800
240.00	1.8881	0.10859	0.014330
300.00	1.8676	0.12641	0.017040
360.00	1.8402	0.14157	0.029250
420.00	1.8263	0.15712	0.027610

UV: C123D (22.17 μM) and *p*-NPA

[S] (mM)	v (μM min^{-1})
0.0000	0.0000
1.0000	0.61620
1.0000	0.68230
1.0000	0.60710
1.5000	0.78480
1.5000	0.84300
1.5000	0.86920
2.0000	0.97140
2.0000	0.96339
2.0000	1.0709
3.0000	1.1971
3.0000	1.2661
3.0000	1.1627
4.0000	1.5697
4.0000	1.5234
4.0000	1.5465

UV: DLH (250.73 nM) and *p*-NPA

[S] (mM)	v (μM min^{-1})
0.0000	0.0000
0.20600	0.85240
0.20600	0.87640
0.20600	0.86160
0.62800	2.4571
0.62800	2.2769
0.62800	2.3913
1.0300	3.7757
1.0300	3.6842
1.0300	3.6842
1.0300	3.5355
1.0300	3.4554
1.0300	3.5469
1.5500	4.8741
1.5500	5.0572
1.5500	4.8169
1.5500	4.8627
1.5500	4.8627
1.5500	4.8055
1.8900	5.1716
1.8900	5.0572
1.8900	5.1259
3.0800	6.2014
3.0800	6.2815
3.0800	6.1899
5.1500	7.1396
5.1500	7.2998
5.1500	7.6201
7.7200	7.3913
7.7200	7.2998

UV: DLI (7.84 μM) and *p*-NPA

[S] (μM)	v (μM min^{-1})
0.0000	0.0000
5.5200	1.1880
5.5200	1.2128
5.5200	1.2300
11.040	1.8764
11.040	1.8650
11.040	1.8879
16.570	2.4314
16.570	2.5029
16.570	2.5744
27.610	3.0435
27.610	3.0778
27.610	3.2151
55.220	4.1762
55.220	4.3478
55.220	4.3135
83.280	4.9085
83.280	4.9199
83.280	5.0229
110.44	5.1602
110.44	5.2059
110.44	5.1144
144.95	4.9428
144.95	5.0229
144.95	4.9199
207.07	5.4005
207.07	5.2403
207.07	5.3432